FINAL SUMMARY REPORT
GER-12842, VOLUME I

Study of EXPANDABLE, TERMINAL DECELERATORS FOR MARS ATMOSPHERE ENTRY

By
GOODYEAR AEROSPACE CORPORATION
AKRON, OHIO

For
JET PROPULSION LABORATORY
JPL CONTRACT NO. 951153

3 October 1966
Copy No. 27

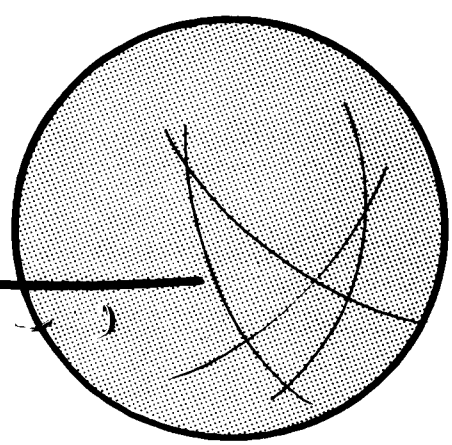

GOODYEAR AEROSPACE
CORPORATION

AKRON 15, OHIO

STUDY OF EXPANDABLE, TERMINAL DECELERATORS FOR MARS ATMOSPHERE ENTRY,

Volume I - Final Summary Report

GER-12842, Rev A 21 October 1966

Jay L. Musil

Goodyear Aerospace Corporation, Akron, Ohio

for

Jet Propulsion Laboratory, California Institute of Technology

Pasadena, Calif.

This work was performed for the Jet Propulsion Laboratory, California Institute of Technology, sponsored by the National Aeronautics and Space Administration under Contract NAS7-100.

FOREWORD

The research described in this final summary report (Volume I) was performed by Goodyear Aerospace Corporation, subsidiary of The Goodyear Tire & Rubber Company, Akron, Ohio, for the Jet Propulsion Laboratory, California Institute of Technology, under the authority of Contract No. 951153. The work was conducted from December 1965 to October 1966. Mr. James M. Brayshaw, Jr., was the Jet Propulsion Laboratory Technical Representative.

The work was performed under the general direction of Mr. R. L. Ravenscraft, manager of the Aero-Mechanical Engineering Division and Mr. Fred R. Nebiker, manager of the Recovery Systems Engineering Department. The program was directed by Mr. Jay L. Musil, project engineer.

Personnel contributing to this effort were Mssrs. A. P. Ahart, configuration, weight, and strength analyses; K. Birklein and J. W. Schlemmer, computer analyses; I. M. Jaremenko, pressure distribution analyses; and W. W. Sowa, thermal analyses.

This is Volume I of two volumes. Volume II presents the supporting technical information.

TABLE OF CONTENTS

Section	Title	Page
FOREWORD		iii
LIST OF ILLUSTRATIONS		vii
LIST OF TABLES		xi
I	DESCRIPTION OF PROGRAM	1
	1. Introduction	1
	2. Present Analysis Procedure for Aerodynamic Decelerator Applications	2
	3. Analysis Procedure Established for Program	4
II	ENVIRONMENTAL CONSIDERATIONS	9
	1. Atmospheres and Trajectories	9
	2. Decelerator Configurations	15
III	ANALYTICAL CONSIDERATIONS	21
	1. Basis of Analysis	21
	2. Decelerator Weight Relationships	22
IV	RESULTS OF ANALYSIS	27
	1. Trajectories Considered	27
	2. Decelerator Size	27
	3. Decelerator Weight	30
	4. Temperature and Material Considerations	33
	5. Effect of Target Mach Number Variation	42
V	SYSTEM COMPARISONS	47
	1. Basis for Comparison and Selection	47
	2. Dynamic Analysis	49

Section	Title	Page
	3. Comparisons of Composite Systems.	61
	a. General	61
	b. Items 1 and 2 - Decelerator Diameter and Altitude at Mach Number 1.	61
	c. Items 3 and 4 - Decelerator Weight and Envelope Weight	63
	d. Items 5 and 6 - Design and Actual Maximum Decelerator Envelope Temperature	64
	e. Item 7 - Auxiliary Gas Inflation System Weight	64
	f. Items 8, 9 and 10 - Ancillary Equipment Weight, Attachment Design Safety Factor, and Packaging Volume	65
	g. Item 11 - Composite System Velocity at 5,000 ft above Terrain	66
	h. Item 12 - Composite System Flight-Path Angle at 5,000 ft above Terrain	66
	i. Items 13 and 14 - System Oscillation Amplitude and Rate.	67
	j. Item 15 - Maximum Operating g-Level . . .	67
	k. Items 16 and 17 - Total Decelerator System Weight and Weight Fraction	68
VI	RECOMMENDATIONS.	69
VII	CONCLUSIONS	73
LIST OF REFERENCES		75
Appendix		
A	DECELERATOR CHARACTERISTICS	77
B	REFINED POINT-MASS TRAJECTORY COMPUTATIONS AND TRANSIENT HEATING CALCULATIONS .	103
C	DYNAMIC STABILITY ANALYSES	117

LIST OF ILLUSTRATIONS

Figure	Title	Page
1	Interrelationships of Decelerator Applications	3
2	Functional Flow Diagram of Constraining Factors and Variable Parameters	5
3	Trajectories for Mars Atmosphere Entry (VM7 Atmosphere)	11
4	Trajectories for Mars Atmosphere Entry (VM8 Atmosphere)	12
5	JPL Mars Entry Capsule	13
6	Trajectories for Mars Atmosphere Entry (Atmospheres VM3 and VM4)	14
7	Decelerator Concepts	16
8	Drag Coefficient Variation with Mach Number	18
9	Decelerator Weight	22
10	Six Steps for Determing Decelerator Size (All Values are Typical)	25
11	Decelerator Size Requirements (Trajectories A1 and A4; Atmospheres VM7 and VM8)	28
12	Decelerator Size Requirements (Trajectory 19 and Atmosphere VM8)	29
13	Decelerator-to-Total Weight (Trajectories A1 and A4; Atmospheres VM7 and VM8)	31
14	Decelerator-to-Total Weight (Trajectory 19 and Atmosphere VM8)	32
15	Aerodynamic and Thermal Effects on Decelerator Envelope (Trajectories 19 and A1)	35

Figure	Title	Page
16	Minimum Decelerator Envelope Unit Weight (Trajectory A1, h_T = 20,000 ft, Dacron)	38
17	Minimum Decelerator Envelope Unit Weight (Trajectory A1, h_T = 20,000 ft, Nomex)	39
18	Minimum Decelerator Envelope Unit Weight (Trajectory 19, h_T = 20,000 ft, Dacron)	40
19	Minimum Decelerator Envelope Unit Weight (Trajectory 19, h_T = 30,000 ft, Dacron)	41
20	Change in Percent Total Drag Area (Trajectory 19 and Atmosphere VM8)	43
21	Change in Altitude with Variation of Target Mach Number from 1.0 (Trajectory 19 and Atmosphere VM8)	44
22	Variation of Decelerator Weight with Target Mach Number (Trajectory 19; Attached BALLUTE)	46
23	Trailing BALLUTE	51
24	Attached BALLUTE	53
25	Tucked-Back BALLUTE	55
26	AIRMAT Cone	57
27	Decelerator Oscillation Characteristics (Atmosphere VM8; Trajectory 19)	59
28	Decelerator Oscillation Characteristics (Atmosphere VM8; Trajectory 22)	60
29	Rocket Boost Technique for Simulation Test	71
B-1	Space/Time and Envelope Transient Temperature versus Mach Number (Trajectory A1)	105
B-2	Space/Time and Envelope Transient Temperature versus Mach Number (Trajectory B3)	107
B-3	Space/Time and Envelope Transient Temperature versus Mach Number (Trajectory 19)	109
B-4	Space/Time and Envelope Transient Temperature versus Mach Number (Trajectory 22)	111

Figure	Title	Page
B-5	Space/Time and Envelope Transient Temperature versus Mach Number (Trajectory 23)	113
B-6	Space/Time and Envelope Transient Temperature versus Mach Number (Trajectory 30)	115
C-1	Decelerator Oscillation Characteristics for Trailing BALLUTE (Atmosphere VM7; Trajectory 22; p = 0.0 rad/sec)	131
C-2	Decelerator Oscillation Characteristics for Trailing BALLUTE (Atmosphere VM7; Trajectory 22; p = 0.5 rad/sec)	132
C-3	Decelerator Oscillation Characteristics for Trailing BALLUTE (Atmosphere VM7; Trajectory 22; p = 0.75 rad/sec)	133
C-4	Decelerator Oscillation Characteristics for Trailing BALLUTE (Atmosphere VM7; Trajectory 22; p = 1.0 rad/sec)	134
C-5	Decelerator Oscillation Characteristics for Trailing BALLUTE (Atmosphere VM8; Trajectory 19; p = 0.5 rad/sec)	135
C-6	Decelerator Oscillation Characteristics for Trailing BALLUTE (Atmosphere VM8; Trajectory 19; p = 1.0 rad/sec)	136

LIST OF TABLES

Table	Title	Page
I	Characteristics of VM Atmospheres	10
II	Initial Entry Conditions	13
III	Cases Selected for Extended Consideration	47
IV	Comparison of Decelerator Systems	62
A-I	Comparison of Decelerator Characteristics	81
A-II	Comparison of Decelerator Characteristics	83
A-III	Comparison of Decelerator Characteristics	85
A-IV	Comparison of Decelerator Characteristics	87
A-V	Comparison of Decelerator Characteristics	89
A-VI	Comparison of Decelerator Characteristics	91
A-VII	Comparison of Decelerator Characteristics	93
A-VIII	Comparison of Decelerator Characteristics	95
A-IX	Comparison of Decelerator Characteristics	97
A-X	Comparison of Decelerator Characteristics	99
A-XI	Comparison of Decelerator Characteristics	101
C-I	Manhours and Cost	117

SECTION I - DESCRIPTION OF PROGRAM

1. INTRODUCTION

Goodyear Aerospace Corporation (GAC) has conducted a parametric study to determine the suitability of expandable terminal decelerators for a Mars lander capsule. Under the terms of Contract No. 951153 from the Jet Propulsion Laboratory (JPL), the study was based on the analytical formulation of the effects associated with the model environments of Mars and specified entry capsule characteristics and entry conditions. These effects, characteristics, and conditions governed the requirements for the engineering applications of expandable decelerator devices.

The main objective was to determine fundamental engineering system design requirements for initial-stage, expandable decelerators that provide stabilization and retardation for Mars lander capsules (the entire system including the entry vehicle and decelerator is referred to as the entry capsule). To fulfill this objective the following characteristic's were analyzed:

1. Structural integrity
2. Performance effectiveness
3. Aerodynamic stability
4. Bulk and weight
5. Heat insulation
6. Materials
7. Ancillary equipment
8. Deployment and inflation
9. Packaging

The final objective was to compare and recommend:

1. Desirable configurations
2. Areas of additional study and analysis
3. Simulation and test requirements

The characteristics of various expandable decelerators were determined by the formulation of uncomplicated straightforward engineering analysis and design. Then, desirable decelerators that retard capsules to about Mach 1 near heights of 10,000, 20,000, and 30,000 ft above the Martian terrain were selected for more-detailed analyses and investigations.

Figure 1 gives the interrelationship of aerodynamic decelerator applications for Mars atmosphere entry. The requirements and technology breakdowns associated with operational functions, system design, basic science, and applied engineering are related directly to those required under the scope of this program.

2. PRESENT ANALYSIS PROCEDURE FOR AERODYNAMIC DECELERATOR APPLICATIONS

To date aerodynamic decelerator design has depended primarily on the available technology developed from specialized previous applications and investigations. The accepted procedure for establishing a design for a new application is given below.

1. Survey performance data relating to various decelerator configurations
2. Evaluate these data to determine the extent that a particular configuration and operating conditions relate to the specified requirements for the new application
3. Conduct a preliminary design effort and build test models

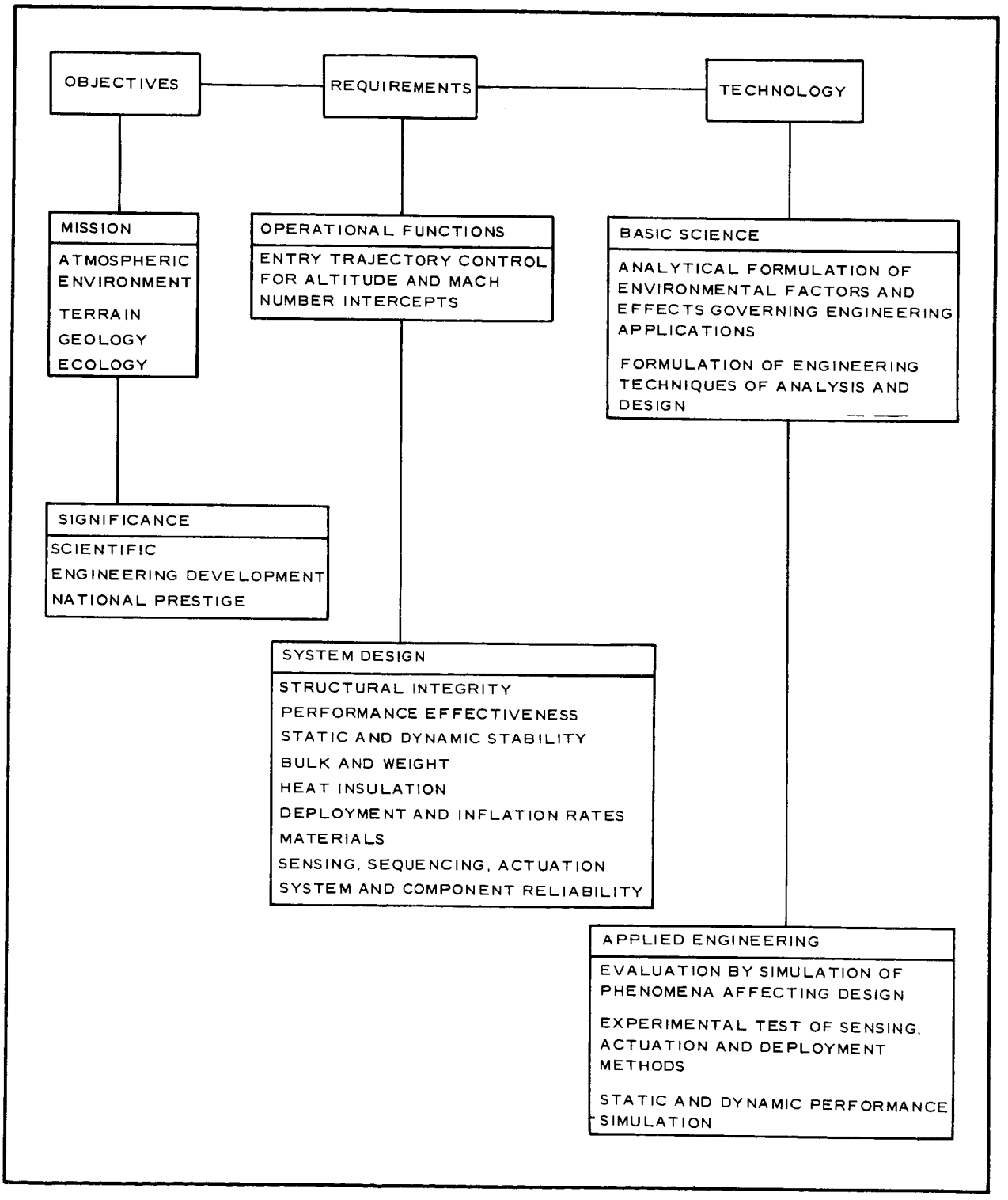

Figure 1 - Interrelationships of Decelerator Applications

Revised 21 October 1966

4. Conduct wind-tunnel, functional, and environmental tests to establish the validity of the predicted performance of a specific design for the new application and operating environments

5. Design, build, and conduct full-scale, free-flight tests of the decelerator system under simulated operational conditions and environments

This procedure has been demonstrated successfully. However, it has been carried out too often with the expense of unscheduled, additional time and cost for redesign and retest One of the major difficulties encountered was the extrapolation of system design data from previous applications. In many cases and usually after the program was well underway, unforseen factors or changes made the avialable data inadequate or not applicable. As a result, interation of Steps 3, 4, and 5 was required. Additionally, procedures and time scales establishing requirements for aerodynamic decelerator applications were often incompatible with the development of the most reliable and efficient decelerator system design.

3. ANALYSIS PROCEDURE ESTABLISHED FOR PROGRAM

This program, which comprised a parameter study, took a different approach to evaluating the characteristics of aerodynamic decelerators as compared with the analysis procedure outlined above. To illustrate this approach, Figure 2 shows a functional flow diagram of the factors and variable parameters appropriate to the application of aerodynamic decelerators for the trajectory control of planetary entry vehicles. The inputs and outputs are associated with the environments, constraints, requirements, and objectives of this study.

The simplicity of the functional diagram is somewhat deceptive. If a servo circuit is used as an analogy, the system is "open-loop," which at once points up the inherent difficulty of aerodynamic decelerator

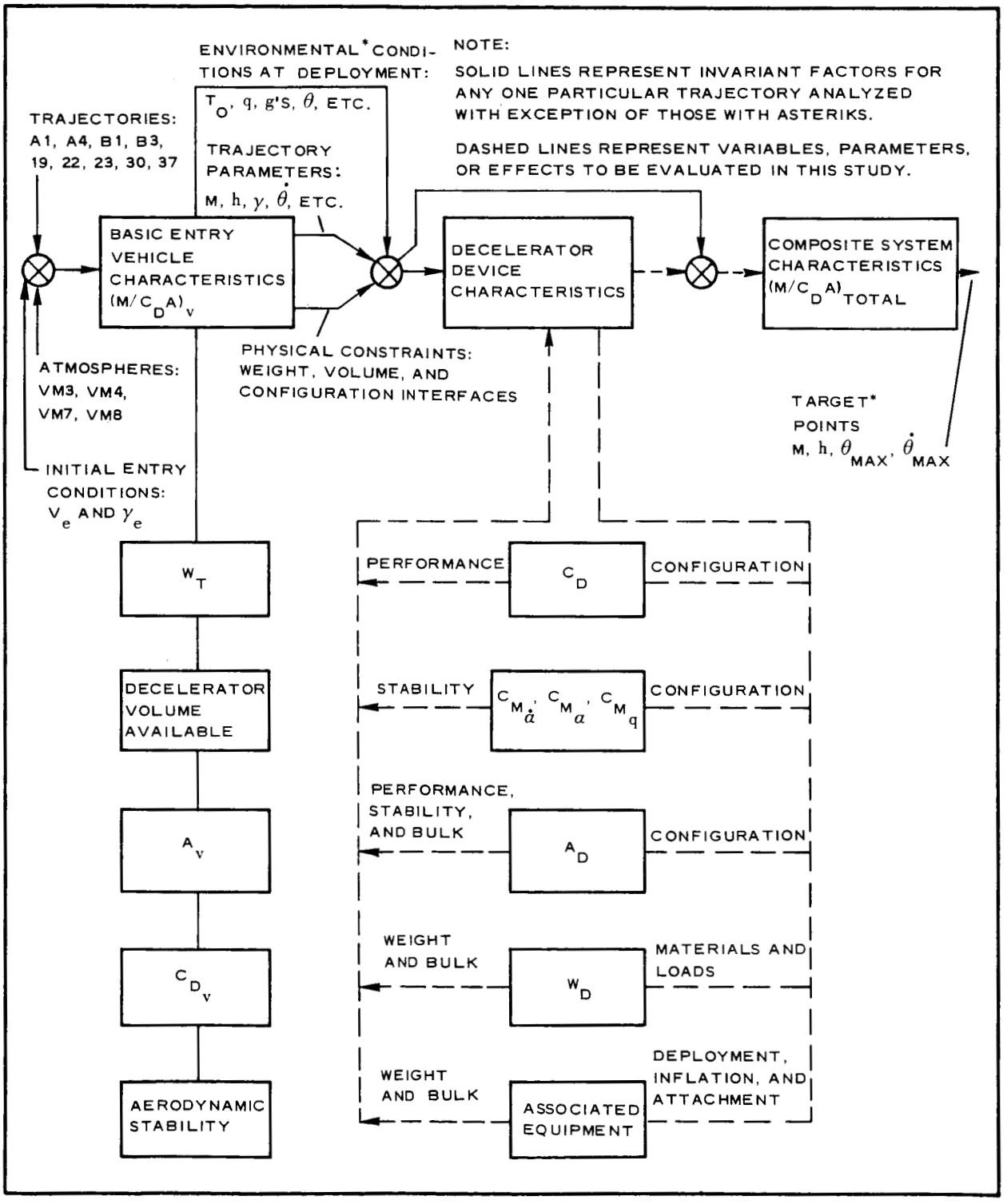

Figure 2 - Functional Flow Diagram of Constraining Factors and Variable Parameters

design technology. "Matching"(that is, achieving an optimized design) the parameters and factors for a desirable system must be accomplished by techniques similar to the graphic solutions for some types of mathematical equations involving transcendental functions.

In reality there is feedback through the dynamic characteristics of the physical system as a result of coupling through the external operating environment and the resulting system motions. Unfortunately this feedback is nonlinear by the very nature of the performance characteristics of aerodynamic decelerator devices when moving through an atmosphere at high speeds, necessitating adaptation of the parameters to the desired system performance.

The purpose of this discussion is not to emphasize the difficulty of this study, but rather to demonstrate the validity of the engineering analysis approach and procedures established. Further, this analysis approach was appropriate since it permitted evaluation for all possible aerodynamic decelerator system concepts.

As shown by Figure 2, the significant factors and parameters that required consideration and evaluation to establish the design of deployable aerodynamic decelerator systems for the Mars lander capsule included:

1. Initial entry conditions (V_e, γ_e, α_e, p, q, r, etc.) associated with the designated JPL trajectories (A1, A4, B1, B3, 19, 22, 23, 30, 37) and the characteristics of the Mars atmosphere (VM3, VM4, VM7, VM8)
2. Basic entry capsule size, mass, and performance characteristics
3. Physical constraints of entry capsule on the decelerator bulk, weight, configuration, attachments, etc.
4. Resulting trajectory parameters associated with

the entry capsule (M, h, γ, θ, etc.) that establish the permissible velocity-time-distance scales for the decelerator operation

5. Environmental conditions at deployment (T_o, q, g's, θ, etc.) and operation of the decelerator that establish design requirements for performance and structural integrity

6. Decelerator characteristics as related to performance, stability, weight, and bulk

7. Composite system characteristics

8. Target points of Mach number, altitude, angular excursions, and attitude rates

The interrelated factors and parameters affecting the application of aerodynamic decelerators are found to be complex with no direct or precise closed-form solution possible. Analysis of the factors and effects had to be studied in discrete, uncomplicated, and orderly fashion and then the separate results for a composite system as applied to representative operational cases had to be synthesized. After definitive trends were established, indicating the more favorable performance characteristics, selections were made. Refined analyses and investigations then were performed leading to the final selection of the concepts and systems recommended for future full-scale development and application.

SECTION II - ENVIRONMENTAL CONSIDERATIONS

1. ATMOSPHERES AND TRAJECTORIES

The various characteristics for the model VM (Voyager/Mars) atmospheres considered in this study are listed in Table I. Figures 3 and 4 show the Mars entry trajectories in the VM7 and VM8 atmosphere profiles for the entry capsule illustrated in Figure 5. Seven entry trajectories were selected by JPL for the entry capsule to establish the environmental conditions under which the decelerators are required to perform successfully with structural integrity. The initial entry velocities and angles, and mass ballistic coefficients associated with the corresponding trajectories are given in Table II. Two additional trajectories (one each in the VM3 and VM4 atmospheres in Figure 6) were investigated to determine effects of atmosphere variation for off-design conditions.

Consideration also was given to controlling factors such as entry capsule size and configuration, sterilization requirements, entry trajectories and Mach number/altitude target points.

Although the surface density for the projected Mars VM8 atmosphere is almost twice that of the VM7, the inverse scale height above the tropopause is greater by a factor of about 2.8 (see Table I). For an entry capsule with a given mass-ballistic coefficient and having the same initial entry conditions, Figures 3 and 4 show that there are shorter time scales and lower altitudes for a given Mach number. Higher dynamic pressures will be associated with deceleration of the entry capsule to the same target points (M = 1.0 at 10,000, 20,000, and 30,000 ft) in the VM8 atmosphere as compared with the VM7. Consequently entry into the VM8 atmosphere established the criteria for the design integrity of an initial-stage supersonic decelerator because higher Mach number performance is required and

TABLE I - CHARACTERISTICS OF VM ATMOSPHERES

Property	Symbol	Dimension	Atmosphere profile			
			VM3	VM4	VM7	VM8
Surface pressure	P_o	mb	10.0	10.0	5.0	5 0
		lb/sq ft	20.9	20.9	10.4	10.4
Surface density	ρ_o	$(gm/cu\ cm)10^5$	1.365	2.57	0.68	1.32
		$(slugs/cu\ ft)10^5$	2.65	4.98	1.32	2.56
Surface temperature	T_o	K	275	200	275	200
		R	495	360	495	360
Stratospheric temperature	T_s	K	200	100	200	100
		R	360	180	360	180
Acceleration of gravity at surface	g	cm/sec^2	375	375	375	375
		ft/sec^2	12.3	12.3	12.3	12.3
Composition						
CO_2 (by mass)			28.2	70.0	28.2	100.0
CO_2 (by volume)			20.0	68.0	20.0	100.0
N_2 (by mass)			71.8	0.0	71.8	0.0
N_2 (by volume)			80.0	0.0	80.0	0.0
A (by mass)			0.0	30.0	0.0	0.0
A (by volume)			0.0	32.0	0.0	0.0
Molecular weight	M	mol^{-1}	31.2	42.7	31.2	44.0
Specific heat of mixture	C_p	cal/gm C	0.230	0.153	0.230	0.166
Specific heat ratio	γ		1.38	1.43	1.38	1.37
Adiabatic lapse rate	Γ	K/km	-3.88	-5.85	-3.88	-5.39
		R/1000 ft	-2.13	-3.21	-2.13	-2.96
Tropopause altitude	h_T	km	19.3	17.1	19.3	18.6
		kilo ft	63.3	56.1	63.3	61.0
Inverse scale height (stratosphere)	β	km^{-1}	0.0705	0.193	0.0705	0.199
		$ft^{-1} \times 10^5$	2.15	5.89	2.15	6.07
Continuous surface wind speed	v	ft/sec	155.5	155.5	220.0	220.0
Peak surface wind speed	v_{max}	ft/sec	390.0	390.0	556.0	556.0
Design vertical wind gradient	dv/dh	ft/sec/1000 ft	2	2	2	2

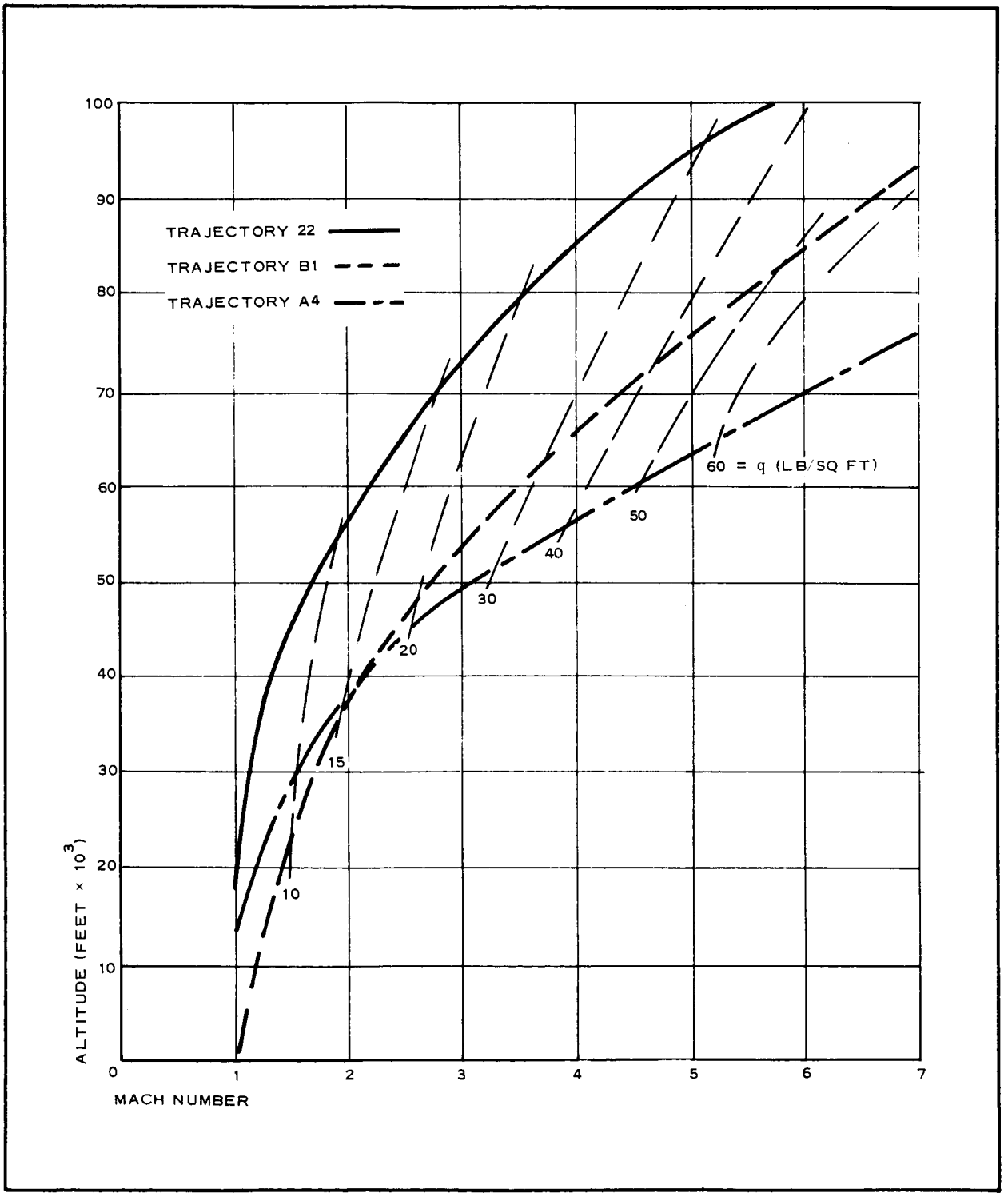

Figure 3 - Trajectories for Mars Atmosphere Entry
(VM7 Atmosphere)

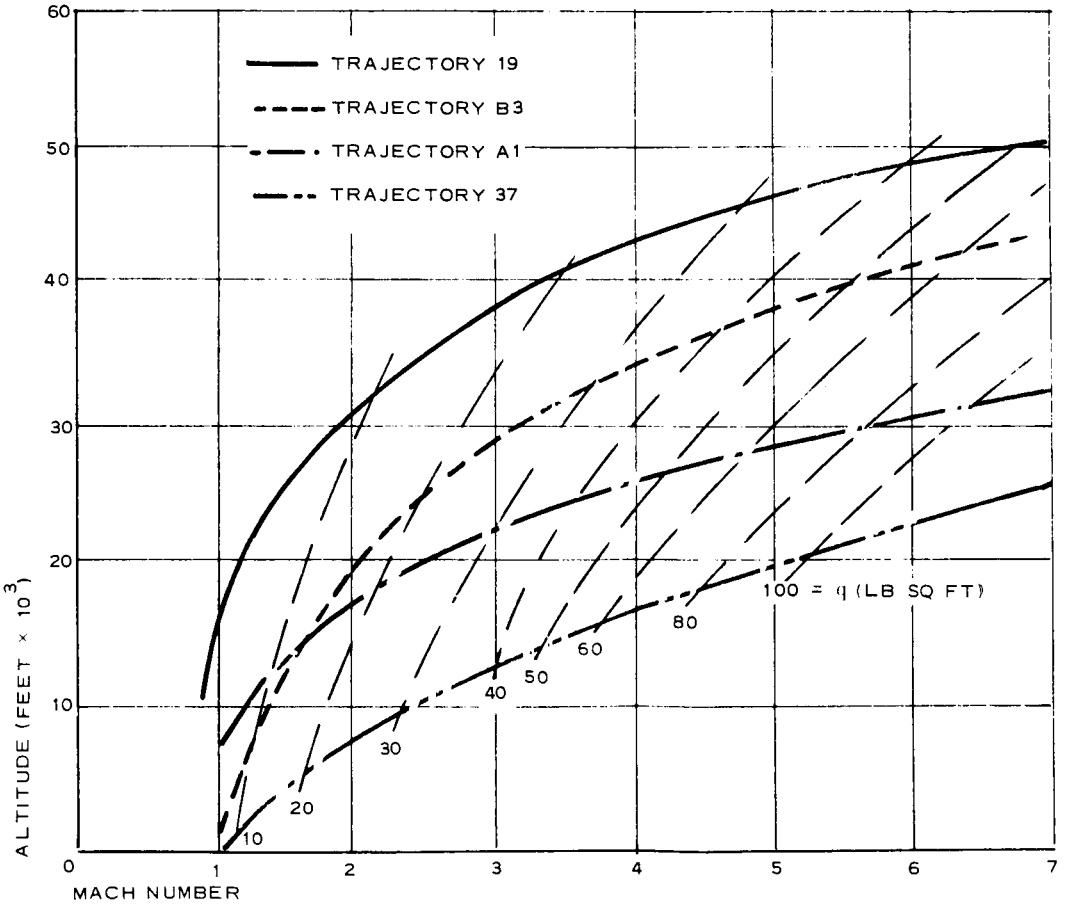

Figure 4 - Trajectories for Mars Atmosphere Entry
(VM8 Atmosphere)

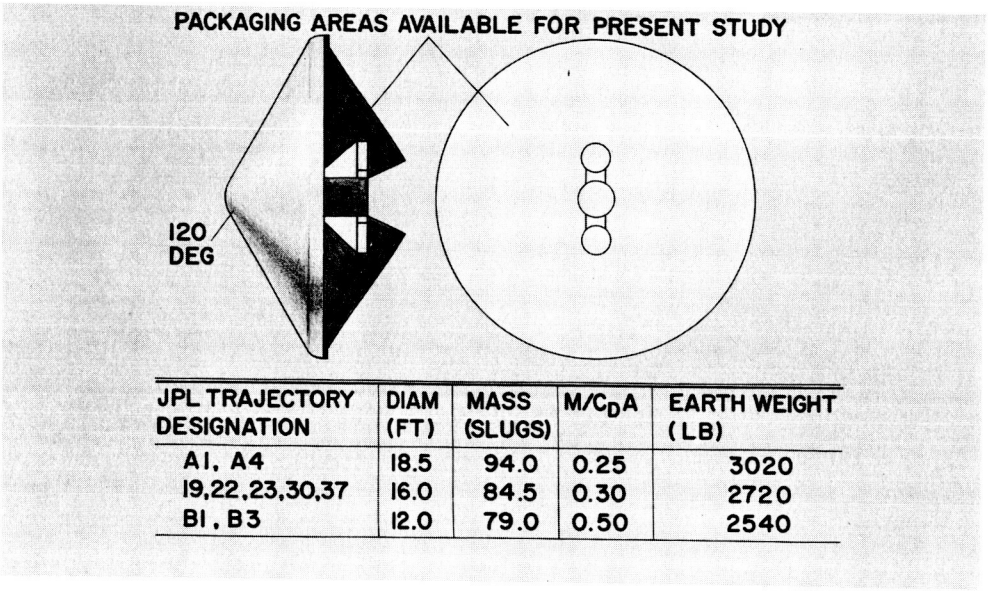

JPL TRAJECTORY DESIGNATION	DIAM (FT)	MASS (SLUGS)	M/C_DA	EARTH WEIGHT (LB)
A1, A4	18.5	94.0	0.25	3020
19,22,23,30,37	16.0	84.5	0.30	2720
B1, B3	12.0	79.0	0.50	2540

Figure 5 - JPL Mars Entry Capsule

TABLE II - INITIAL ENTRY CONDITIONS

JPL trajectory designation	Entry velocity, V_e (fps)	Entry angle, γ_e (deg)	Capsule mass ballistic parameter, M/C_DA (slugs/sq ft)	Atmosphere profile
A1	23,000	25	0.25	VM8
A4	23,000	25	0.25	VM7
B1	15,000	15	0.5	VM7
B3	15,000	15	0.5	VM8
19	16,000	16	0.3	VM8
22	16,000	16	0.3	VM7
23	16,000	16	0.3	VM3
30	16,000	16	0.3	VM4
37	23,000	28	0.3	VM8

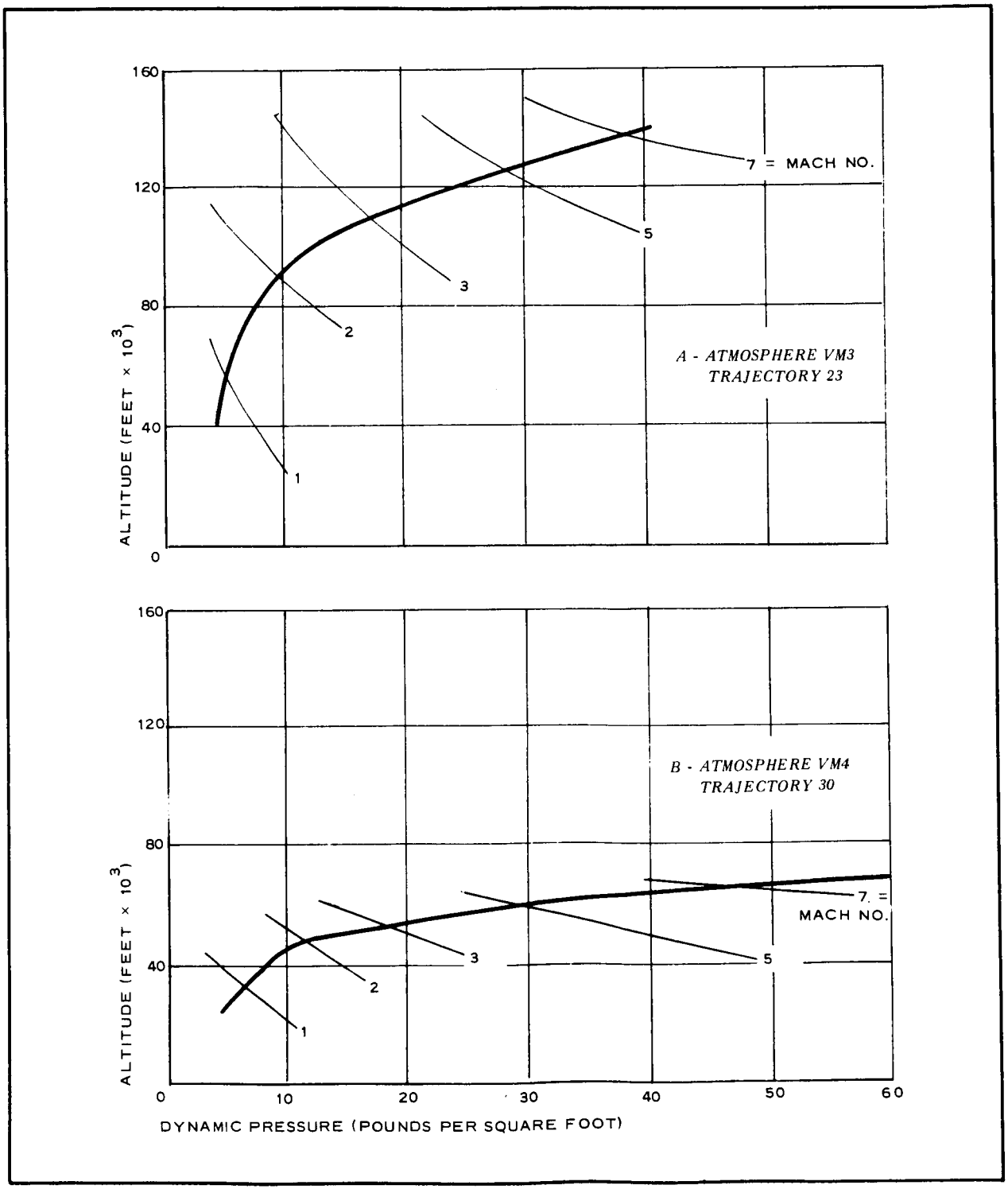

Figure 6 - Trajectories for Mars Atmosphere Entry
(Atmospheres VM3 and VM4)

correspondingly higher aerodynamic pressure loads are encountered.

Note that higher driving temperatures are associated with the VM7 atmosphere at Mach numbers corresponding with those in the VM8. However, in the VM7 atmosphere the results of analyses indicate a trend toward considerably lower deployment Mach number requirements for first-stage decelerators. This trend minimizes aerodynamic heating effects as a critical design factor for the VM7 entry cases considered in this study (see Appendixes A and B). For this study a basic entry capsule was specified with a blunted cone configuration, as shown in Figure 5. The capsule has an included angle of 120 deg and the size and mass characteristics as tabulated in Figure 5, corresponding with the designated JPL trajectories. The study allowed substantial volume availability and a minimum of interface constraints aft of the capsule base so that assessment of the various decelerator configurations was not unduly restricted by this consideration. However intergration forward from the capsule base to the payload was beyond the scope of the study and this affect is not reflected.

2. DECELERATOR CONFIGURATIONS

An inflatable AIRMAT[a] cone, extending from the base and parallel to the basic entry vehicle forebody angle and ram-air,, self-inflating BALLUTE[a] devices illustrated in Figure 7 were considered in this program. The characteristic size and weight trends for these devices were found to be indicative of all expandable, pressure-inflatable devices, including parachutes and other balloon-like configurations that require auxiliary gas inflation sources. Only the values for the represented cases and configuration studied will change.

The trailing and attached plain-back BALLUTE configurations are shown in Figure 7 with burble fences about 15 deg aft of the maximum BALLUTE diameter. There are various aerodynamic and structural considerations for the use of the fence, one of which is to establish a

[a] TM, Goodyear Aerospace Corporation, Akron, Ohio.

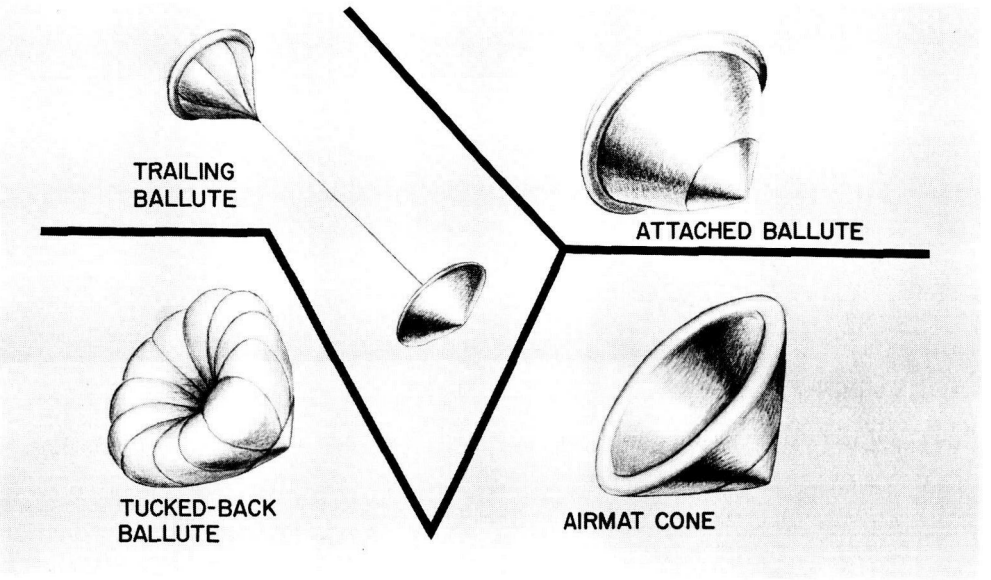

Figure 7 - Decelerator Concepts

point of uniform viscous separation near the maximum diameter of the BALLUTE. Although this consideration is associated primarily with subsonic speeds, that is, before the critical (local sonic) Mach number is encountered near the maximum BALLUTE diameter, there is a possibility of encountering an asymmetric separation effect for a range of transonic Mach numbers near 1.0.

Additionally the fence provides a substantial portion of the overall drag of the BALLUTE and can produce the same drag as a much larger BALLUTE without a fence. Strength, bulk, and weight requirements can be correspondingly less for a given drag effectiveness requirement. Tests have proved that projections as high as 10 percent of the BALLUTE diameter (referred to as a 10-percent burble fence) are effective. This amount of projection provides a 44-percent increase in relation to the BALLUTE reference area and at the same time, the desired uniform viscous separation effect is ensured. It is recommended that a similar

fence be considered for incorporation with the tucked-back BALLUTE configuration.

Figure 8 shows the drag coefficient variation with Mach number for the configurations illustrated in Figure 7. For the attached and trailing BALLUTEs and the AIRMAT cone configurations, there were various sources of data for reasonable engineering confidence in the drag variations indicated throughout the Mach number range in Figure 8. There were no comparable data for the tucked-back BALLUTE. However, for this study, a reasonable approximation was possible for the drag coefficient based on the characteristic trends for blunt, large-angle cone configurations and the results of various BALLUTE development test programs[1-11].

The drag coefficient variation for the trailing BALLUTE shown in Figure 8 is associated with BALLUTE-to-forebody diameter ratios in the range from 1.0 to about 3.0. The characteristic reduction in drag effectiveness with increasing Mach numbers primarily is caused by the reduction of energy in the forebody wake and the wake flow conditions. Numerous tests have demonstrated the good drag effectiveness and low oscillation characteristics of the BALLUTE trailing at a distance within less than four forebody base diameters - even when the BALLUTE is trailing behind an asymmetric lifting forebody at angles of attack up to 30 deg and the forebody has large auxiliary control flaps deflected as much as 40 deg.

Other trailing decelerator configurations for supersonic applications, including all current variations of supersonic parachutes, generally have to be positioned farther aft of the forebody base. They also require a larger diameter to develop the equivalent drag effectiveness of the BALLUTE configuration with a 10-percent burble fence. Furthermore, the characteristic blunt face of the parachute canopy gives rise to exaggerated unsteady flow conditions at supersonic speeds, generally causing violent parachute canopy flutter and instability at off-design

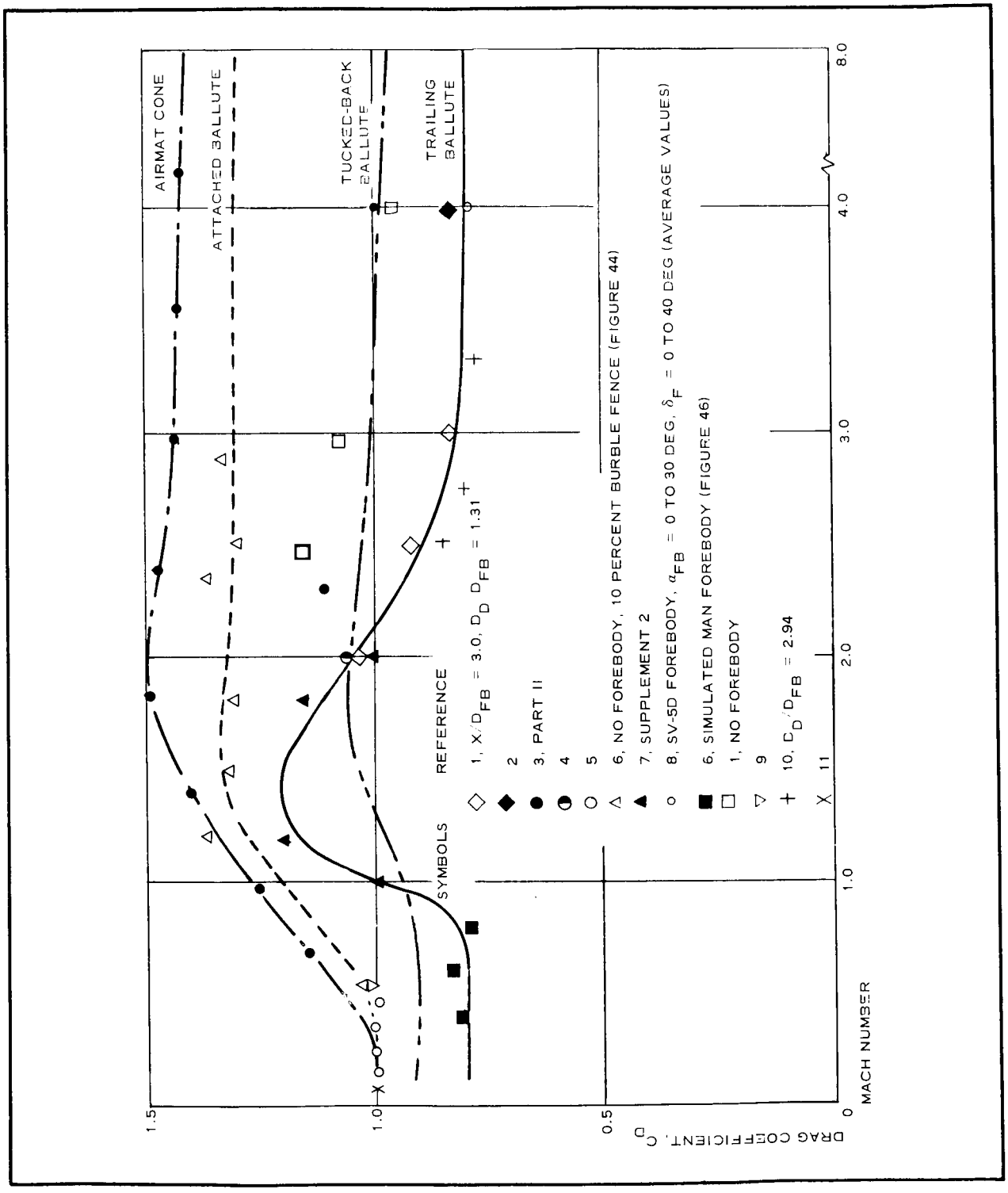

Figure 8 - Drag Coefficient Variation with Mach Number

Mach numbers. This phenomenon is not associated with ram-air-inflated BALLUTE devices during operation primarily because of (1) more steady and uniform flow directed over the symmetrical forward portion, (2) uniform separation as a result of the fence, and (3) strong damping, rigidizing, and added mass and inertia effect of the entrapped inflation gas at high stagnation pressure (that is, total pressure).

The effect of the riser line on the decelerator system weight was established as an important consideration with respect to the trailing BALLUTE. This consideration also is true for trailing parachute decelerators. The GAC analyses (see Appendix A, Volume II) indicate that for a BALLUTE trailing at a distance of four entry-capsule base diameters in the operational environment of interest, the weight breakdown is approximately as follows: 20 percent for the BALLUTE envelope, 33 percent for the meridian cables, 15 percent for the coating (considering both heat insulation and porosity), and 32 percent for the riser. Because of the high percentage of riser weight, a trailing decelerator may weigh more than an attached decelerator even though it may be smaller to develop the same total drag effectiveness.

SECTION III - ANALYTICAL CONSIDERATIONS

1. BASIS OF ANALYSIS

To conduct surface experiments and exploration of Mars effectively, there will have to be a soft landing with equipment. Selecting an expandable terminal decelerator for a Mars lander capsule only can be made by evaluation and assessment of the constraints of the overall mission and related systems. To obtain an optimized, expandable, terminal decelerator, the various interrelationships of Figure 2 must be evaluated within a parametric framework that allows meaningful tradeoffs.

The requirement to achieve a target Mach number and a target altitude above Mars and the evaluation of interrelationships in Figure 2 facilitated the understanding of how parametric formats and engineering analysis procedures could be formulated. The analytical tools used were point-mass trajectory computations, generalized strength/weight and configuration analyses, drag performance estimates, pressure distribution estimates, materials investigations, thermal analyses, and aerodynamic stability analyses (see Volume II).

Decelerator system weight has been established as a fundamental factor in the application of expandable terminal decelerators. With appropriate data, an integrated tradeoff of decelerator weight and entry vehicle system weight was made. The decelerator weight was expressed in terms of allowable Mach number and altitude (or dynamic pressure) at deployment, size, performance effectiveness, and available operation times to achieve the specified target Mach number/altitude conditions. This tradeoff also took into consideration the vehicle's physical characteristics and the operational environments given in this study.

2. DECELERATOR WEIGHT RELATIONSHIPS

The weight for a flexible pressure-inflated decelerator as shown by Figure 9 (also see Appendix A of Volume II) is related to:

$$w_D = f(P, d^3, K_1, K_2),$$

where P is pressure; d, diameter; K_1, a shape factor; and K_2, a material strength factor. The pressure, P, for a ram-air-inflatable BALLUTE is a function of the configuration, dynamic pressure, and the flow conditions of the operating environment. For design purposes and structural integrity, maximum values of the parameters corresponding to the deployment conditions generally are employed in any particular design application. The primary criterion is the pressure recovery at the ram-air inlets of the device. Numerous tests and analyses have shown that by making judicious consideration of geometry and position effects, an almost constant pressure recovery factor of 2.75 at the inlets can be achieved for deployment Mach numbers above about 2.0.

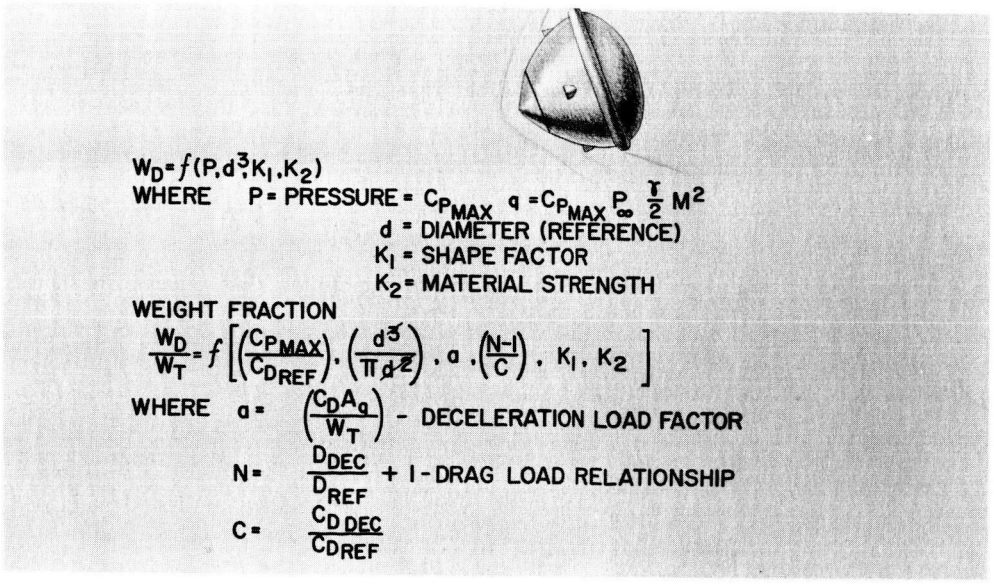

Figure 9 - Decelerator Weight

In terms of a weight ratio, it is shown by Figure 9 that the decelerator weight fraction increases linearly with diameter. This fact reflects the disappointing but well-known effect of the cube/square law for structural scaling with increasing size. Additionally, the decelerator weight fraction is a function of the dynamic pressure or square of the Mach number and is related to the external surface pressure from the aerodynamic loads that requires support by the internal pressure.

Thus, the decelerator weight results were developed from static aerodynamic loading relationships with empirically determined, quasi-static load, temperature, and design factors employed to account for operating environmental effects and material characteristics. The validity of this approach has been demonstrated by the results of this study and has led to optimum designs of systems with minimum practical weight. Considering dynamic loading effects, additional weight advantages are gained by delaying the decelerator device deployment to lower dynamic pressure conditions, when time and distance scales permit, for the following reasons:

1. Energy requirements to deploy and erect the decelerator are reduced since the basic vehicle system is decelerating inertially at a lower rate
2. Snatch loads on the decelerator device, supporting structure, and vehicle as a result of lower relative inertial velocities are reduced
3. Deployment opening shock and inflation loads as a result of lower dynamic pressures are reduced
4. Peak heat flux, integrated heat load, and maximum temperature rise on exposed surfaces of the decelerator are reduced because of the lower deployment velocity and shorter time scales of operation to attain lower specified target altitude/Mach number conditions

Before specific results are presented, it is desirable to establish how the decelerator size was determined (see Section V of Volume II). Figure 10 illustrates the six basic steps in the graphic analysis procedure that lead to a first approximation determination of the decelerator size for achieving the target Mach number/altitude.

I.

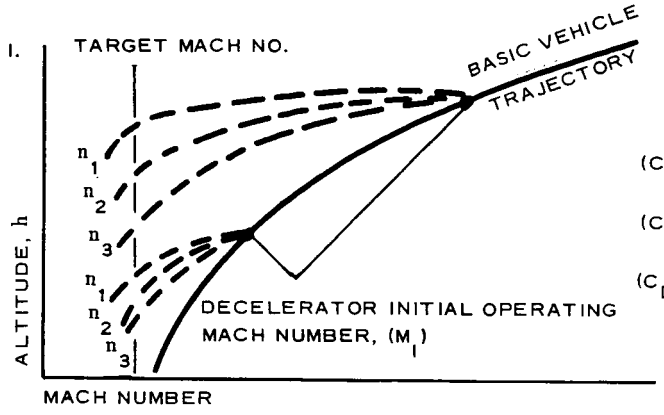

$$n = \text{PERCENT OF} \frac{(C_DA)_T}{(C_DA)_V} \times (C_DA)_V$$

$(C_DA)_V$ = VEHICLE DRAG AREA $\doteq$ 100 PERCENT VALUE

$(C_DA)_D$ = DECELERATOR DRAG AREA

$(C_DA)_T = (C_DA)_V + (C_DA)_D$

II.

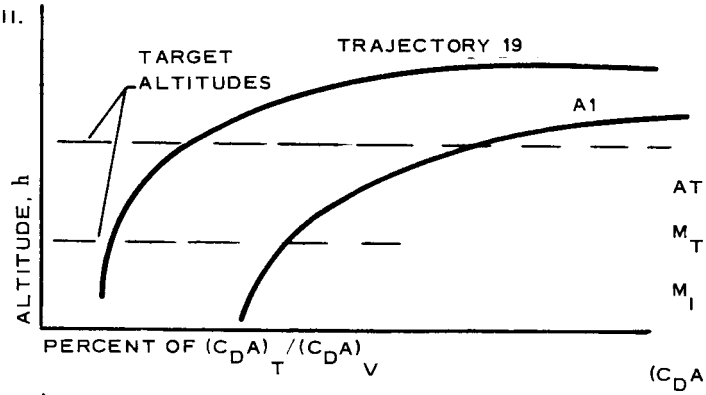

ATMOSPHERE VM8

M_T = 1.0

M_I = 3.0

III.

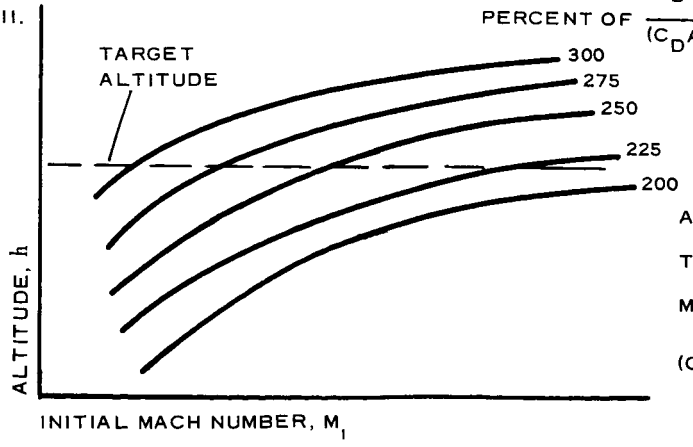

ATMOSPHERE VM8

TRAJECTORY 19

M_T = 1.0

$(C_DA)_V$ = 281.5 SQ FT

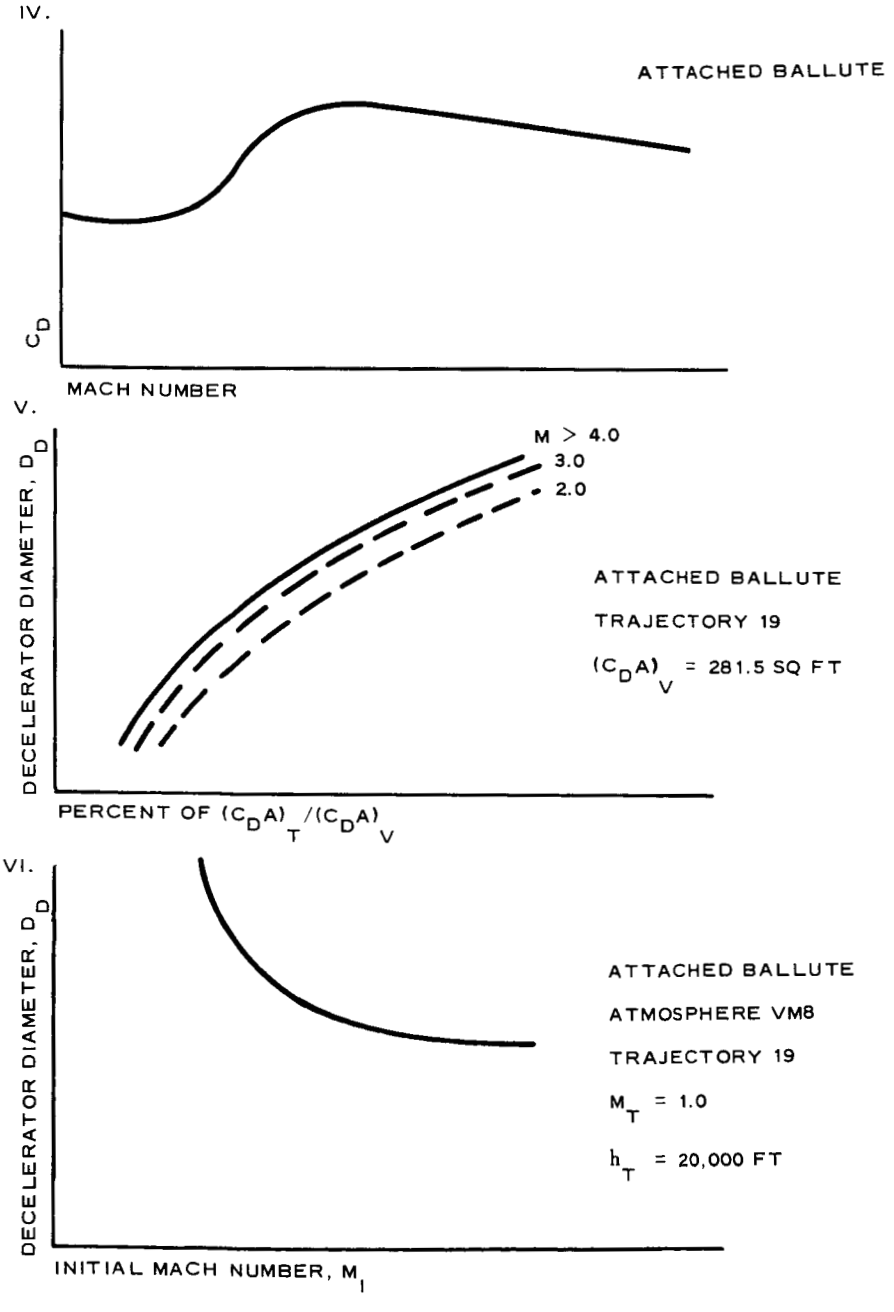

Figure 10 - Six Steps for Determing Decelerator Size
(All Values are Typical)

SECTION IV - RESULTS OF ANALYSIS

1. TRAJECTORIES CONSIDERED

The A1, A4, and 19 trajectories specifically are considered here but the analysis procedures and characteristic trends indicated are appropriate to all the trajectories (see Volume II). Note that the A1 and A4 trajectories have a M/C_DA of 0.25 and are associated with a higher initial entry velocity and steeper entry angle (from Table II, V_e = 23,000 fps and γ_e = 25 deg) when compared with the other trajectories, except for the 37 trajectory that has the same velocity but a steeper initial entry angle of 28 deg and an M/C_DA of 0.3. These entry conditions may be associated with lower accuracy constraints for either orbiting or flyby entry modes of the entry capsule. For the cases considered in this study and as shown by the trajectories of Figures 3 and 4, the severity of environmental conditions encountered at corresponding altitudes in atmosphere VM8 are affected more substantially by initial entry conditions than by the mass-ballistic parameter. For example compare the A1 and 19 entry cases at the altitude of 30,000 ft. It should be recognized that the results shown later pertaining to the A1 trajectory indicate less favorable weight fractions for first-stage decelerators to achieve the same target Mach number/altitude points as compared with the 19 trajectory. The 19 trajectory has a lower initial entry velocity (V_e = 16,000 fps) and a lower entry angle (γ_e = 16 deg) with a higher mass-ballistic parameter (M/C_DA = 0.3).

2. DECELERATOR SIZE

The six-step analysis procedure was used to develop Figures 11 and 12, which establish the decelerator size requirements to retard entry capsules in the A1, A4, and 19 trajectories to a target Mach number

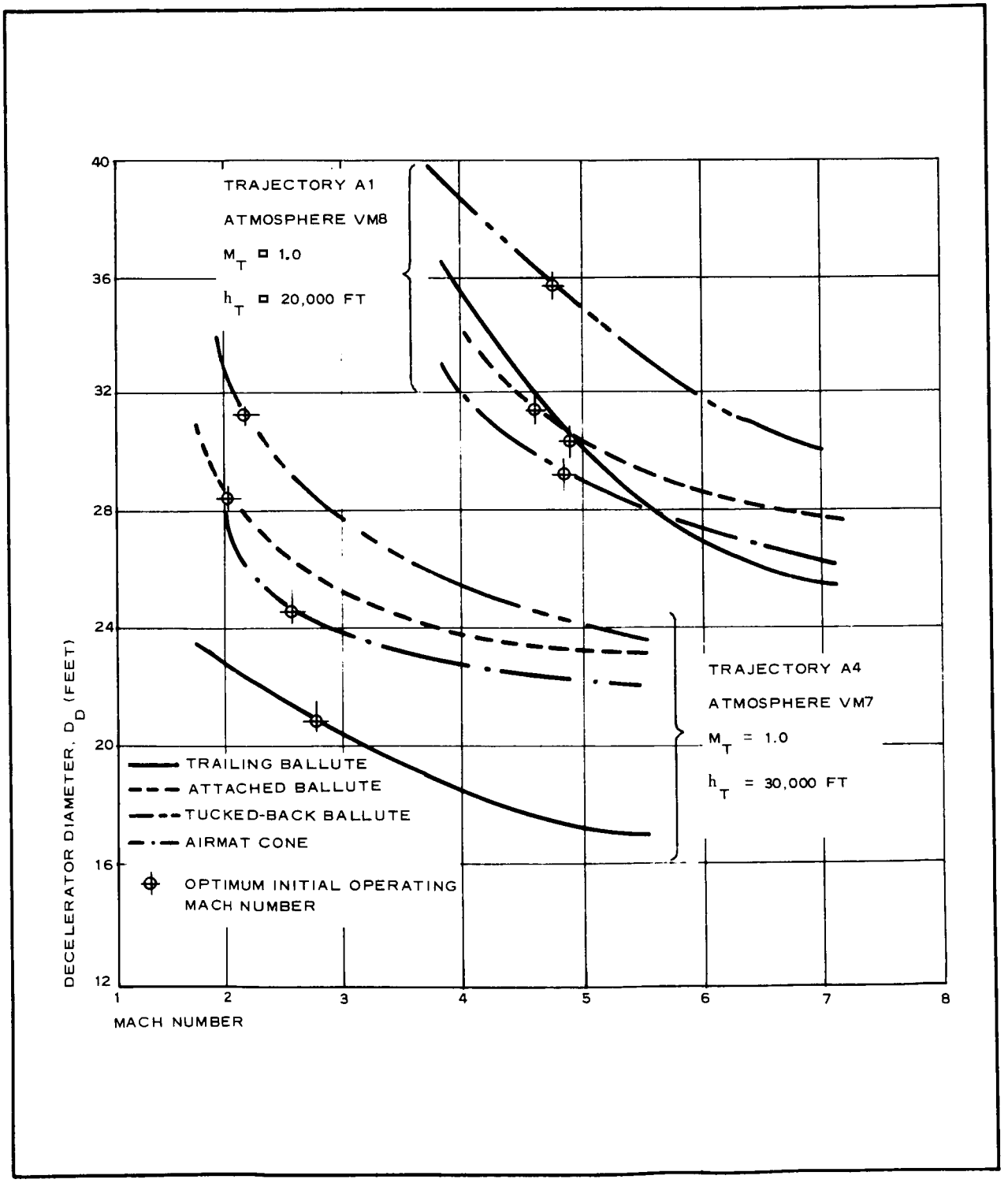

Figure 11 - Decelerator Size Requirements (Trajectories A1 and A4; Atmospheres VM7 and VM8)

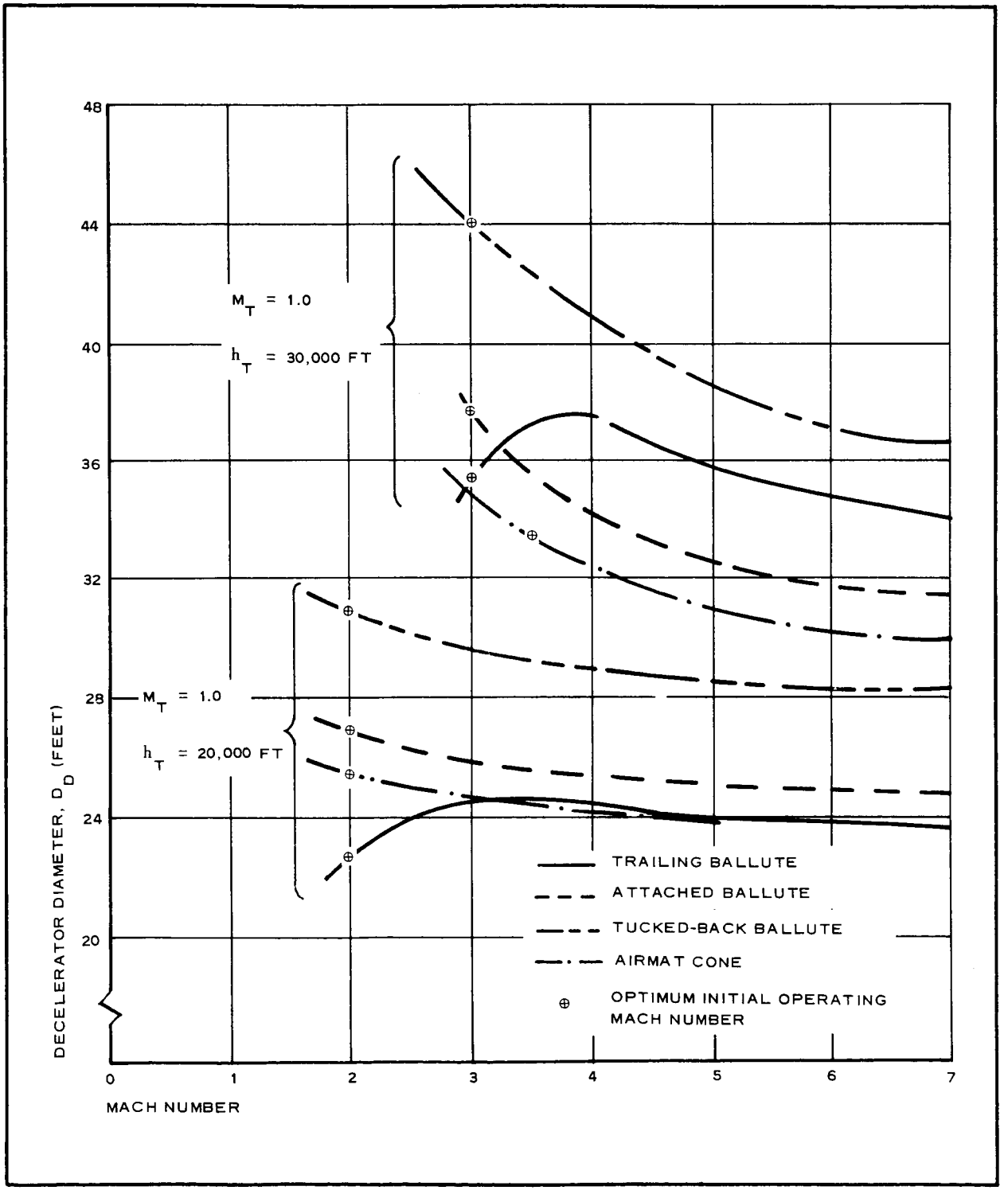

Figure 12 - Decelerator Size Requirements (Trajectory 19 and Atmosphere VM8)

of 1.0 near target altitudes of 20,000 and 30,000 ft (see Section VI of Volume II). The decelerators were defined as developing their full-drag effectiveness at the corresponding Mach numbers on the abscissa scale. In other words, for the first approximation of decelerator size, time scales for decelerator deployment and inflation were not required to be reflected in these results. Note, however, that for the corresponding Mach numbers in the figures in this section illustrating the characteristics of the decelerators there is a slightly higher Mach number (about 5 percent) and a higher dynamic pressure (about 10 percent) at which the decelerator device is deployed initially and begins to inflate (see Items 16 and 17 of Tables A-I through A-XI of Appendix A). Figures 11 and 12 show the trend to asymptotic values of decelerator size as Mach number is increased.

Thus, this study has pointed out that in relation to the size of a decelerator, there is an upper practical limit to the initial operating Mach number. Above this limit there is no appreciable reduction in decelerator size to achieve lower specified target Mach number/altitude points for the trajectories considered in this study. In comparing the curves associated with the target point Mach number of 1.0 and the 20,000-ft altitude for trajectory 19, the smaller decelerator sizes are indicated because of the increasing density of the atmosphere.

3. DECELERATOR WEIGHT

Figures 13 and 14 present the percent of decelerator weight to total entry capsule weight for the four decelerator configurations in trajectories A1, A4, and 19. The results were obtained by the analysis procedure in Appendix A of Volume II. For these figures the decelerator strength requirements are predicated on the use of dacron assumed to be operating at an elevated temperature of 350 F. A material strength design factor of 2.0 also is reflected in the results presented.

When it is possible to attain specified target altitude/Mach number conditions within physical constraints and within allowable time and distance

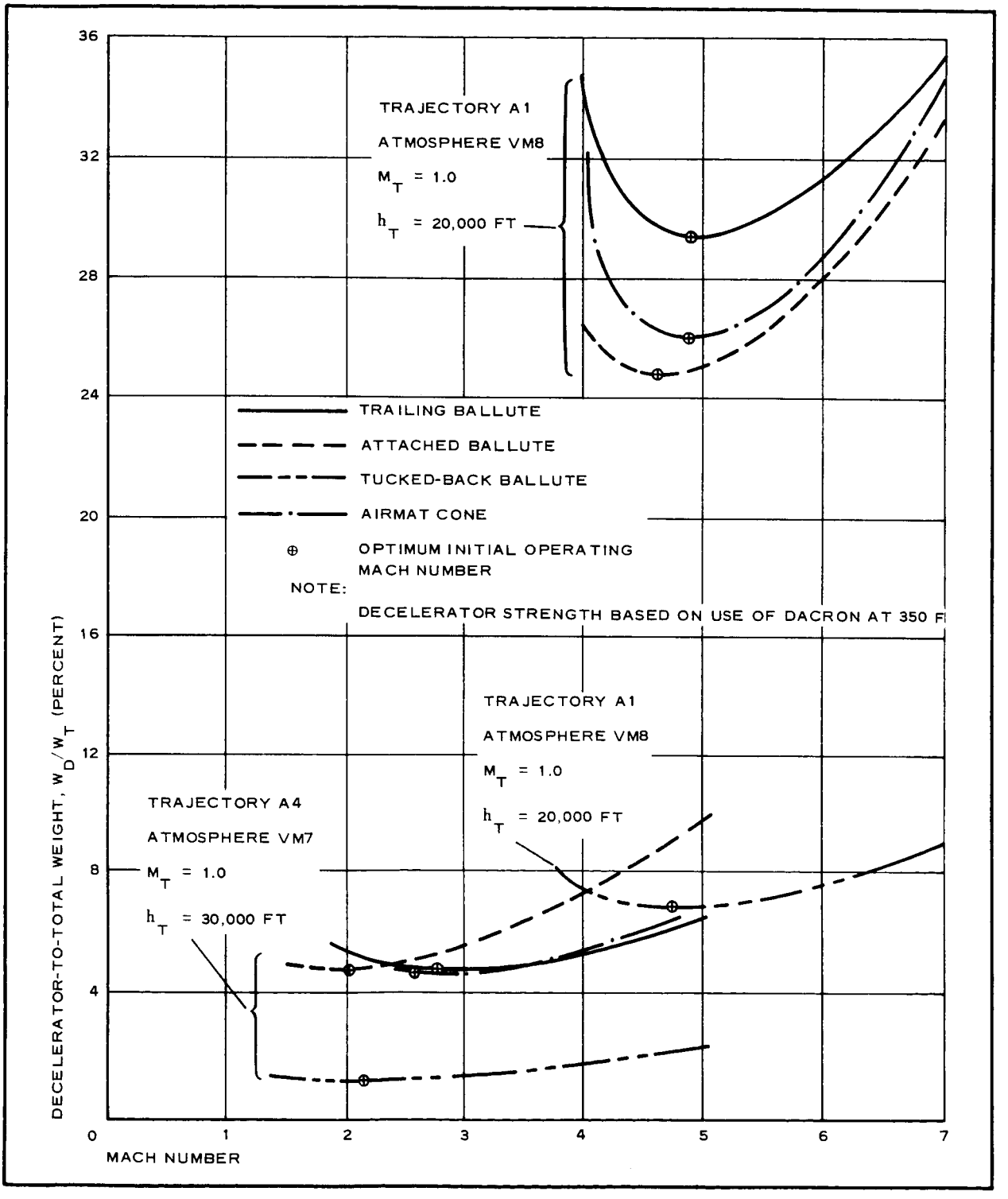

Figure 13 - Decelerator-to-Total Weight (Trajectories A1 and A4; Atmospheres VM7 and VM8)

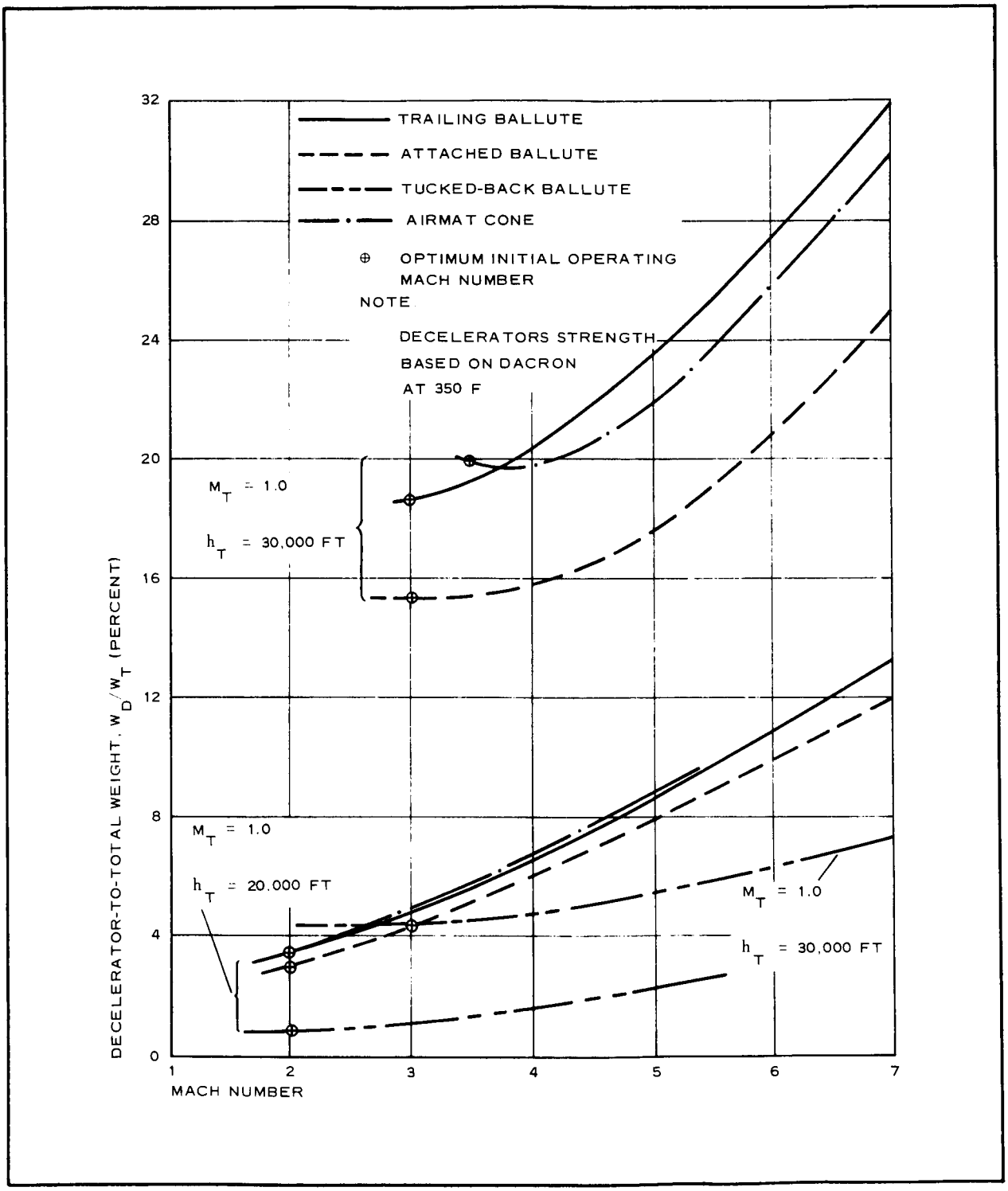

Figure 14 - Decelerator-to-Total Weight (Trajectory 19 and Atmosphere VM8)

scales, Figures 11 through 14 indicate that it is desirable to accept a larger decelerator diameter and delay operation of the device to a corresponding lower Mach number. This consideration leads to the trend of arriving at a minimum percentage of decelerator-to-total system weight and corresponding optimum initial operating Mach number. For trajectory 19 in Figure 14 and the target conditions of Mach number = 1.0 and altitude = 20,000 ft, the same trends are indicated. However as a result of the extended available time and distance scales and higher atmosphere density, the values for the decelerator size, weight fraction, and operational Mach number all are reduced substantially as compared with the requirements for the 30,000-ft target altitude case. The interaction of Mach number effect (that is, dynamic pressure) on the decelerator strength and weight requirements has a compounding effect.

4. TEMPERATURE AND MATERIAL CONSIDERATIONS

Figure 15 has been developed by the analysis procedure of Section IV of Volume II to indicate the degree of validity in choosing dacron when operating at a temperature of 350 F for the decelerators analyzed and in leading to the results presented in Figures 13 and 14 for trajectories A1 and 19. The thermal requirement curves for dacron and Nomex for trajectory A1 represent the envelope fabric weight per unit area required to limit the total temperature rise to 350 F with dacron and 600 F with Nomex. These curves correspond with the decelerator sizes in Figures 11 and 12 that begin effective operation at the corresponding Mach number on the abscissa scale. The material temperature results from the local heat flux and integrated heat load corresponding with the velocity-time-distance scales (appropriate to initial operating conditions for the decelerators) to achieve the target points of M_T = 1.0 and h_T = 20,000 ft. The analyses (see Section II of Volume II) assumed that the local heat flux is 0.30 of the stagnation point value.

Boundaries for both 30,000- and 20,000-ft target altitudes for trajectory 19 have been included in Figure 15 to indicate the effect of a lower

target altitude requirement. For the lower target altitude, there are associated lower optimum initial operating Mach number requirements with the resulting fact that aerodynamic heating effects are minimized. At the higher initial operating Mach numbers for this target altitude, larger values for the fabric unit weight are required as a result of the extended time scales of operation and consequent increase in total heat load in addition to the effect of the higher values of Mach number. To develop the thermal requirement curves, the heat absorbed by the decelerator material was assumed simply to be that of its heat capacity.

In Figure 15 are the curves of decelerator envelope fabric weight per unit area for the attached and trailing BALLUTE decelerators established by aerodynamic loading requirements. There are symbols for the other configurations as determined also by the aerodynamic loading encountered at the corresponding initial operating Mach number to achieve the desired target point conditions. For trajectory A1 with target conditions of $M_T = 1.0$ and $h_T = 20,000$ ft, it is shown that the use of dacron at a 350-F "static" temperature for the AIRMAT cone (initially operating at the indicated optimum Mach number from Figures 13 and 14) is conservative. For the attached BALLUTE, the assumption of dacron at 350 F is quite accurate; for the trailing and tucked-back BALLUTEs, the assumption is optimistic.

It is pointed out here that the static strength/weight analysis and the thermal analysis did not include provision for coating weight. Some coating must be provided in any event to ensure minimum acceptable leakage rates to maintain the desired pressurization within the decelerator envelope. Typical coating materials employed for this purpose are also good heat insulating materials (see Section III of Volume II). A nominal coating thickness of about 0.01 psf of Vitron or Neoprene will provide a net porosity of about 0.02 cu ft/sq ft/sec, which is an acceptable value based on experimental results for the upper values of pressure ratios and operating environment encountered in this study.

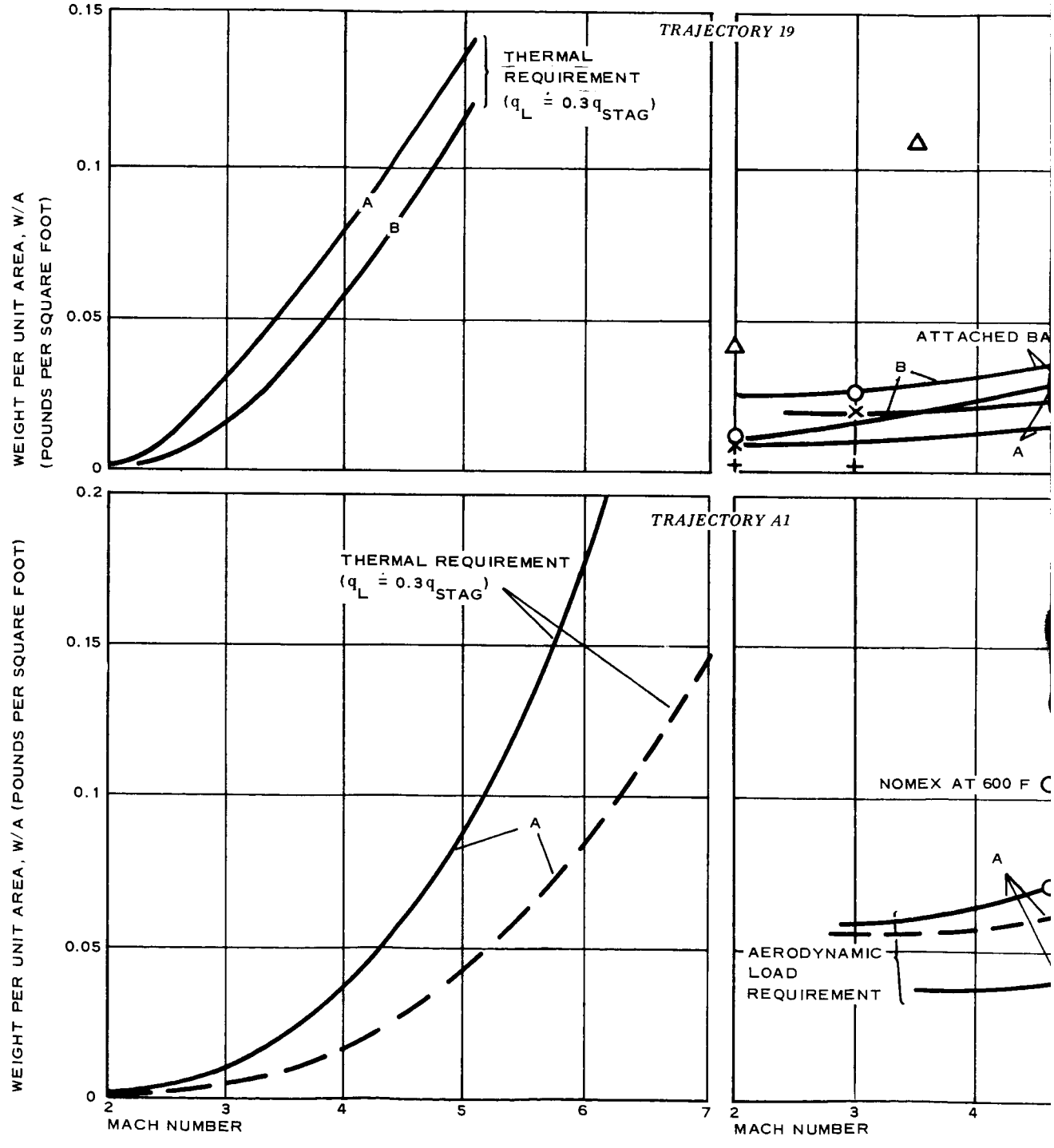
TRAJECTORY 19
THERMAL REQUIREMENT ($q_L \doteq 0.3 q_{STAG}$)
A
B
ATTACHED BA
WEIGHT PER UNIT AREA, W/A (POUNDS PER SQUARE FOOT)
0.15
0.1
0.05
0
TRAJECTORY A1
THERMAL REQUIREMENT ($q_L \doteq 0.3 q_{STAG}$)
NOMEX AT 600 F
AERODYNAMIC LOAD REQUIREMENT
0.2
0.15
0.1
0.05
0
2
3
4
5
6
7
MACH NUMBER

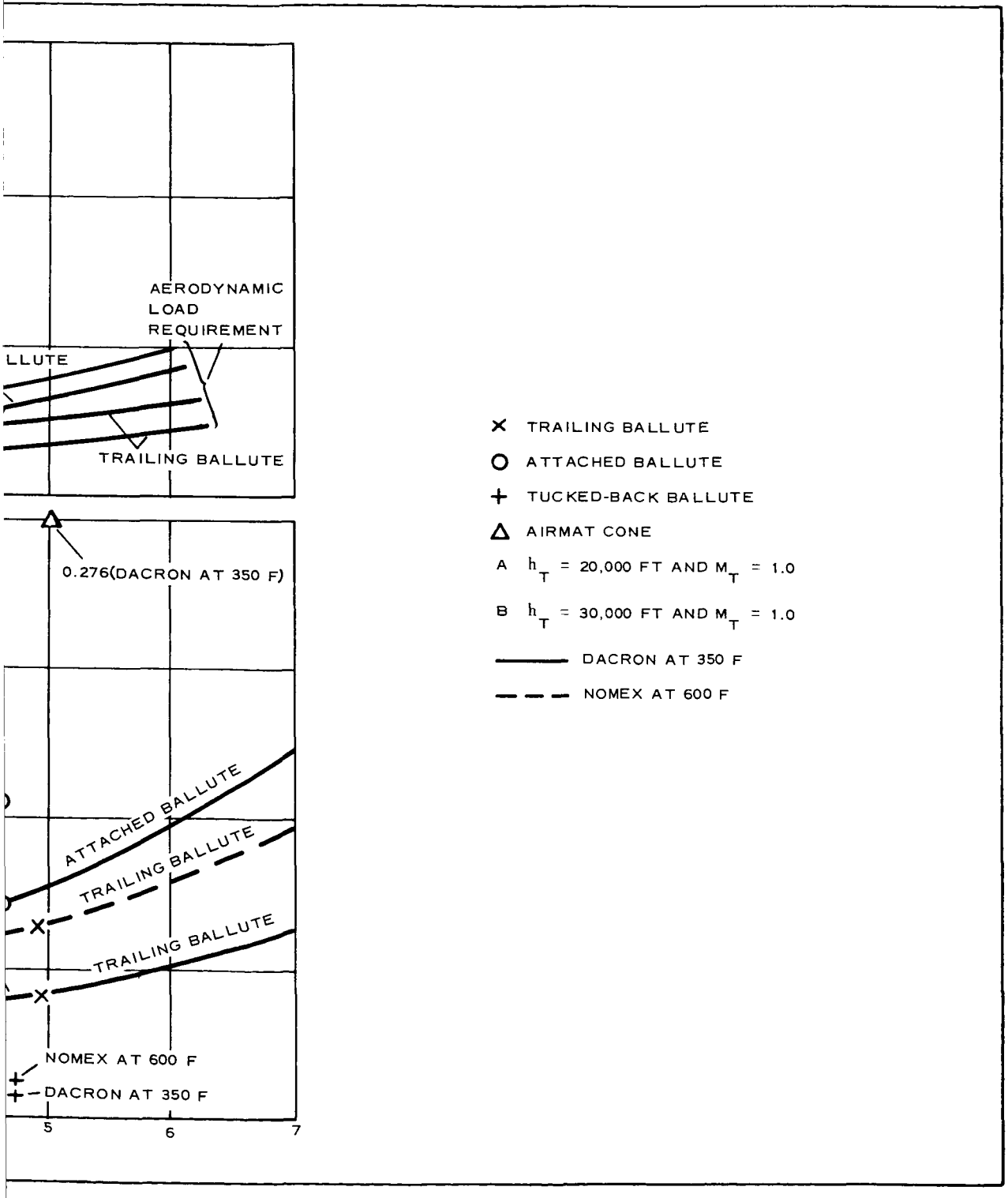

Figure 15 - Aerodynamic and Thermal Effects on Decelerator Envelope (Trajectories 19 and A1)

#2

Figures 16 through 19 present curves to establish a more refined estimate for the minimum required decelerator envelope unit weight that would be compatible with both the aerodynamic heating and aerodynamic loading environment for the several entry cases considered in this study (also see Section VI of Volume II). Each figure is associated with the decelerator configurations that provide deceleration of the basic entry capsule to $M_T = 1.0$ near the target altitude specified on the figures. In each figure is the callout "optimum Mach no.," which is associated with a minimum percentage of decelerator-to-total entry capsule weight.

On the ordinate in these figures is the callout "minimum practical weight", which is the minimum weight of the envelope for each of the decelerator types. The thermal requirement curves are limited to a maximum temperature of 450 F for dacron and 700 F for Nomex. The symbols for each decelerator located on the "optimum Mach no." line correspond to the envelope material thickness required to sustain the aerodynamic loading at the indicated temperature. The "minimum practical weight" includes provision for a coating of 0.01 lb/sq ft of Neoprene or Vitron to give the decelerator envelope a low value of porosity. For this study it is assumed that the coating has the same specific heat as the envelope material, which is a valid assumption (see Section III of Volume II).

The fabric weight per unit area is in reference to the thin envelope of the decelerator device. The proportion of decelerator envelope weight to total decelerator weight (see Appendix A of Volume II) is nominally 20 percent for the trailing BALLUTE, 38 percent for the attached BALLUTE, and 10 percent for the tucked-back BALLUTE. For the AIRMAT cone, the envelope comprises about 67 percent of the total expandable decelerator weight. Furthermore for the cases under study, the period of the significant heat pulse is of the order of 5 sec (see Section II of Volume II and Figures B-1 through B-6 in Appendix B). In this interval the speed of the entry capsule will have been reduced

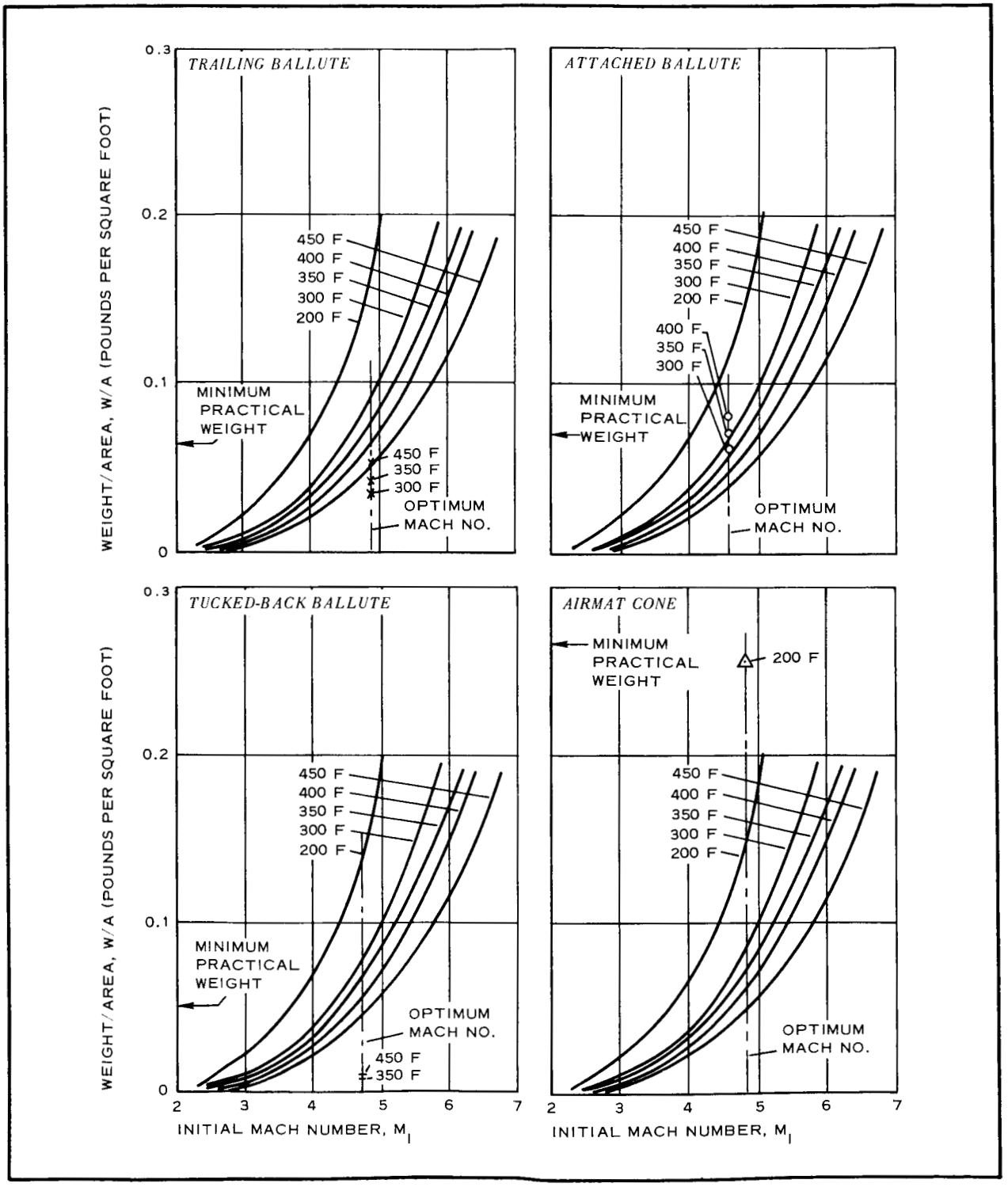

Figure 16 - Minimum Decelerator Envelope Unit Weight (Trajectory A1, h_T = 20,000 ft, Dacron)

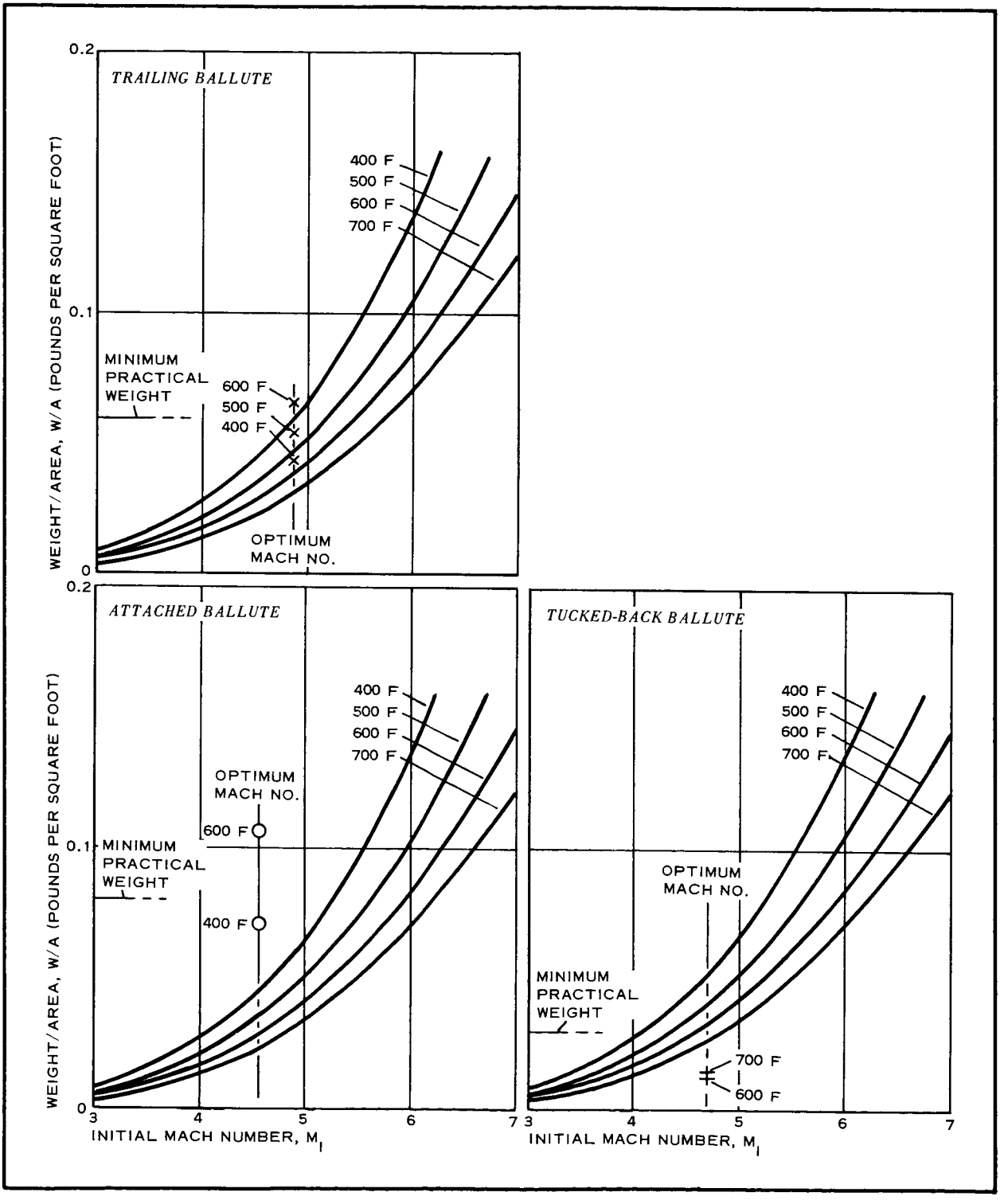

Figure 17 - Minimum Decelerator Envelope Unit Weight (Trajectory A1, h_T = 20,000 ft, Nomex)

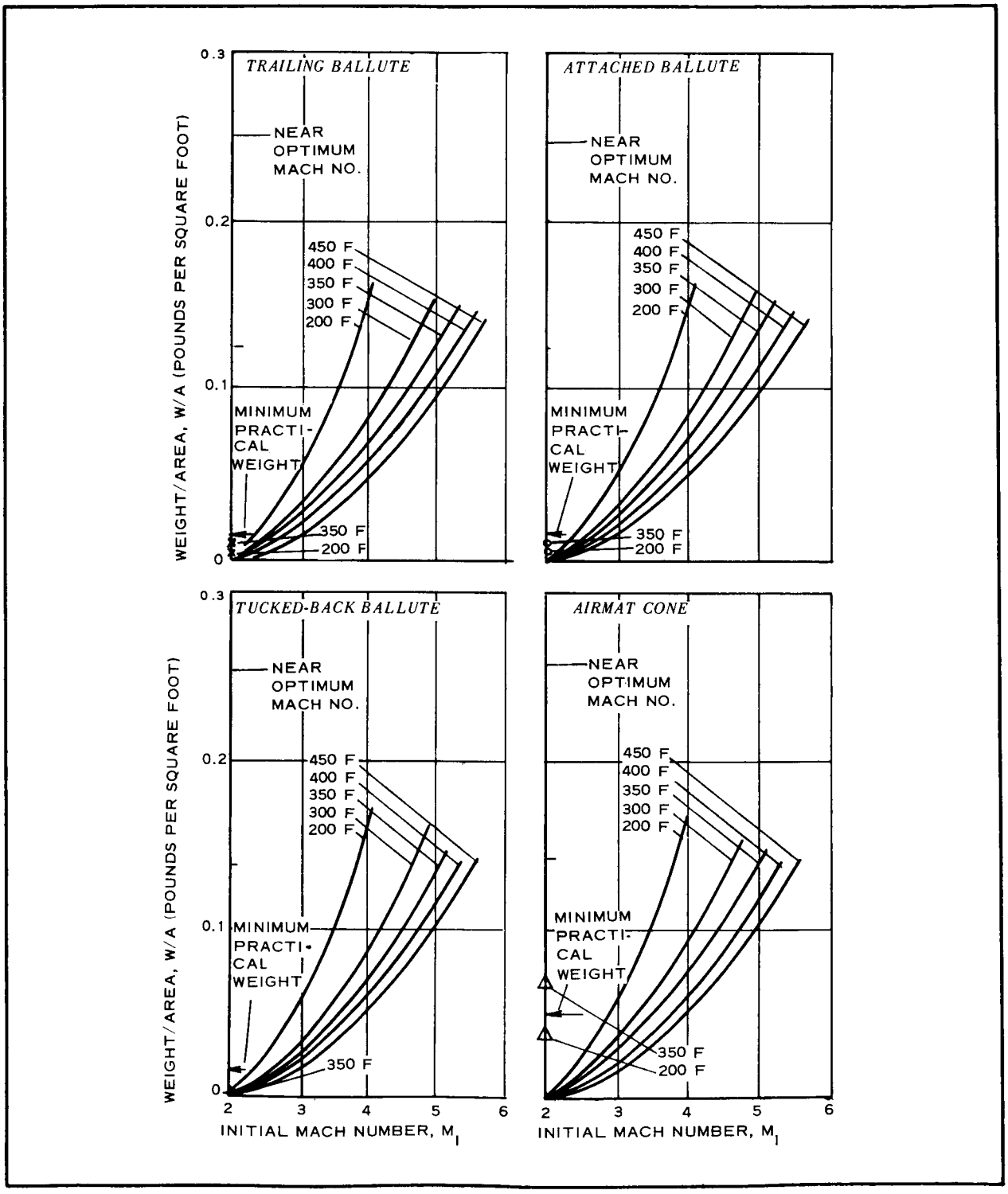

Figure 18 - Minimum Decelerator Envelope Unit Weight (Trajectory 19, h_T = 20,000 ft, Dacron)

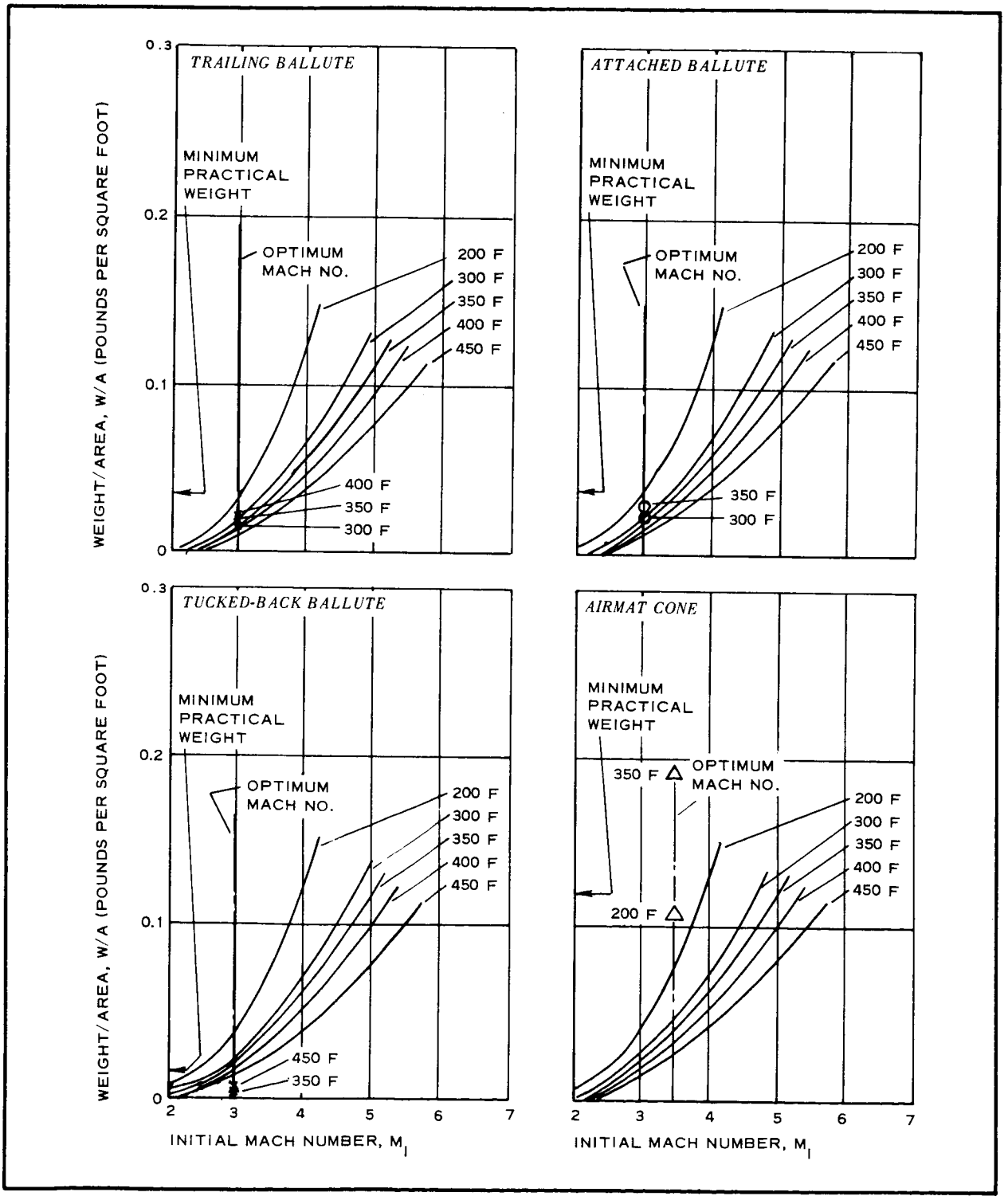

Figure 19 - Minimum Decelerator Envelope Unit Weight
(Trajectory 19, h_T = 30,000 ft, Dacron)

significantly and the corresponding aerodynamic loads will be smaller by the time the material reaches the assumed elevated operating temperatures used in this study (note Figures 16 through 19). Thus, it is indicated (see Item 11, Tables A-I through A-XI of Appendix A) that for the decelerator envelope with coating thickness based on acceptable leakage rate and heat insulation, reasonable decelerator weight fractions can be obtained.

5. EFFECT OF TARGET MACH NUMBER VARIATION

The determination of how the decelerator size and target altitude are affected by the target point Mach number as it varies from 0.7 to 1.5 is important as relating to size and performance operating tolerances. Figures 20 and 21 illustrate these effects for trajectory 19. Considering the effect on size (Figure 20), increasing the target Mach number to 1.4 reduces the required total system drag area by about 100 percent from the value required at Mach 1.0. At the Mach number 1.0 reference point (the zero value on the ordinate scale of Figure 20) for trajectory 19, the percentage of total system drag area to the entry capsule drag area is required to have a nominal value of about 500 percent to attain an M_T = 1.0 at 30,000 ft. If the M_T is increased to 1.4 at 30,000 ft, the percentage of decelerator drag area to the entry capsule drag area can be reduced to about 400 percent. In this case, this reduction is the same as decreasing the decelerator diameter by about 10 percent for an initial operating Mach number of 3.0. The trend is for a smaller reduction in size with higher initial operating Mach number.

On the other hand for a lower target Mach number of 0.7, a 10-percent increase in decelerator size is indicated. This increase is made while assuming a constant value of drag coefficient for the system, which is optimistic compared with the characteristic lower drag coefficient of bodies at subsonic velocities. At the subsonic target Mach numbers, the effect of the initial operating Mach number is nominal.

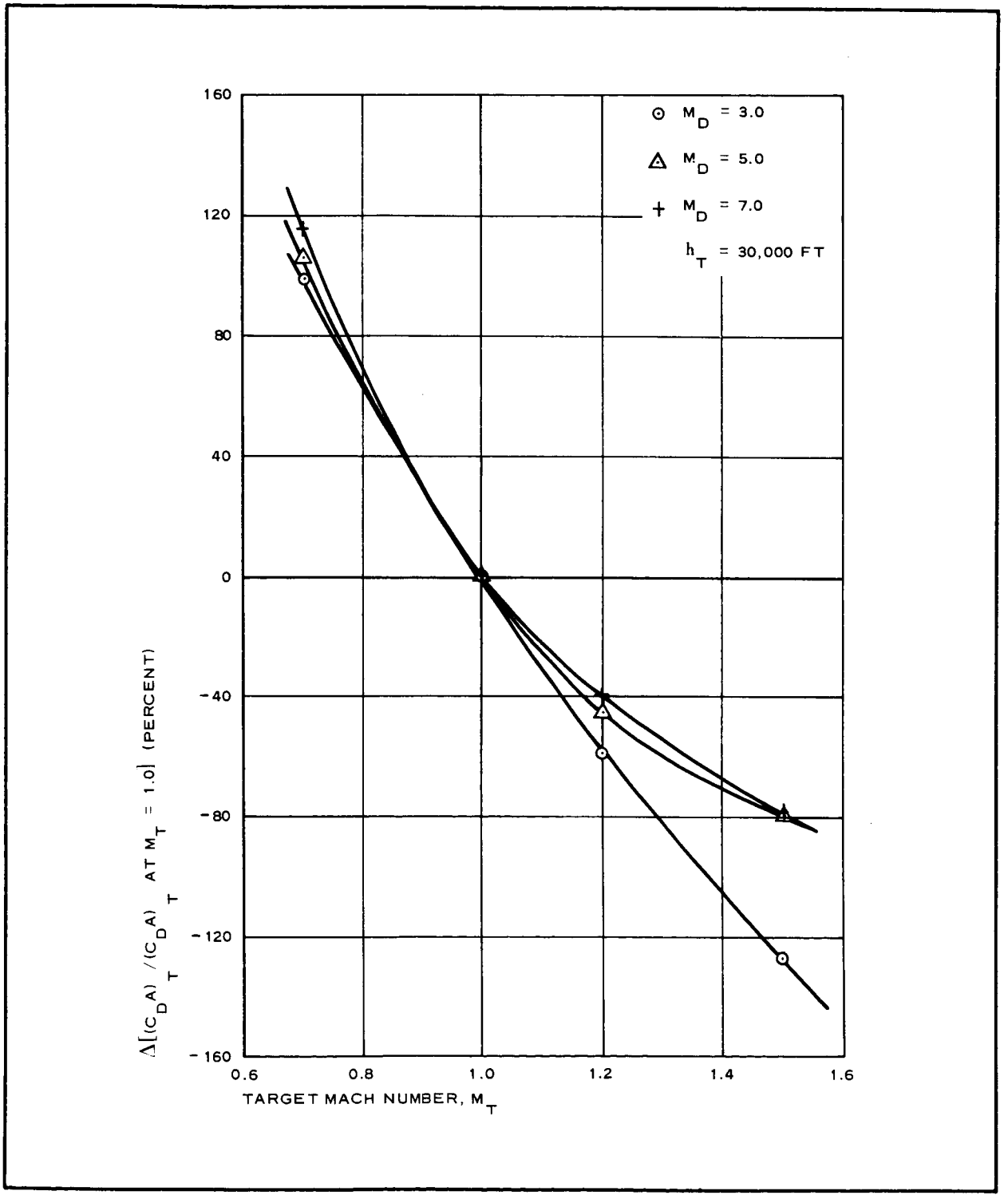

Figure 20 - Change in Percent Total Drag Area (Trajectory 19 and Atmosphere VM8)

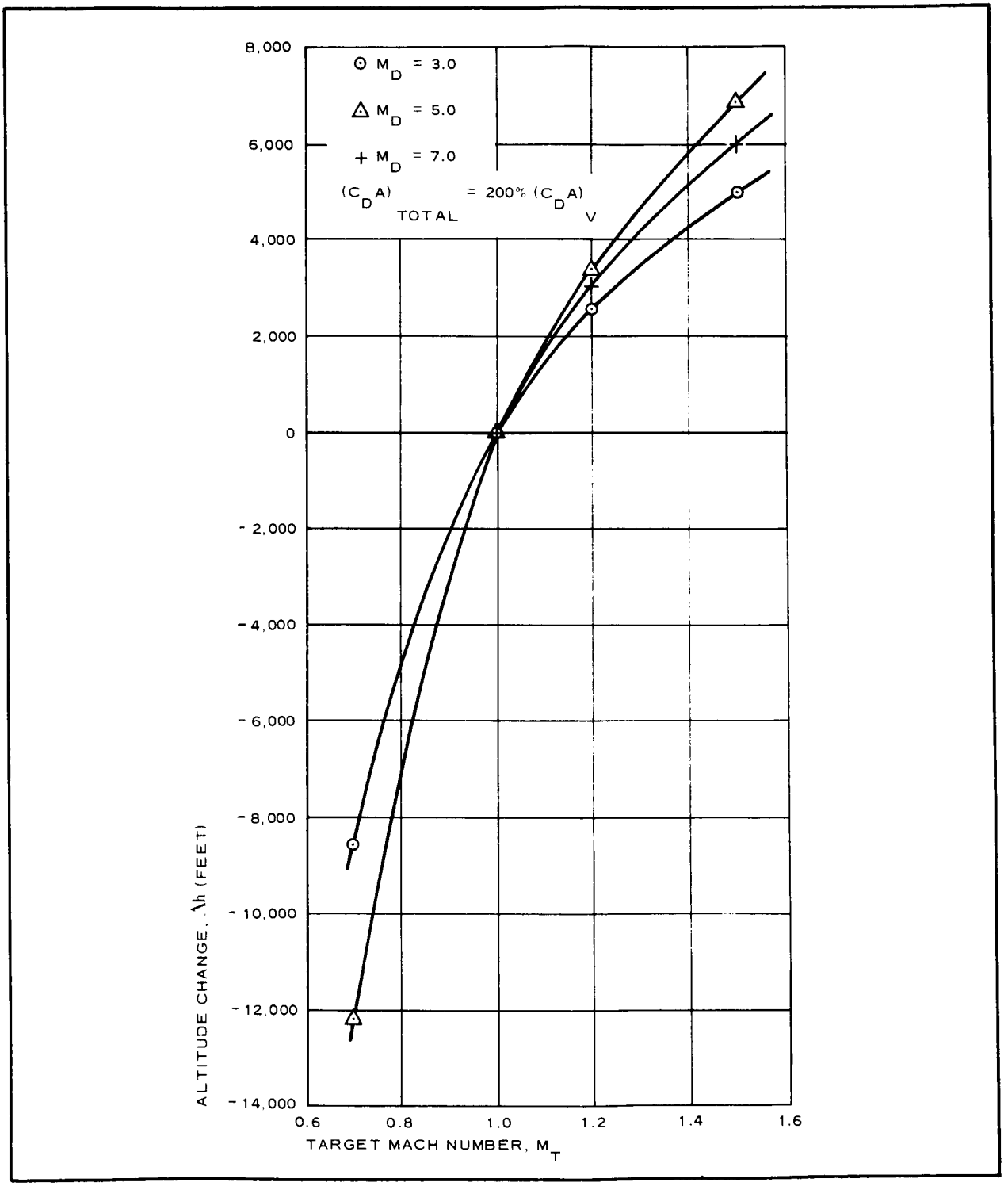

Figure 21 - Change in Altitude with Variation of Target Mach Number from 1.0 (Trajectory 19 and Atmosphere VM8)

The effect of target point Mach number variation on altitude shows that if the target Mach number is allowed to increase above 1.0, there is an incremental gain in target altitude. Conversely the target altitude decreases with decreasing values of target point Mach number.

A higher initial operating Mach number results in an additional gain in altitude primarily because the higher Mach number is also associated with a higher initial operating altitude (see Step 1 in Figure 10). For lower target Mach numbers a higher initial operating Mach number causes loss in altitude. This loss occurs because of the lower air density corresponding with the higher altitude at which the reference target Mach number of 1.0 is attained and because the required decelerator drag area corresponding with the higher initial operation Mach number also is smaller.

Figure 22 illustrates the trend of decelerator-to-total entry capsule weight as a function of target Mach number variation with target altitude as a parameter for trajectory 19. The intersection of the curves with the abscissa scale is the Mach number to which the entry capsule decelerates without an auxiliary decelerator. For trajectory 19 it is indicated that fairly low values of subsonic Mach number can be attained for decelerators weighing less than 10 percent of the total entry capsule weight. To achieve target Mach numbers of less than about 0.4 for trajectory 19, substantial weight penalties are incurred regardless of target altitude.

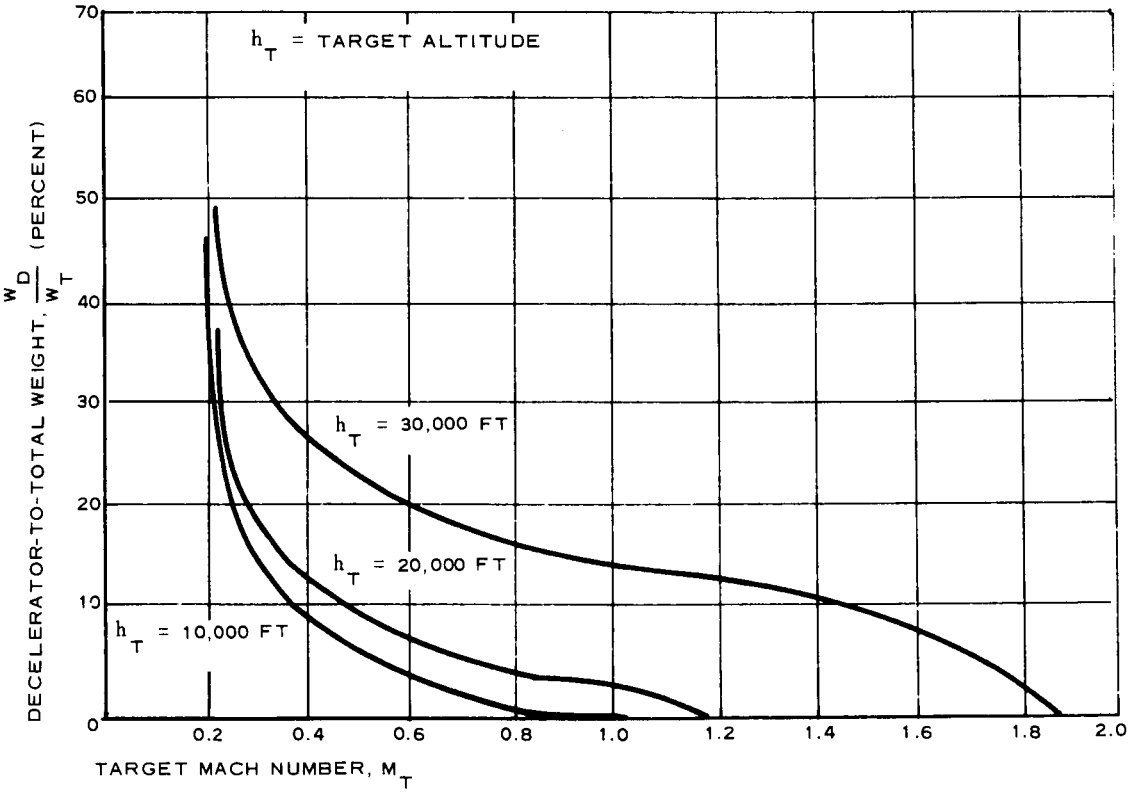

Figure 22 - Variation of Decelerator Weight with Target Mach Number (Trajectory 19 ; Attached BALLUTE)

SECTION V - SYSTEM COMPARISONS

1. BASIS FOR COMPARISON AND SELECTION

The comparison and subsequent selection of decelerator configurations and their suitable areas of application for final study and analysis were facilitated by a tabulation scheme. Thirty separate factors associated with each of the four decelerator configurations for the various entry cases under study were evaluated as shown in Tables A-I through A-XI in Appendix A. The tabulation includes those engineering design factors that establish realistic total decelerator system weight estimates and that were necessary for use with the dynamic computer analyses.

Seventeen cases were selected as indicated in Table III below, for refined point-mass trajectories that incorporated a transient, heating analysis program to determine more realistically the temperature to which the fabric of the decelerator envelope will be subjected. Figures B-1 through B-6 in Appendix B show the results of the refined point-mass trajectory computations and transient heating calculations.

TABLE III - CASES SELECTED FOR EXTENDED CONSIDERATION

JPL trajectory number	Target altitude (ft $\times 10^3$)	Decelerator		Configurations	
		TB	AB	TBB	AC
A1	20			X	X
B3	20		X	X	X
19	20	X	X	X	X
22	30	X	X	X	X
23	30		X	X	
30	20	X		X	

The selection of the entry cases in Table III for extended analyses was considered appropriate since these cases encompass the broad range of parameters associated with the study, including: (1) mass ballistic parameter, size, and weight of entry capsule, (2) initial trajectory conditions, (3) Mars atmosphere profiles, and (4) the four basic expandable decelerator configurations. Thus, a reasonable assessment of the effect these parameters have on the characteristics of expandable terminal decelerators could be made. Trajectories 19 and 22 were emphasized since all the decelerator configurations were evaluated for these two trajectories, including the dynamic stability analyses. These trajectories are considered the more appropriate for the early Mars lander missions and, as will be discussed, show that expandable terminal decelerators can provide desirable system performance with reasonable weights within current expandable decelerator technology.

The refined point-mass trajectory computations included provision for a linear increase in decelerator drag area from initiation of deployment to full inflation during an interval of 1.5 sec. The choice of this inflation interval and linear drag area variation was based on experience with ram-air inflated BALLUTEs for the Mach number and dynamic pressure range of current interest. This choice includes tradeoff considerations of a minimum desired time to achieve full-drag effectiveness and low opening shock and to avoid material fatigue failure as a result of flutter during the inflation interval.

With the ram-air-inflated configurations, the size and number of the inlets must provide the required mass flow into the decelerator envelope consistent with the decelerator internal volume and the inflation interval of 1.5 sec. For the 120-deg AIRMAT cone with an auxiliary gas inflation source, gas pressure, gas volume, valve sizes, and valve numbers also must be compatible with the inflation interval of 1.5 sec.

Layout drawings of selected decelerator/vehicle combinations for the

four decelerator configurations under study were made as shown in Figures 23 through 26. From these an assessment of the packaging, attachment, deployment requirements, and constraints was gained. Additionally realistic weight estimates for the ancillary equipment associated with these items were obtained as tabulated in these figures. Note that packaged volume requirements are not beyond the range of practical considerations (see Item 13 of Tables A-I through A-XI in Appendix A).

As illustrated in the layout drawings of Figures 23 through 26, Marmon clamps accomplish attachment and separation functions of the various decelerator devices and associated equipments. The Marmon clamp is significantly lighter and has less bulk with higher reliability and uniformity in accomplishing separation functions. Furthermore, this attachment method is suitable for all the decelerator concepts including the trailing decelerators. In this case the suspension lines between the capsule base and the confluence point of the riser are attached to the ring as illustrated in Figure 23. Additionally the assembly requirements are simple with a minimum of parts. All of these characteristics for this method of attachment further lend themselves to simplifying the sterilization of this assembly.

2. DYNAMIC ANALYSIS

Dynamic stability characteristics for each of the four decelerator configurations for the 19 and 22 trajectories were analyzed. In the case of attached decelerator configurations, a six-degree-of-freedom computer program was used (see Appendix B of Volume II) for the formulation of the dynamic stability analysis. For the trailing BALLUTE two additional degrees of freedom were included.

Figures 27 and 28 show the oscillation characteristics for each of the four basic decelerator configurations as applied to the 19 and 22 trajectories. In the case of the trailing decelerators, the effect of the kinematic coupling between rolling velocity and angle of attack caused

the capsule to continually diverge to large angles of attack and coning angles for both the 19 and 22 trajectories. The present description for the system dynamics with the trailing decelerator is not adequate and should be studied in greater detail in future programs. The larger amplitude of oscillation for the 22 trajectory is caused by the reduced damping moments in the lower density of the VM7 atmosphere as compared with the VM8 atmosphere.

The drag force and moment of the trailing decelerator has the natural effect of providing stabilization for the composite capsule/decelerator system. However, because of kinematic (roll-yaw) coupling effects there is considerable divergence in angle of attack of the composite system. For the attached decelerator there was no divergence caused by the kinematic coupling effect. There is a nominal reduction in the rolling velocity of the entry capsule when the decelerators are deployed since the moment of inertia in roll has been increased. The composite system rolling velocity is reduced a small amount since conservation of the rolling angular momentum is preserved prior to and immediately after decelerator device deployment.

It should be recognized that the values used for the pitch and yaw damping factor ($C_{m_q} + C_{m_{\dot{\alpha}}}$) in the dynamic analyses may be questionable for the attached decelerator configurations (see Item 28 in Tables A-I through A-XI of Appendix A and Section I of Volume II). In view of the paucity of data relating to this factor for the configurations under study, this term was evaluated using Figure 10 in Section I of Volume II (referenced to the parameter of qD_o/v) to account for the composite capsule/decelerator cg position. The term then was doubled to account for Mach number effect (for the range of Mach numbers of interest, $M \approx 2$ to 5). This approach was predicated on the trend of data and theory for ($C_{m_q} + C_{m_{\dot{\alpha}}}$) versus Mach number for conical configurations as shown by Figure 14 in Section I of Volume II.

BASIC BALLUTE PACKAGE INFORMATION FOR SEVERA

JPL TRAJECTORY NO.	D_v (FT)	D_B (FT)	$(C_DA)_v$ (SQ FT)	$(C_DA)_T$ (SQ FT)	q_D (LB/SQ FT)	DESIGN DRAG LOAD (LB)	ATTACHMEN AND RELEAS DEVICE (LB)
B3	12.0	23.7	158.0	536	20.3	15,320	13.2
37	16.0	25.4	281.5	690	112.5	91,700	47.7
A1	18.5	30.7	376.0	961	76.5	89,500	54.8
19	16.0	23.0	281.5	749	9.9	9,260	4.8
A4	18.5	21.1	376.0	692	26.2	16,600	10.1
B1	12.0	17.5	158.0	359	25.4	10,200	8.8
22	16.0	19.95	281.5	632	10.4	7,300	3.8

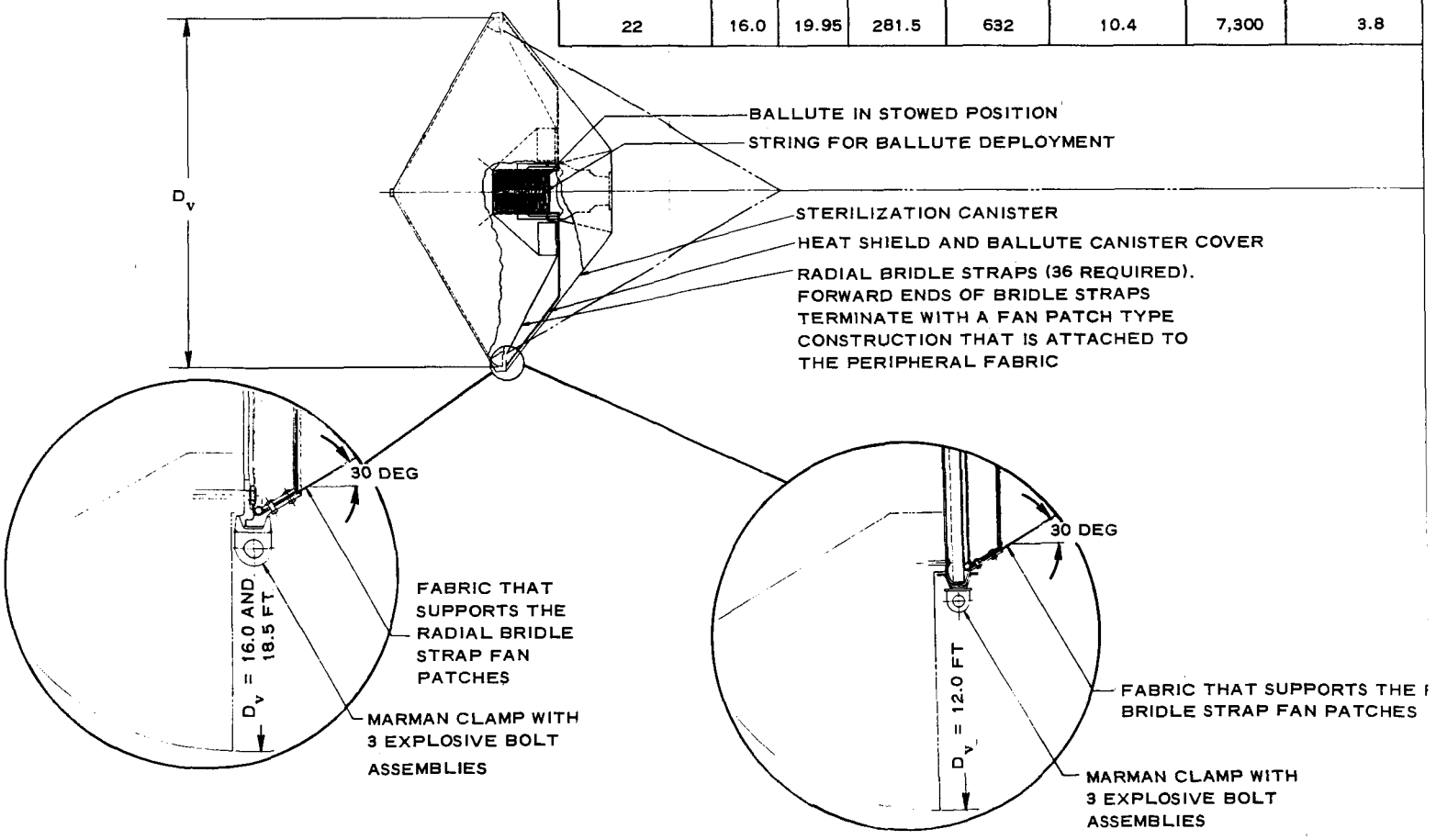

AL CAPSULE DIAMETERS (D_v)

IT SE	AUXILIARY EQUIPMENT FOR STOWING (LB)	BALLUTE CANISTER AND HEAT SHIELD (LB)	BALLUTE DACRON FABRIC (LB)	TOTAL PACKAGE CONCEPT (LB)
	12.9	60	129.3	215.4
	106.1	80	1061.0	1294.8
	108.3	110	1083.0	1356.1
	5.6	80	56.1	146.5
	18.6	110	185.9	324.6
	13.3	60	132.9	215.0
	7.4	80	74.3	165.5

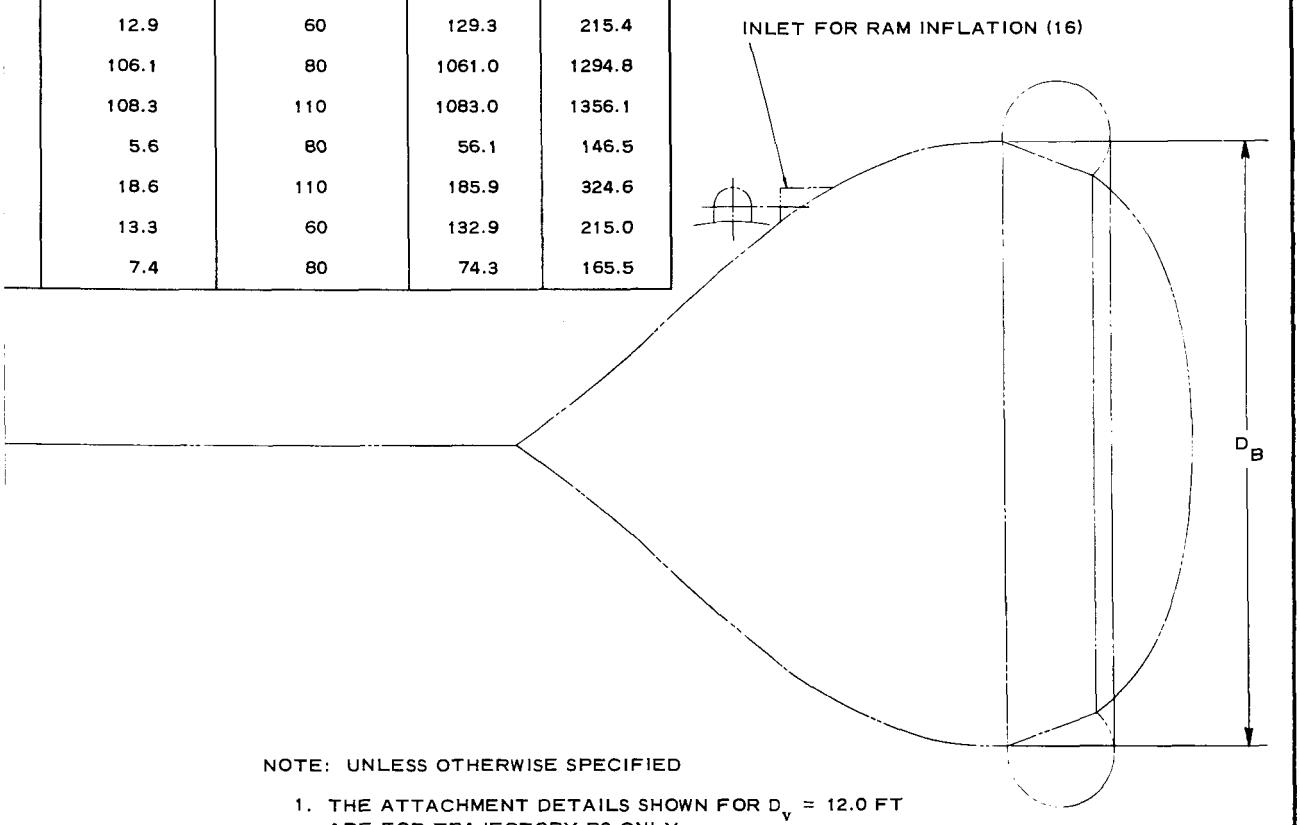

NOTE: UNLESS OTHERWISE SPECIFIED

1. THE ATTACHMENT DETAILS SHOWN FOR D_v = 12.0 FT ARE FOR TRAJECTORY B3 ONLY
2. THE ATTACHMENT DETAILS SHOWN FOR D_v = 16.0 FT ARE FOR TRAJECTORY 37 ONLY
3. THE ATTACHMENT DETAILS SHOWN FOR D_v = 18.5 FT ARE FOR TRAJECTORY A1 ONLY
4. THE ATTACHMENT DETAILS ARE BASED ON THE USE OF 7075-T6 ALUMINUM UNDER LOAD AT 350 F WITH THE FOLLOWING VALUES:

   F_{t_y} = 0.62 × 67,000 = 41,500 LB/SQ IN.

   F_{br_y} = 0.67 × 94,000 = 63,000 LB/SQ IN.

   F_{s_u} = 0.74 × 46,000 = 34,000 LB/SQ IN.

RADIAL

Figure 23 - Trailing BALLUTE

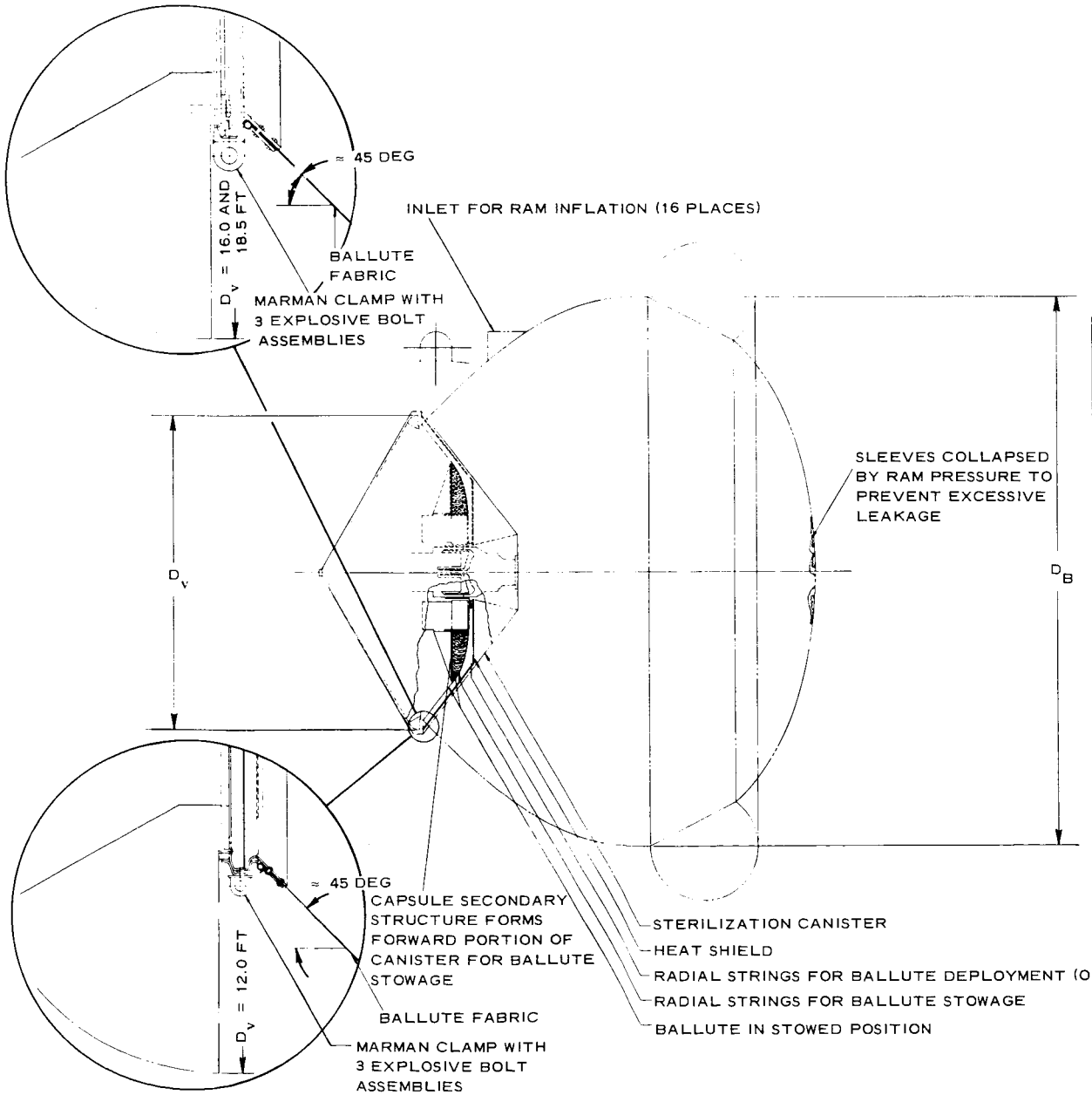

JPL TRAJECTORY NO.	D_v (FT)	D_B (F
B3	12.0	22
37	16.0	28
A1	18.5	31
19	16.0	27
A4	18.5	28
B1	12.0	18
22	16.0	24

BASIC BALLUTE PACKAGE INFORMATION FOR SEVERAL CAPSULE DIAMETERS (D_v)

T)	$(C_DA)_v$ (SQ FT)	$(C_DA)_T$ (SQ FT)	q_D (LB/SQ FT)	DESIGN DRAG LOAD (LB)	ATTACHMENT AND RELEASE DEVICE (LB)	AUXILIARY EQUIPMENT FOR STOWING (LB)	BALLUTE CANISTER AND HEAT SHIELD (LB)	BALLUTE DACRON FABRIC (LB)	TOTAL PACKAGE CONCEPT (LB)
.9	158.0	536	20.3	15,330	13.9	10.1	60	100.7	184.7
.0	281.5	796	88.0	90,500	56.9	63.1	80	631.0	831.0
.7	376.0	1023	68.8	89,400	65.6	68.6	110	686.0	930.2
.1	281.5	750	9.9	9,260	5.8	6.2	80	61.9	153.9
.6	376.0	842	16.0	14,900	10.9	18.4	110	183.5	322.8
.9	158.0	359	25.4	10,200	9.2	11.6	60	116.3	197.1
.9	281.5	633	10.4	7,310	4.6	7.7	80	77.0	169.3

NOTE: UNLESS OTHERWISE SPECIFIED

1. THE ATTACHMENT DETAILS SHOWN FOR D_v = 12.0 FT ARE FOR TRAJECTORY B3 ONLY
2. THE ATTACHMENT DETAILS SHOWN FOR D_v = 16.0 FT ARE FOR TRAJECTORY 37 ONLY
3. THE ATTACHMENT DETAILS SHOWN FOR D_v = 18.5 FT ARE FOR TRAJECTORY A1 ONLY
4. THE ATTACHMENT DETAILS ARE BASED ON THE USE OF 7075-T6 ALUMINUM UNDER LOAD AT 350 F WITH THE FOLLOWING VALUES:

   F_{t_y} = 0.62 × 67,000 = 41,500 LB/SQ IN.

   F_{br_y} = 0.67 × 94,000 = 63,000 LB/SQ IN.

   F_{s_u} = 0.74 × 46,000 = 34,000 LB/SQ IN.

RAP)

Figure 24 - Attached BALLUTE

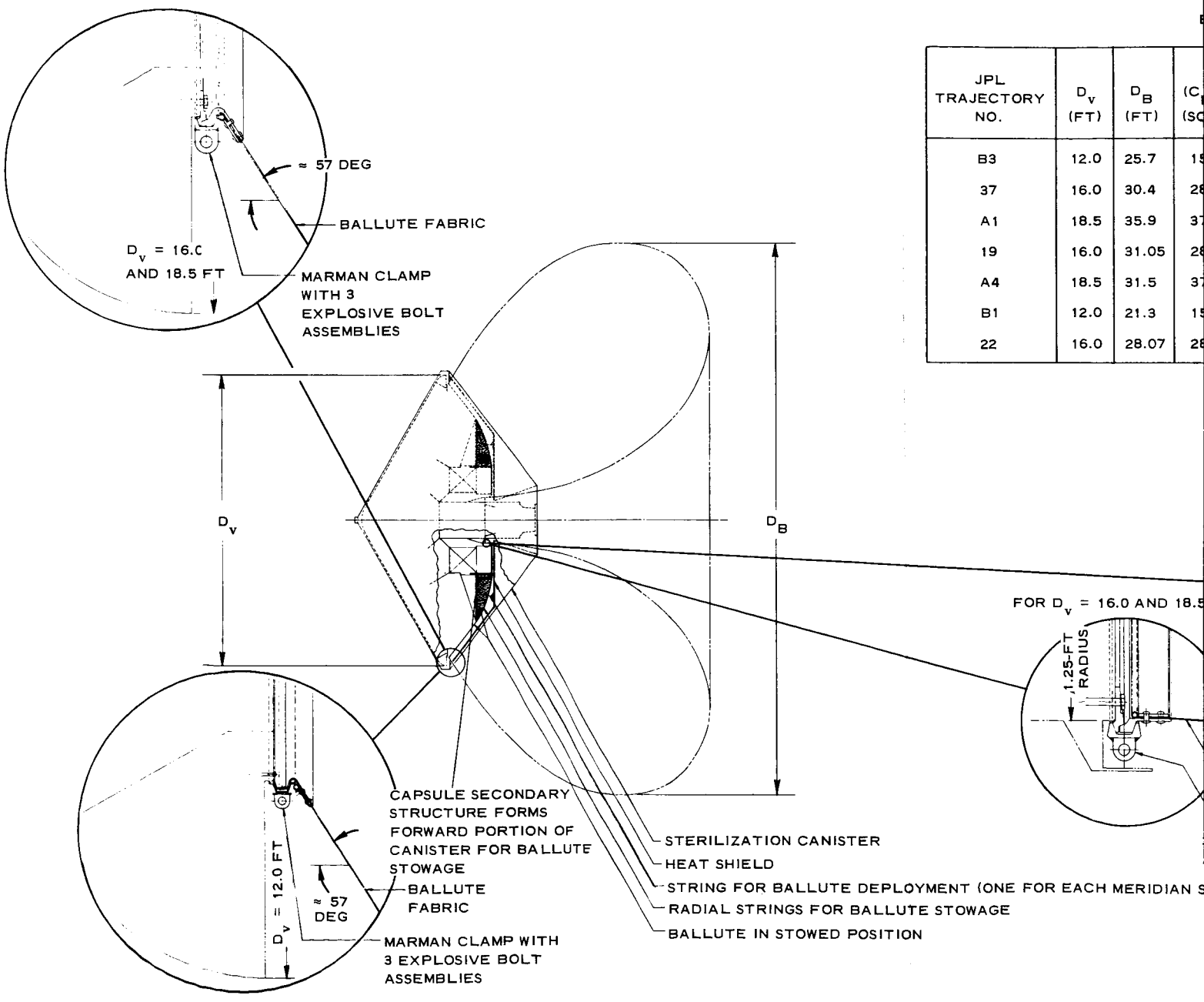

JPL TRAJECTORY NO.	D_v (FT)	D_B (FT)	($C_$ (SC
B3	12.0	25.7	1
37	16.0	30.4	2
A1	18.5	35.9	3
19	16.0	31.05	2
A4	18.5	31.5	3
B1	12.0	21.3	1
22	16.0	28.07	2

55-1

55-2

BASIC BALLUTE PACKAGE INFORMATION FOR SEVERAL CAPSULE DIAMETERS (D_v)

$(C_DA)_v$ FT)	$(C_DA)_T$ (SQ FT)	q_D (LB/SQ FT)	DESIGN DRAG LOAD (LB)	ATTACHMENT AND RELEASE DEVICE (LB)	AUXILIARY EQUIPMENT FOR STOWING (LB)	BALLUTE CANISTER AND HEAT SHEILD (LB)	BALLUTE DACRON FABRIC (LB)	TOTAL PACKAGE CONCEPT (LB)
58.0	536	20.3	15,400	13.4	4.3	60	42.6	120.3
31.5	735	103.0	93,300	51.8	35.1	80	351.0	517.9
76.0	1005	72.15	90,900	57.7	36.3	110	363.0	567.0
31.5	749	9.9	9,260	5.1	2.9	80	29.4	117.4
76.0	800	17.5	14,820	9.4	6.6	110	65.6	191.6
58.0	359	25.4	10,200	8.9	5.9	60	58.8	133.6
31.5	633	10.4	7,310	4.1	3.7	80	36.9	124.7

NOTE: UNLESS OTHERWISE SPECIFIED

1. THE ATTACHMENT DETAILS SHOWN FOR D_v = 12.0 FT ARE FOR TRAJECTORY B3 ONLY
2. THE ATTACHMENT DETAILS SHOWN FOR D_v = 16.0 FT ARE FOR TRAJECTORY 37 ONLY
3. THE ATTACHMENT DETAILS SHOWN FOR D_v = 18.5 FT ARE FOR TRAJECTORY A1 ONLY
4. THE ATTACHMENT DETAILS ARE BASED ON THE USE OF 7075-T6 ALUMINUM UNDER LOAD AT 350 F WITH THE FOLLOWING VALUES:

   F_{t_y} = 0.62 × 67,000 = 41,500 LB/SQ IN.

   F_{br_y} = 0.67 × 94,000 = 63,000 LB/SQ IN.

   F_{s_u} = 0.74 × 46,000 = 34,000 LB/SQ IN.

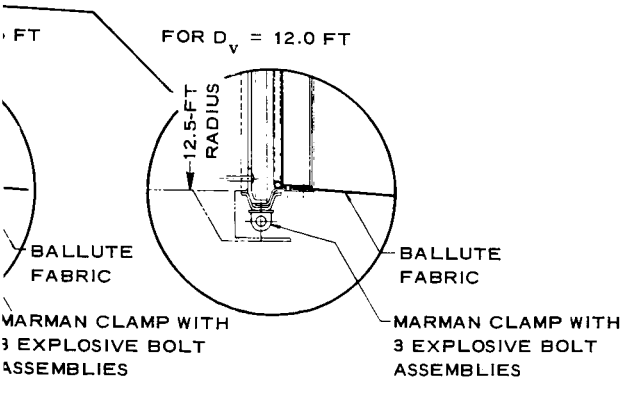

Figure 25 - Tucked-Back BALLUTE

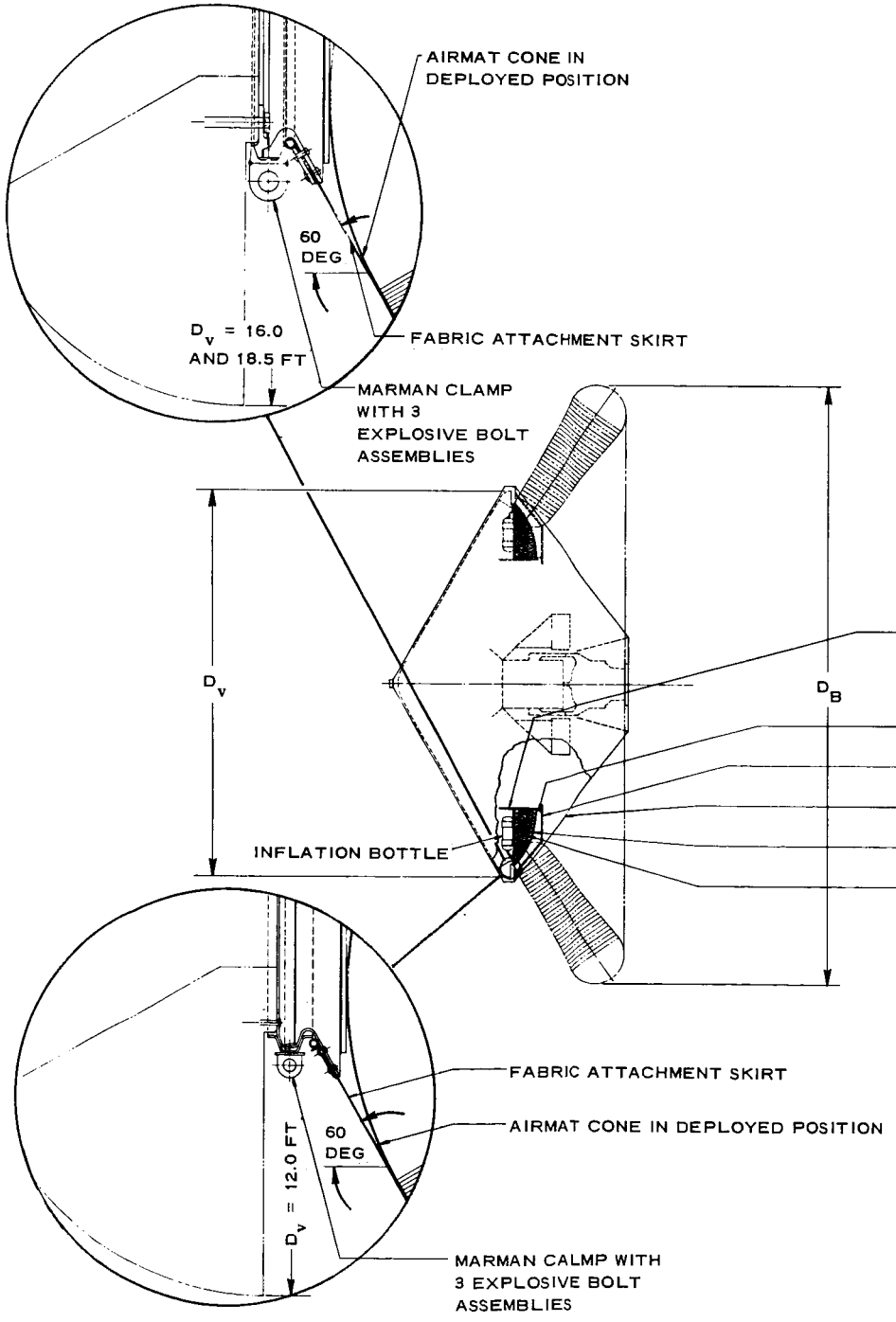

BASIC ATTACHED 12

JPL TRAJECTORY NO.	D_v (FT)	D_B (FT)	$(C_DA)_v$ (SQ FT)	$(C_D$ (SQ
B3	12.0	21.9	158.0	5
37	16.0	24.8	281.5	6
A1	18.5	29.5	376.0	9
19	16.0	25.8	281.5	7
A4	18.5	24.8	376.0	6
B1	12.0	18.2	158.0	3
22	16.0	23.7	281.5	6

0-DEG AIRMAT CONE PACKAGE INFORMATION FOR SEVERAL CAPSULE DIAMETERS (D_v)

$(A)_T$ FT)	q_D (LB/SQ FT)	DESIGN DRAG LOAD (LB)	ATTACHMENT AND RELEASE DEVICE (LB)	AUXILIARY EQUIPMENT FOR STOWING (LB)	AIRMAT CONE CANISTER AND HEAT SHIELD (LB)	AIRMAT CONE DACRON FABRIC (LB)	TOTAL PACKAGE CONCEPT (LB)
36	20.3	15,330	14.4	7.2	60	71.8	153.4
88	112.5	91,500	58.4	77.6	80	776.0	992.0
85	75.4	92,100	67.3	42.8	110	428.0	648.1
49	9.9	9,260	5.9	5.4	80	53.8	145.1
94	23.2	14,800	10.8	15.1	110	151.0	286.9
70	22.93	9,740	9.1	5.9	60	58.7	133.7
33	10.4	7,310	4.7	3.9	80	39.4	128.0

RTS

IE (36)

NOTE: UNLESS OTHERWISE SPECIFIED

1. THE ATTACHMENT DETAILS SHOWN FOR D_v = 12.0 FT ARE FOR TRAJECTORY B3 ONLY
2. THE ATTACHMENT DETAILS SHOWN FOR D_v = 16.0 FT ARE FOR TRAJECTORY 37 ONLY
3. THE ATTACHMENT DETAILS SHOWN FOR D_v = 18.5 FT ARE FOR TRAJECTORY A1 ONLY
4. THE ATTACHMENT DETAILS ARE BASED ON THE USE OF 7075-T6 ALUMINUM UNDER LOAD AT 350 F WITH THE FOLLOWING VALUES:
   F_{t_y} = 0.62 × 67,000 = 41,500 LB/SQ IN.
   F_{br_y} = 0.67 × 94,000 = 63,000 LB/SQ IN.
   F_{s_u} = 0.74 × 46,000 = 34,000 LB/SQ IN.

Figure 26 - AIRMAT Cone

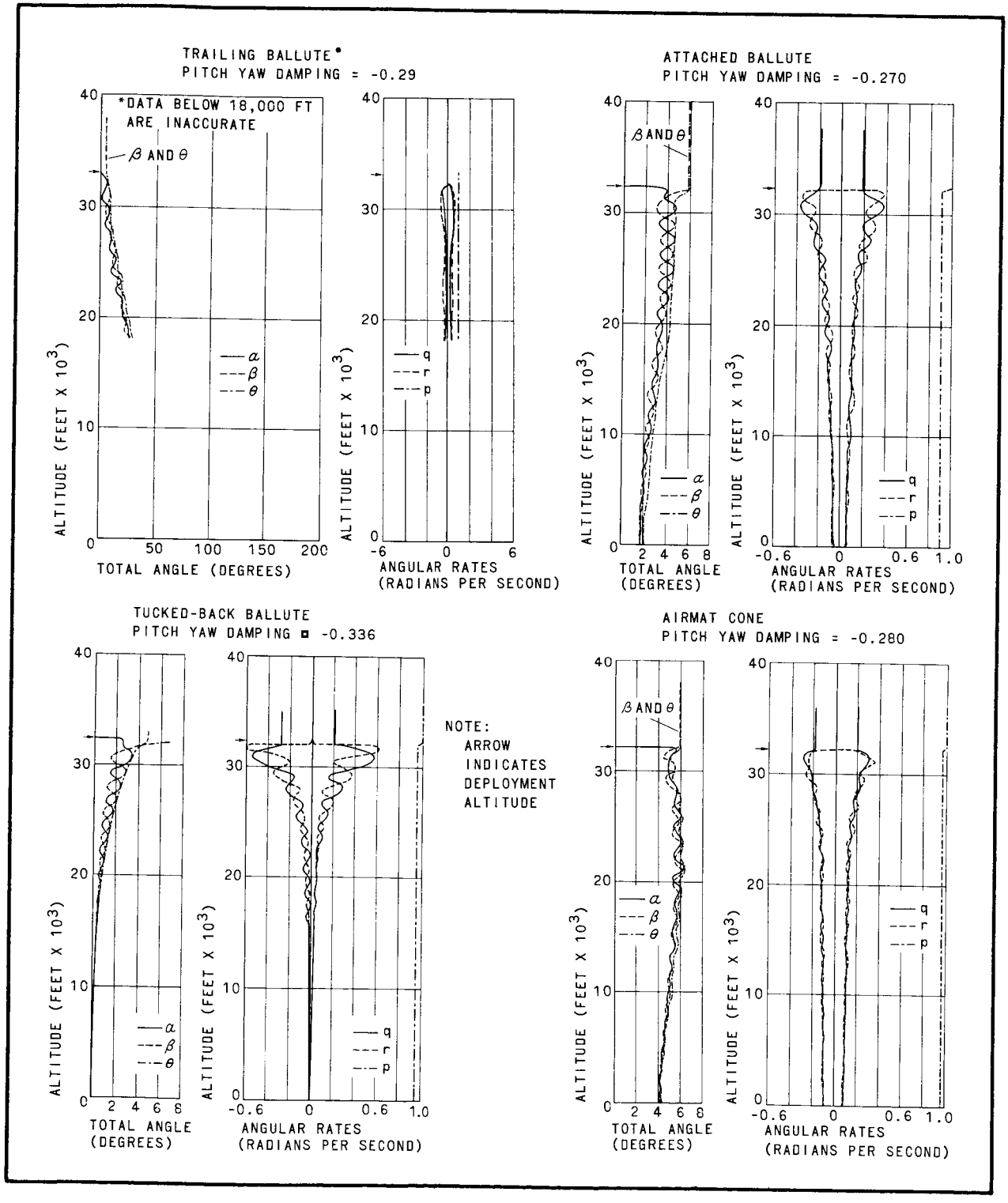

Figure 27 - Decelerator Oscillation Characteristics (Atmosphere VM8; Trajectory 19)

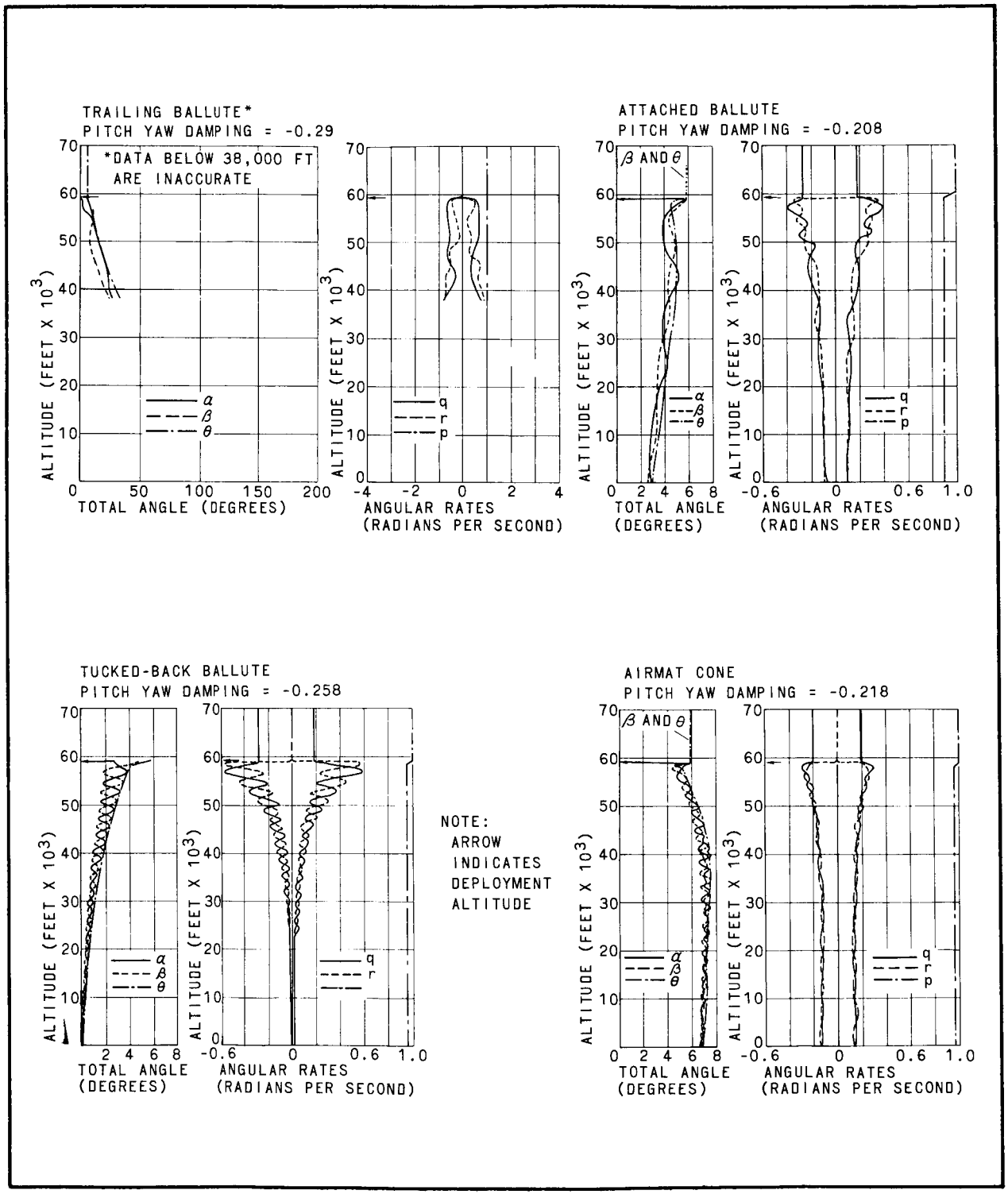

Figure 28 - Decelerator Oscillation Characteristics (Atmosphere VM7; Trajectory 22)

3. COMPARISONS OF COMPOSITE SYSTEMS

a. General

The final comparison of the expandable decelerator characteristics was made primarily in terms of engineering design considerations. In other words since all the configurations initially were "sized" to attain specified target Mach number/altitude conditions (see Appendix B), the comparison was made on the basis of the 17 characteristics in Table IV. Table IV shows the results of this comparison. Dacron was used for the envelope fabric of all the decelerators. The results for the various characteristics in Table IV are discussed below.

b. Items 1 and 2 - Decelerator Diameter and Altitude at Mach Number 1

The decelerator diameter was determined by the first approximation analysis procedure described in Section V of Volume II and illustrated in Figure 10 of this volume. The numerical values of decelerator size were selected as corresponding with or tending toward the minimum weight fraction for the decelerator device that would achieve a target point Mach number of about one near a target altitude of 20,000 ft for the A1, B3 and 19 entry cases and a target altitude near 30,000 ft for the 22 entry case. The values were obtained from Figures 67, 68, 69, 70, 73, 74, 87 and 88 in Section VI of Volume II. Note that the decelerator sizes for the 23 and 30 trajectories are the identical designs for the 22 and 19 trajectories, respectively. The purpose was to assess the effect of atmosphere variation on system performance and engineering design considerations.

Also note that the decelerator sizes established on the basis of the first approximation analysis procedure was reasonably accurate for the A1 and B3 entry cases to achieve a target Mach number of about one near 20,000 ft.

For the 19 trajectory with a target altitude near 20,000 ft and 22

TABLE IV - COMPARISON OF DECELERATOR SYSTEMS

No.	Characteristic	Dimension	Trajectory A1		Trajectory B3			Trajectory 19				Trajectory 22				Trajectory 23		Trajectory 30	
			TBB*	AC+	AB‡	TBB	AC	TB§	AB	TBB	AC	TB	AB	TBB	AC	AB	TBB	TB	TBB
1	Decelerator diameter	Ft	35.9	29.5	22.9	25.7	21.9	23	27.1	31.1	25.8	19.95	24.9	28.1	23.7	24.9	28.1	23	31.1
2	Altitude at Mach 1	Ft × 10^3	22.9	23	19.8	19.6	19.7	25.4	27.5	27.5	27.5	44.5	49	49	49	86.7	86.7	43.8	44.8
3	Decelerator weight including porosity coating)	Lb	363	428	100.7	42.6	71.8	56.1	61.9	29.4	53.8	74.3	77	36.9	39.4	77	36.9	56.1	29.4
4	Design envelope unit weight	Lb/sq ft	0.05	0.266	0.03	0.015	0.075	0.015	0.016	0.012	0.049	0.02	0.019	0.013	0.046	0.019	0.013	0.015	0.012
5	Design envelope temperature	Deg F	420	150	240	310	150	< 100	< 100	< 100	< 100	250	260	350	100	260	350	< 100	< 100
6	Actual maximum envelope temperature	Deg F	449	153	97	126	81	70	70	70	70	174	147	182	102	104	119	70	70
7	Auxiliary gas inflation system weight	Lb	25.4	40	13.7	7.1	7.0	11	13.7	8.7	6.0	3.9	7.2	4.4	8.0	7.2	4.4	11	8.7
8	Ancillary equipment weight (includes attachment and heat shield	Lb	204	220 1	84.0	77.7	81.6	90.4	92	88	91.3	91.2	92.3	87.8	88.6	92.3	87.8	90.4	88
9	Attachment design safety factor	. . .	2.4	2.6	1.7	1.7	1.6	2.4	1.7	1.4	1.4	2.3	1.2	1.2	1.25	0.6	0.6	1.6	0.96
10	Packaged volume of decelerator at 30 lb/cu ft	Cu ft	13	14.3	3.35	1.42	2.4	1.87	2.06	1.0	1.79	2.48	2.56	1.23	1.31	2.56	1.23	1.87	1.0
11	Velocity at 5000 ft	Ft/sec	297	319	392	385	399	418	342	329	349	615	492	479	503	460	448	513	421
12	Flight path angle at 5000 ft	Deg	-82	-80	-68	-69	-68	-74	-81	-82	-81	-72	-80.4	-81	-80	-90	-90	-85	-89
13	Oscillation amplitude near 5000 ft																		
	θ - Coning	Deg	. . .	. . .	. . .	. . .	. . .	. . .	2.15	0.09	4.42	. . .	3.09	0.18	6.83	. . .	. . .	. . .	. . .
	β - yaw	Deg	. . .	. . .	. . .	. . .	. . .	. . .	-0.27	0.08	-0.56	. . .	1.05	0.15	6.82	. . .	. . .	. . .	. . .
	α - angle of attack	Deg	. . .	. . .	. . .	. . .	. . .	. . .	2.14	-0.05	-4.39	. . .	-2.9	0.10	0.29	. . .	. . .	. . .	. . .
14	Oscillation rate near 5000 ft																		
	p - roll rate	Rad/sec	. . .	. . .	. . .	. . .	. . .	. . .	0.90	0.955	0.96	. . .	0.9	0.955	0.96	. . .	. . .	. . .	. . .
	q - pitch rate	Rad/sec	. . .	. . .	. . .	. . .	. . .	. . .	0.0008	-0.004	0.011	. . .	-0.02	-0.0015	-0.13	. . .	. . .	. . .	. . .
	r - yaw rate	Rad/sec	. . .	. . .	. . .	. . .	. . .	. . .	-0.06	0.007	0.098	. . .	0.08	0.0003	-0.0004	. . .	. . .	. . .	. . .
15	g's at full inflation	Earth g	21.4	21	4.9	4.9	5	2.5	3.1	3.5	3.4	2.3	3.3	3.3	3.2	6.8	6.7	3.8	5.1
16	Total decelerator system weight	Lb	592.4	688.1	198.4	127.4	160.4	157.5	167.6	126.1	151.5	169.4	176.5	129.1	136	176.5	129.1	157.5	126.1
17	Decelerator-to-total entry weight	Percent	19.6	22.75	7.82	5.01	6.32	5.75	6.11	4.6	5.56	6.18	6.44	4.71	5	6.44	4.71	5.75	4.6

*TBB Tucked-back BALLUTE

+AC AIRMAT cone

‡AB Attached BALLUTE

§TB Trailing BALLUTE

trajectory with a target altitude of 30,000 ft, the procedure was conservative. Consequently it can be expected that slightly smaller decelerator sizes could be employed to achieve the specified target conditions for these entry cases with a small amount of weight saving.

c. Items 3 and 4 - Decelerator Weight and Envelope Weight

As discussed in Section III, Item 1 useful integrated tradeoffs can be made between decelerator and total weight in terms of Mach number and altitude at deployment, decelerator size, performance effectiveness, and material characteristics. The formulation of the tradeoffs for the specific decelerators is established in Appendix A of Volume II.

Note that the weight/strength analysis of Appendix A, Volume II assumes that the decelerator materials were operating at a static elevated design temperature. In the case of dacron this temperature level was taken as 350 F where the strength is nominally one half the value compared to room temperature or about 70 F. Additionally, a design safety factor of 2.0 is reflected in the weight/strength analysis. A half-strength operating level with corresponding temperature is considered as a practical design point for inflatable structures fabricated of flexible materials.

On the basis of the above considerations, a first approximation weight was established for the decelerator sizes corresponding with Item 1 of Table IV (see Item 6 of Tables A-I through A-XI in Appendix A). Using these values, the proportion of weight allocated to the decelerator envelope was determined. Then using the thermal analysis procedures of Section IV of Volume II, a second approximation was made to secure a more likely value for the operating temperature (Item 5) and unit weight of the decelerator envelope (Item 4). The values determined are shown in Figures 46 through 50 of Volume II and Item 9 of Tables A-I through A-XI of Appendix A. Note that for all cases the decelerator envelope weight includes a unit coating weight of at least 0.01 lb/sq ft to provide a

low value of porosity for the envelope . The coating limits the internal pressurized gas leakage to no greater than 0.02 lb/sq ft/sec.

In reiteration the strength and therefore the weight of the meridian cables for all the decelerators and the riser line of the trailing BALLUTE is based on the half strength of dacron material with a design safety factor of 2.0. The weights for Item 3 in this Table are based on the above considerations.

d. Items 5 and 6 - Design and Actual Maximum Decelerator Envelope Temperature

In comparing Items 5 and 6, note that the second approximation for the assumed operating temperature for the dacron decelerator envelope was quite accurate for the A1 and 19 trajectories and for the AIRMAT cone in the 22 trajectory. For the other trajectories the second approximation was still conservative by as much as a factor of 1.5 to 2.5. However as noted above (see Item 4) the decelerator unit weight includes a minimum coating of at least 0.01 lb/sq ft.

Thus with the possible exception of the attached BALLUTE for the B3 trajectory where a 10 percent saving in decelerator weight might be realized, only nominal weight would be saved for the other cases. Also as noted above the meridian cable and riser-line strength and weight would correspond approximately to an operating temperature of 350 F with a design safety factor of 2. Considering the 19 and 30 trajectories,where the operating temperature is equivalent to room temperature, the decelerator meridian cables and risers actually would have a design safety factor of about 4 based on the weights of Item 3. The design safety factors corresponding with the B3, 22 and 23 trajectories would range between about 3.2 and 3.8 for the indicated values of operating temperature.

e. Item 7 - Auxiliary Gas Inflation System Weight

For the ram-air inflated decelerators, this item may be considered

as optional. By the definition of this study, however, it is mandatory with the 120-deg AIRMAT cone. The weight of auxiliary inflation aid gas for the ram-air inflated configurations was approximated as 50 percent of that required for the fully inflated decelerator at the design initial deployment Mach number, altitude, and internal pressure corresponding to the pressure recovery at the ram-air inlets of the decelerator. This value was multiplied by a factor of 1.5 to account for the container weight (see Item 12 of Table A-I through A-XI in Appendix A). For the AIRMAT cone the inflation gas and container weight was determined from Figure 100 in Section VII of Volume II corresponding to the size and supporting pressure requirements encountered at the initial deployment Mach number and altitude for this configuration.

f. Items 8, 9 and 10 - Ancillary Equipment Weight, Attachment Design Safety Factor, and Packaging Volume

Item 8 includes the weight estimates for the decelerator attachments, packaging equipment, separation and deployment means, and base heat shield. Figures 23 through 26 illustrate how attachment and separation means are provided for each of the decelerators considered in this study.

Note that the ancillary equipment weight includes the capsule base heat shield to protect the decelerator and equipment from the base heating encountered during entry. The shield probably will be fabricated of fiberglass with a thickness capable of maintaining the internal temperature below 200 F for a total heat input load of about 1000 BTU's/sq ft. On the basis of Mars entry energy levels and typical base heating levels encountered in orbital entry of blunt body shapes, this heat input is considered realistic. The weight of the heat shield allows for additional reinforcing to support the base pressure and deceleration loads of entry. The separation function of the heat shield would be utilized to extract and deploy the decelerator.

Item 9 indicates the attachment design factor. The values correspond with the load developed at full inflation of the decelerators and the design yield stress for the attachment components are indicated in Figures 23 through 26. The attachment supports are conservatively designed by assuming operation at an elevated temperature of 350 F and the material stress capability corresponding to this temperature level was used.

The packaging volume indicated by Item 10 for the decelerators is referenced to a packaging density of 30 lb/cu ft, which is a typical value for expandable decelerators fabricated of flexible material. Even if the packaging density were reduced to 20 lb/cu ft, the volume requirements are not excessive in terms of the volume availability provided in this study.

g. Item 11 - Composite System Velocity at 5,000 ft above Terrain

The tabulated data for this item and the space-time histories of Figures B-1 through B-6 in Appendix B show that reasonably low subsonic velocities will be attained so that conventional parachute systems could be deployed to limit terrain impact velocities to acceptable levels. This finding is for the decelerator sizes of Item 1 established on the basis of achieving a target point Mach number of about one near or above an altitude of 20,000 ft in the VM8 atmosphere and 30,000 ft in the VM7 atmosphere.

h. Item 12 - Composite System Flight-Path Angle at 5,000 ft above Terrain

The attached expandable decelerators can deflect the entry capsule flight-path for the A1, 19, 22, 23 and 30 entry cases to within 10 deg of the vertical at an altitude of 5000 ft. This deflection would be compatible with the levels of subsonic velocities of Item 11 and the energy and control capabilities of a soft-landing, terminal-stage, retrosystem of the Surveyor type.

i. Item 13 and 14 - Oscillation Amplitudes and Rates at 5000-ft Altitude

As described previously, for the case of the trailing decelerators there is a divergence tendency in angle of attack resulting primarily from the inadequate description of the 8-degree-of-freedom computer formulation (see Figures 27 and 28 and Appendix C.) Limited experience with the application of trailing decelerators attached to a spinning forebody generally has not exhibited this tendency, at least to the magnitude encountered in this study. It is apparent that the analytical (mathematical) description of the system dynamics should be studied and evaluated in much greater detail in future programs for the application of trailing decelerators. The system motion involving the use of the attached decelerators did not result in a large angular divergence. See Appendix C for a comprehensive discussion of the dynamic analysis considerations and results.

Comparing the magnitudes of oscillation amplitude and rate for the corresponding decelerator configurations, the effect of atmospheric density is apparent. The reduced damping moments in all modes of oscillation for trajectory 22 result in larger values of angular amplitude and rate. The comparison of the separate decelerators indicates that the attached configurations provide better stability than the trailing decelerator for the reason previously discussed. The best of the attached configurations is the tucked-back BALLUTE; primarily because of higher and more favorable values for C_{N_α}, X_{cp}/D_v and $(C_{m_q} + C_{m_{\dot{\alpha}}})$. See Items 26, 27, and 28 in Tables A-III and A-XI in Appendix A.

j. Item 15 - Maximum Operating g-Level

The deceleration g-levels encountered at full inflation of the decelerators are not excessive in relation to those in earth entry applications. Except for trajectory A1, the load levels would be less than the peak loads at launch and boost in the entry of the basic capsule for the trajectories studies.

As in Item 1, the decelerators for trajectories 23 and 30 are the same designs for trajectories 22 and 19, respectively. The corresponding g-loads at full inflation of the decelerators for trajectories 23 and 30 are 2 and 1.5 times greater than the 22 and 19 cases. Refering back to Item 9 (Attachment Design), the attachment design for both configurations in trajectory 23 and for the tucked-back BALLUTE in trajectory 30 would not be adequate. Some structural strengthening of the attachments would be required with nominal increase in the decelerator attachment weight. Recall, however, that the attachment design is conservative on the basis of the assumed elevated operating temperature. Appendix C considers the effects of the system dynamics on the decelerator strength and weight.

k. Items 16 and 17 - Total Decelerator System Weight and Weight Fraction

Item 16 is the sum of Items 3, 7, and 8 and Item 17 is the percentage of the total decelerator weight to the total entry capsule weight. The tucked-back BALLUTE has the more favorable weight fraction by a slight margin over the AIRMAT cone, which is the next best configuration. For trajectories 19 and 22 the weight difference among all configurations does not exceed two percent of the total entry capsule weight, much less than the accuracy of the assumptions and approximations made in the parametric analyses of this study.

Factors other than weight and performance will be important in choosing the most suitable expandable terminal decelerator for a Mars lander system. These factors would include static and dynamic aerodynamic stability, complexity and cost of fabrication methods, sequencing and control functions, interface constraints, etc. The accurate evaluation of these factors only can be made by a more comprehensive and detailed system design than encompassed by this study (see next section).

SECTION VI - RECOMMENDATIONS

As inferred from the statement of work for this program, this study was not expected to yield data in sufficient detail for complete and final engineering designs of expandable decelerators for Mars atmosphere entry. Consequently recommendations were made for areas requiring additional investigation and analyses. Additionally descriptions of development, simulation, and proof-test procedures to qualify aerodynamic decelerator systems for the Mars mission, including the types of facilities required, were made (see Sections VIII, IX, and X of Volume II).

The areas recommended as requiring additional investigation include:

1. Detailed configuration design analyses for an attached expandable decelerator associated with a specific entry capsule and performance envelope within the broad limits encompassed by this study
2. Fabrication techniques and constraints for an approximately full-scale, ram-air-inflated attached expandable configuration
3. Conventional wind-tunnel and free-flight wind-tunnel model tests to determine the aerodynamic performance and stability of an entry capsule/attached expandable configuration under simulated operating environments (see Section VIII of Volume II)
4. Design and fabrication of a full- or near-full-scale functional mockup of an entry capsule/attached expandable configuration for packaging, deployment, and inflation tests in the NASA Ames or Langley full-scale, wind-tunnel facilities

5. Large-scale, free-flight simulation tests of an entry vehicle/attached expandable configuration using rocket boost techniques, as illustrated by Figure 29 (see Section IX of Volume II)

6. Functional, environmental, sterilization and reliability tests of materials, hardware, and ancillary equipment associated with the entry capsule/attached expandable configuration

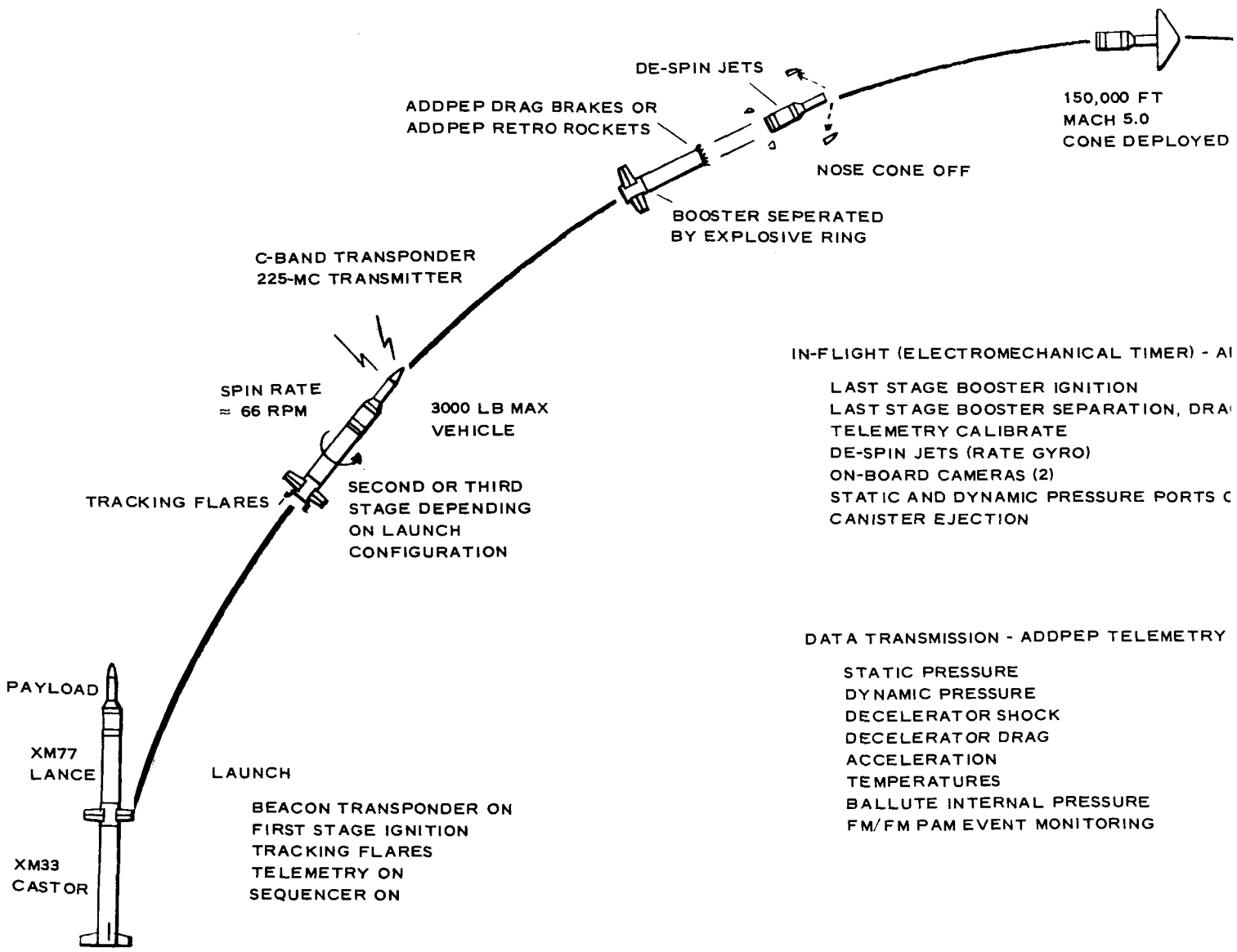
DE-SPIN JETS
ADDPEP DRAG BRAKES OR
ADDPEP RETRO ROCKETS
150,000 FT
MACH 5.0
CONE DEPLOYED
NOSE CONE OFF
BOOSTER SEPERATED
BY EXPLOSIVE RING
C-BAND TRANSPONDER
225-MC TRANSMITTER
SPIN RATE
≈ 66 RPM
3000 LB MAX
VEHICLE
TRACKING FLARES
SECOND OR THIRD
STAGE DEPENDING
ON LAUNCH
CONFIGURATION
PAYLOAD
XM77
LANCE
XM33
CASTOR
LAUNCH
BEACON TRANSPONDER ON
FIRST STAGE IGNITION
TRACKING FLARES
TELEMETRY ON
SEQUENCER ON
IN-FLIGHT (ELECTROMECHANICAL TIMER) - AI
LAST STAGE BOOSTER IGNITION
LAST STAGE BOOSTER SEPARATION, DRA
TELEMETRY CALIBRATE
DE-SPIN JETS (RATE GYRO)
ON-BOARD CAMERAS (2)
STATIC AND DYNAMIC PRESSURE PORTS C
CANISTER EJECTION
DATA TRANSMISSION - ADDPEP TELEMETRY
STATIC PRESSURE
DYNAMIC PRESSURE
DECELERATOR SHOCK
DECELERATOR DRAG
ACCELERATION
TEMPERATURES
BALLUTE INTERNAL PRESSURE
FM/FM PAM EVENT MONITORING

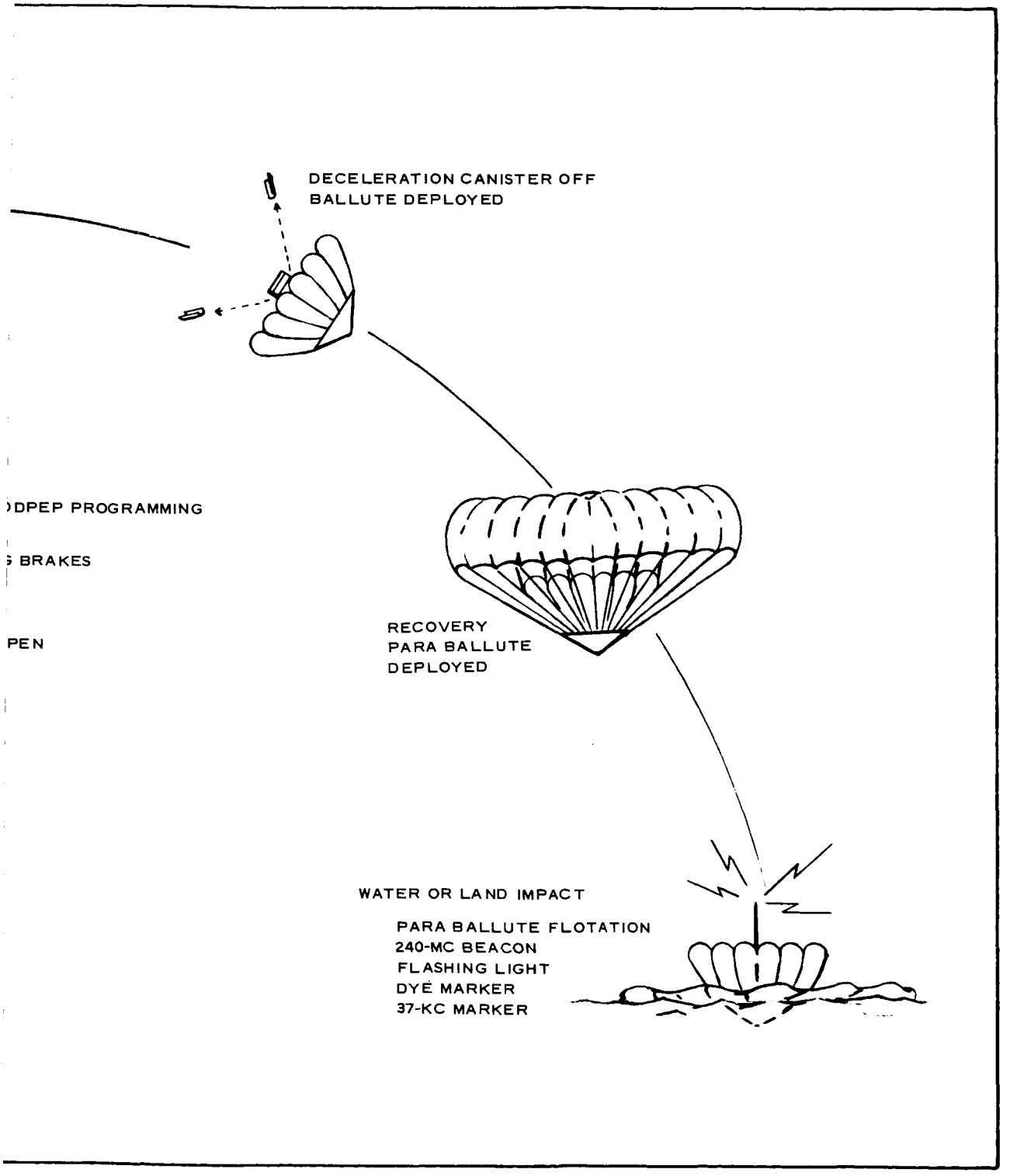

Figure 29 - Rocket Boost Technique for Simulation Test

SECTION VII - CONCLUSIONS

The research conducted during this study has led to the following conclusions:

1. The suitable application of expandable terminal decelerators for Mars atmosphere entry can be established by the analytical formulation of environmental factors and effects governing engineering applications and straightforward engineering techniques of analysis and design.

2. Definitive trends toward minimum weight fractions (of reasonable magnitude) for expandable terminal decelerators with corresponding optimum values for initial operating Mach number (that is, dynamic pressure) to aerodynamically retard entry capsules to Mach numbers of less than 1.0 at altitudes of 20,000 and 30,000 ft above Mars for specific model atmospheres has been established. For all the entry cases considered in this study, the suitable applications for expandable terminal decelerators for Mars atmosphere entry are within the current decelerator technology.

3. Dacron and Nomex, which are compatible with planetary sterilization requirements, can be employed safely for fabrication of expandable terminal decelerators under the combined aerodynamic and thermal loading environments encountered in Mars entry for the trajectories considered in the study. For all cases analyzed minimum coating thickness of the order of 0.01 lb/sq ft can be employed to maintain low acceptable values of

porosity for the decelerator envelope and to maintain the material temperature to acceptable design values with only minimum weight penalties.

4. The effect of varying target point Mach number from a nominal value of 1.0 at a specified target altitude has a measurable effect on decelerator size and weight fraction.

5. Detailed engineering analysis, design, and simulation testing pointed toward a specific expandable decelerator configuration and performance envelope within the broad range of values and trends encompassed by this study can be undertaken confidently. Such a program could be implemented over a reasonable period of 24 months from go-ahead and result in a prototype expandable decelerator system that could be flight-qualified subsequently for as early as the 1973 Mars lander mission (see Section X of Volume II). For budgetary purposes it was estimated (see Appendix D) that a program for the design, development, and test of an expandable terminal aerodynamic decelerator for a Mars lander capsule could be accomplished at an overall cost to the government of less than $3 million.

LIST OF REFERENCES

1. AEDC TR-65-218: Drag Characteristics of Three BALLUTE Decelerators in the Wake of the ALARR Payload at Mach Numbers 2 to 4. Arnold Air Force Station, Tenn. Arnold Engineering Development Center. 1965.

2. AEDC TDR-63-119: Performance of Flexible Aerodynamic Decelerators at Mach Numbers from 1.5 to 6. Arnold Air Station, Tenn. Arnold Engineering Development Center. 1963.

3. Alexander, W. C.: Investigation to Determine the Feasibility of Using Inflatable Balloon Type Drag Devices for Recovery Applications in the Transonic, Supersonic, and Hypersonic Flight Regime. Part II. Mach 4 to Mach 10 Feasibility Investigation. Akron, Ohio.Goodyear Aircraft Corp. ASD TDR-62-702. December 1965.

4. Charczenko, N.: Aerodynamic Characteristics of Towed Spheres, Conical Rings and Cones Used as Decelerators at Mach Numbers from 1.57 to 4.65. TN D-1789. NASA, April 1963.

5. Charczenko, N.; and McShera, J. T.: Aerodynamic Characteristics of Towed Cones Used as Decelerators at Mach Numbers from 1.57 to 4.65. TN D-994. NASA, December 1965.

6. Altgelt, R.: Gemini BALLUTE System Development. GER-11538 Akron, Ohio. Goodyear Aerospace Corporation. January 1965.

7. GER-11665: Aerodynamic Deployable Decelerator Performance Evaluation Program. Akron, Ohio. Goodyear Aerospace Corporation.

8. AEDC-TR-65-266: The Characteristics of a BALLUTE in the Wake of the Martin Fullscale SV-5D Vehicle at Mach Numbers from 0.6 to 2.9. Arnold Air Station, Tenn. Arnold Engineering Development Center. 1965.

9. AEDC-TR-64-131: Gemini BALLUTE Structural Test at Mach Numbers 0.55 and 1.92. Arnold Air Station, Tenn. Arnold Engineering Development Center. 1964.

10. McShera, J. T.: Aerodynamic Drag and Stability Characteristics of Towed Inflatable Decelerators at Supersonic Speeds. TN D-1601. NASA.

11. GER-11762: BALLUTE Evaluation Program for Project Sleigh Ride. Akron, Ohio. Goodyear Aerospace Corporation.

APPENDIX A - DECELERATOR CHARACTERISTICS

An explanation of each item in Tables A-I through A-XI is given below. Each number in the list corresponds with each item number in the tables.

1. Optimum initial operating Mach number at full-drag effectiveness - Defined as the Mach number selected or corresponding with the value for or trend toward the minimum weight fraction of the decelerator that will achieve the target point Mach number/altitude conditions. This Mach number is obtained from Figures 67 through 99 in Section VI of Volume II. Also see Appendix A of Volume II.

2. Dynamic pressure at initial Mach number - Value obtained from point-mass trajectory computations corresponding with the Mach number of Item 1 above

3. Altitude at initial Mach number - Value secured from point-mass trajectory computations corresponding to Item 1 above

4. Adiabatic wall temperature at initial Mach number - Value corresponding with Item 1 for temperature recovery factor of 0.9 (see Section II of Volume II)

5. Drag area at initial Mach number (C_DA) - Value based on drag area determined as required to achieve the target Mach number/altitude conditions (obtained from Figures 52 through 62 in Section V of Volume II)

6. Diameter - Value based on decelerator drag coefficient corresponding to Item 1 (see Section V and VI, Volume II) and Item 5 above

7. Drag coefficient, C_D (total) - See Item 6 above (also, Figure 8)

8. Decelerator weight - Value based on weight fraction corresponding to Item 1 multiplied by the entry capsule weight associated with the specific entry case (see Appendix A of Volume II)

9. Minimum practical decelerator envelope unit weight for combined thermal and aerodynamic loading environment including porosity coating weight of 0.01 lb/-sq ft - Value taken from Figures 89 through 99 by the analysis described in Section IV of Volume II

10. Total decelerator surface area - Value taken from Figure A-9 by the analysis described in Appendix A of Volume II

11. Total decelerator weight (based on Item 9) - Item 8 $\times \left[1 - \left(W_e/W_D\right)\right]$ + Item 9 $\times$ Item 10; for $\left(W_e/W_D\right)$ (see Appendix A of Volume II)

12. Auxiliary gas inflation aid weight - Defined as 1.5 $\times$ (50 percent of Item 29) g_e for Trailing BALLUTE (TB), Attached BALLUTE (AB), and Tucked-Back BALLUTE (TBB) configurations; for the AIRMAT cone (AC) configuration see Figure 100 of Section VII, Volume II

13. Packaging volume required - Based on Item 11 for packing densities indicated. The weights given are the maximum weights of the decelerators from Item 11

14. Inflated decelerator volume - Taken from Figure A-9 by analysis described in Appendix A of Volume II

15. Specified inflation time (from start of deployment) -

Specified on basis of size, minimum desired time to full-inflation, reduction of fabric flutter, and reduced loads

16. Mach number at deployment initiation - Taken from point-mass trajectory computations as the value occurring 1.5 sec before Item 1

17. Dynamic pressure at deployment - Obtained in the same manner as Item 16 above

18. Adiabatic wall temperature at deployment - Corresponds with Item 16 for temperature recovery factor of 0.9

19. Centroid of inflated volume - Derived from Figure A-9 by the analysis in Appendix A, Volume II

20. Transverse radius of gyration of decelerator squared - Obtained in the same manner as Item 19

21. Transverse radius of gyration of composite system squared -

$$K_{y,z}^{2} = \frac{1}{M_T}\left\{ I_{y,z_v} + \frac{1}{g}(\text{Item 11} \times \text{Item 20}) + \frac{\text{Item 11}}{g}\left[D_v \times (\text{Item 25} - 0.25) \right]^2 \right\}$$

22. Rotational radius of gyration of decelerator squared - Obtained in same manner as Item 19

23. Rotational radius of gyration of composite system squared -

$$K_x^2 = \frac{1}{M_T}\left[I_{x_v} + \frac{1}{g}(\text{Item 11} \times \text{Item 22}) \right]$$

24. Centroid of decelerator weight (from capsule base) - Derived in same manner as Item 19

25. Composite system cg position -

$$\left(\frac{X_{cg}}{D_v}\right)_{comp} = 0.25 + \frac{W_D}{W_T}\left[0.385 + \text{Item 24}\right]$$

26. Composite system cp position - Approximated as Item 19 + 0.865 for attached configurations only

27. Estimated C_{N_α} - Approximated from Munk's theory (per degree)

28. Estimated $\left(C_{m_q} + C_{m_{\dot{\alpha}}}\right)$ - Approximated from Figure 10 of Section I, Volume II and doubled to account for Mach number effect. See Figure 14 of Section I of Volume II (per radian about composite system cg)

29. Added mass of inflation gas (approximate) - Approximated as

$$\frac{P_T \times (\text{Item 14})}{g_m R_m T_m}$$

Defining $P_T = 2.75 \times f\left[(M),\ (P_l/P_\infty)\right]$; see Section II of Volume II, Figures 22, 23 and 24

30. Apparent mass effect of boundary layer -

$$\lambda_m = \frac{P_T}{g_m R_m T_m} \times \text{Item 10} \times \delta \ ;$$

where $\delta \doteq 0.03\, D_D$[a]

[a] Hoerner, S.: Fluid Dynamic Drag. Published by the author. New York, N.Y. 1958.

TABLE A-I - COMPARISON OF DECELERATOR CHARACTERISTICS

Trajectory no. A1

Atmosphere VM8

Vehicle characteristics

Diameter, D_v (ft) 18.5

Mass (slugs) 94

Ballistic parameter, $\left(M/C_D A\right)_v$ 0.25

Drag area, $\left(C_D A\right)_v$

(sq ft) 376

Weight, W_E (Earth lb) 3025

Initial entry angle (deg) 25

Initial entry velocity (fps) 23,000

Target altitude (ft) 20,000

Target Mach no. 1.0

Decelerator configuration code

TB - trailing BALLUTE (80 deg with plain back)

AB - attached BALLUTE

TBB - tucked-back BALLUTE

AC - AIRMAT cone (120 deg)

Item no. *	Characteristic	Dimension	Decelerator configuration			
			TB	AB	TBB	AC
1	Optimum initial operating Mach number at full-drag effectiveness	M = V/C	4.87	4.57	4.7	4.82
2	Dynamic pressure at initial Mach number	Lb/sq ft	61	56	58	60
3	Altitude at initial Mach number	Ft × 10^3	27.7	27	27.5	27.6
4	Adiabatic wall temperature at initial Mach number	F	800	710	780	790
5	Drag area at initial Mach number ($C_D A$)	Sq ft	585	1023	1005	985
6	Diameter	Ft	30.7	31.7	35.9	29.5
7	Drag coefficient, C_D (total)		0.79	1.3	1.0	1.44
8	Decelerator weight based on					
	Dacron at 350F	Lb	893	756	215	794
	Nomex at 600F	Lb	1351	1131	329	1310
9	Minimum practical decelerator envelope unit weight for combined thermal and aerodynamic loading environment including porosity coating weight of 0.01 lb/sq ft					
	Dacron	Lb/sq ft	0.065	0.07	0.05	0.266
	Operating temperature	F	400	300	420	150
	Nomex	Lb/sq ft	0.06	0.08	0.03	N/A
	Operating temperature	F	400	300	630	N/A
10	Total decelerator surface area	Sq ft	4130	4050	2610	1189

11	Total decelerator weight (based on Item 9)					
	Dacron	Lb	1083	686	363	428
	Nomex	Lb	969	675	389	N/A
12	Auxiliary gas inflation aid weight based on gas source					
	BALLUTEs	Lb	39.6	42	25.4	. . .
	AIRMAT cone	Lb	. . .	. . .	. . .	40
13	Packaging volume required based on					
	Packing density = 20 lb/cu ft	Cu ft	54.1	34.3	19.5	21.4
	Packing density = 30 lb/cu ft	Cu ft	36.1	22.9	13	14.3
14	Inflated decelerator volume	Cu ft	16520	17480	10600	1104
15	Specified inflation time (from start of deployment)	Sec	1.5	1.5	1.5	1.5
16	Mach number at deployment initiation		5.55	5.16	5.3	5.49
17	Dynamic pressure at deployment	Lb/sq ft	76.5	68.8	72.2	75.4
18	Adiabatic wall temperature at deployment	F	1100	950	980	1070
19	Centroid of inflated volume	X_v/D_v	4.971	0.735	0.386	0.154
20	Transverse radius of gyration of decelerator squared	Sq ft	129.6	135.7	123.7	79.7
21	Transverse radius of gyration of composite system squared	Sq ft	960	70.55	42.4	37.55
22	Rotational radius of gyration of decelerator squared	Sq ft	203.8	233.9	203.0	139.5
23	Rotational radius of gyration of composite system squared	Sq ft	98.5	78.5	49.9	45.25
24	Centroid of decelerator weight (from capsule base)	X_o/D_v	4.996	0.856	0.501	0.154
25	Composite system cg position	X_{cg}/D_v	1.86	0.451	0.315	0.277
26	Composite system cp position	X_{cp}/D_v	N/A	1.2	1.36	1.118
27	Estimated C_{N_α} (average) = C_{Y_β} (per degree)		0.01	0.01	0.02	0.005
28	Estimated $(C_{m_q} + C_{m_{\dot{\alpha}}})$	(qD_v/V) (ref)	0	-0.06	-0.026	-0.105
29	Added mass of inflation gas (approximate)	Slugs	1.65	1.75	1.06	N/A
30	Apparent mass effect of boundary layer	Slugs	0.38	0.39	0.28	0.16

*For explanation of each item, see comments at beginning of Appendix A.

TABLE A-II - COMPARISON OF DECELERATOR CHARACTERISTICS

Trajectory no. B3
Atmosphere VM8

Vehicle characteristics
Diameter, D_v (ft) 12
Mass (slugs) 79
Ballistic parameter, $\left(M/C_D A\right)_v$ 0.5
Drag area, $\left(C_D A\right)_v$
(sq ft) 158
Weight, W_E (Earth lb) 2540

Initial entry angle (deg) 15
Initial entry velocity (fps) 15,000

Target altitude (ft) 20,000
Target Mach no. 1.0

Decelerator configuration code
TB - trailing BALLUTE (80 deg with plain back)
AB - attached BALLUTE
TBB - tucked-back BALLUTE
AC - AIRMAT cone (120 deg)

Item no. *	Characteristic	Dimension	Decelerator configuration			
			TB	AB	TBB	AC
1	Optimum initial operating Mach number at full-drag effectiveness	M = V/C	2.5	2.5	2.5	2.5
2	Dynamic pressure at initial Mach number	Lb/sq ft	19	19	19	19
3	Altitude at initial Mach number	Ft × 10^3	25	25	25	25
4	Adiabatic wall temperature at initial Mach number	F	50	50	50	50
5	Drag area at initial Mach number ($C_D A$)	Sq ft	378	536	536	536
6	Diameter	Ft	23.7	22.9	25.7	21.9
7	Drag coefficient, C_D (total)		0.86	1.3	1.03	1.42
8	Decelerator weight based on					
	Dacron at 350F	Lb	129.8	97.8	28.4	122
	Nomex at 600F	Lb	189.2	146	42.1	182
9	Minimum practical decelerator envelope unit weight for combined thermal and aerodynamic loading environment including porosity coating weight of 0.01 lb/sq ft					
	Dacron	Lb/sq ft	0.02	0.03	0.015	0.075
	Operating temperature	F	270	240	310	150
	Nomex	Lb/sq ft	N/A	N/A	N/A	N/A
	Operating temperature	F	N/A	N/A	N/A	N/A
10	Total decelerator surface area	Sq ft	2460	1970	1338	728

11	Total decelerator weight (based on Item 9)					
	Dacron	Lb	129.3	100.7	42.6	71.8
	Nomex	Lb	N/A	N/A	N/A	N/A
12	Auxiliary gas inflation aid weight based on gas source					
	BALLUTEs	Lb	16.8	13.7	7.1	. . .
	AIRMAT cone	Lb	. . .	. . .	. . .	7.0
13	Packaging volume required based on					
	Packing density = 20 lb/cu ft	Cu ft	6.5	5.05	2.15	3.6
	Packing density = 30 lb/cu ft	Cu ft	4.3	3.35	1.42	2.4
14	Inflated decelerator volume	Cu ft	7510	6060	3150	501
15	Specified inflation time (from start of deployment)	Sec	1.5	1.5	1.5	1.5
16	Mach number at deployment initiation		2.6	2.6	2.6	2.6
17	Dynamic pressure at deployment	Lb/sq ft	20.3	20.3	20.3	20.3
18	Adiabatic wall temperature at deployment	F	100	100	100	100
19	Centroid of inflated volume	X_v/D_v	5.325	0.855	0.431	0.204
20	Transverse radius of gyration of decelerator squared	Sq ft	77.2	71.1	63.4	41.8
21	Transverse radius of gyration of composite system squared	Sq ft	21.2	9.38	7.41	7.51
22	Rotational radius of gyration of decelerator squared	Sq ft	121.5	120.5	104.0	72.7
23	Rotational radius of gyration of composite system squared	Sq ft	13.65	12.23	9.22	9.54
24	Centroid of decelerator weight (from capsule base)	X_o/D_v	5.363	0.981	0.56	0.204
25	Composite system cg position	X_{cg}/D_v	0.526	0.29	0.26	0.257
26	Composite system cp position	X_{cp}/D_v	. . .	1.34	1.5	1.28
27	Estimated C_{N_α} (average) = C_{Y_β} (per degree)		0.01	0.01	0.02	0.005
28	Estimated $(C_{m_q} + C_{m_{\dot{\alpha}}})$	(qD_v/V) (ref)	0	-0.105	-0.153	-0.17
29	Added mass of inflation gas (approximate)	Slugs	0.7	0.57	0.295	N/A
30	Apparent mass effect of boundary layer	Slugs	0.163	0.127	0.097	0.06

*For explanation of each item, see comments at beginning of Appendix A.

TABLE A-III - COMPARISON OF DECELERATOR CHARACTERISTICS

Trajectory no. 19
Atmosphere VM8

Vehicle characteristics
- Diameter, D_v (ft) 16
- Mass (slugs) 84.5
- Ballistic parameter, $\left(M/C_D A\right)_v$ 0.3
- Drag area, $\left(C_D A\right)_v$ (sq ft) 281.5
- Weight, W_E (Earth lb) 2720

Initial entry angle (deg) 16
Initial entry velocity (fps) 16,000

Target altitude (ft) 20,000
Target Mach no. 1.0

Decelerator configuration code
- TB - trailing BALLUTE (80 deg with plain back)
- AB - attached BALLUTE
- TBB - tucked-back BALLUTE
- AC - AIRMAT cone (120 deg)

Item no. *	Characteristic	Dimension	Decelerator configuration			
			TB	AB	TBB	AC
1	Optimum initial operating Mach number at full-drag effectiveness	M = V/C	2	2	2	2
2	Dynamic pressure at initial Mach number	Lb/sq ft	9.5	9.5	9.5	9.5
3	Altitude at initial Mach number	Ft × 10^3	31.3	31.3	31.3	31.3
4	Adiabatic wall temperature at initial Mach number	F	-50	-50	-50	-50
5	Drag area at initial Mach number ($C_D A$)	Sq ft	467	749	749	749
6	Diameter	Ft	23	27.1	31.05	25.8
7	Drag coefficient, C_D (total)		1.12	1.3	0.99	1.43
8	Decelerator weight based on					
	Dacron at 350F	Lb	93.2	81.1	23.2	93.2
	Nomex at 600F	Lb	141.5	122.5	34.8	139.2
9	Minimum practical decelerator envelope unit weight for combined thermal and aerodynamic loading environment including porosity coating weight of 0.01 lb/sq ft					
	Dacron	Lb/sq ft	0.015	0.016	0.012	0.049
	Operating temperature	F	< 100	< 100	< 100	< 100
	Nomex	Lb/sq ft	N/A	N/A	N/A	N/A
	Operating temperature	F	N/A	N/A	N/A	N/A
10	Total decelerator surface area	Sq ft	2320	2975	1950	918

11	Total decelerator weight (based on Item 9)					
	Dacron	Lb	56.1	61.9	29.4	53.8
	Nomex	Lb	N/A	N/A	N/A	N/A
12	Auxiliary gas inflation aid weight based on gas source					
	BALLUTEs	Lb	11	13.7	8.7	. . .
	AIRMAT cone	Lb	. . .	. . .	. . .	6.0
13	Packaging volume required based on					
	Packing density = 20 lb/cu ft	Cu ft	2.8	3.1	1.47	2.69
	Packing density = 30 lb/cu ft	Cu ft	1.87	2.06	1.0	1.79
14	Inflated decelerator volume	Cu ft	8870	10900	6880	747
15	Specified inflation time (from start of deployment)	Sec	1.5	1.5	1.5	1.5
16	Mach number at deployment initiation		2.07	2.07	2.07	2.07
17	Dynamic pressure at deployment	Lb/sq ft	9.9	9.9	9.9	9.9
18	Adiabatic wall temperature at deployment	F	0	0	0	0
19	Centroid of inflated volume	X_v/D_v	4.964	0.719	0.391	0.158
20	Transverse radius of gyration of decelerator squared	Sq ft	72.7	99.2	92.6	47.6
21	Transverse radius of gyration of composite system squared	Sq ft	21.12	19.23	17.9	17.82
22	Rotational radius of gyration of decelerator squared	Sq ft	114.4	171.7	151.9	105.7
23	Rotational radius of gyration of composite system squared	Sq ft	20.3	21.8	19.58	20
24	Centroid of decelerator weight (from capsule base)	X_o/D_v	4.992	0.834	0.509	0.158
25	Composite system cg position	X_{cg}/D_v	0.354	0.27	0.256	0.254
26	Composite system cp position	X_{cp}/D_v	. . .	1.19	1.36	1.13
27	Estimated C_{N_α} (average) = C_{Y_β} (per degree)		0.01	0.01	0.02	0.005
28	Estimated $(C_{m_q} + C_{m_{\dot{\alpha}}})$	(qD_v/V) (ref)	0	-0.135	-0.168	-0.14
29	Added mass of inflation gas (approximate)	Slugs	0.46	0.57	0.36	N/A
30	Apparent mass effect of boundary layer	Slugs	0.083	0.126	0.095	0.055

*For explanation of each item, see comments at beginning of Appendix A.

TABLE A-IV - COMPARISON OF DECELERATOR CHARACTERISTICS

Trajectory no. 19

Atmosphere VM8

Vehicle characteristics

Diameter, D_v (ft) 16

Mass (slugs) 84.5

Ballistic parameter, $\left(M/C_D A\right)_v$ 0.3

Drag area, $\left(C_D A\right)_v$

(sq ft) 281.5

Weight, W_E (Earth lb) 2720

Initial entry angle (deg) 16

Initial entry velocity (fps) 16,000

Target altitude (ft) 30,000

Target Mach no. 1.0

Decelerator configuration code

TB - trailing BALLUTE (80 deg with plain back)

AB - attached BALLUTE

TBB - tucked-back BALLUTE

AC - AIRMAT cone (120 deg)

Item no. *	Characteristic	Dimension	Decelerator configuration			
			TB	AB	TBB	AC
1	Optimum initial operating Mach number at full-drag effectiveness	M = V/C	3	3	3	3.5
2	Dynamic pressure at initial Mach number	Lb/sq ft	16	16	16	19
3	Altitude at initial Mach number	Ft $\times 10^3$	38.3	38.3	38.3	40.7
4	Adiabatic wall temperature at initial Mach number	F	100	100	100	250
5	Drag area at initial Mach number ($C_D A$)	Sq ft	1127	1409	1409	1290
6	Diameter	Ft	35.45	37.8	44.1	33.8
7	Drag coefficient, C_D (total)		1.14	1.25	0.92	1.44
8	Decelerator weight based on					
	Dacron at 350F	Lb	506	416	119.2	543
	Nomex at 600F	Lb	. . .	602	178	800
9	Minimum practical decelerator envelope unit weight for combined thermal and aerodynamic loading environment including porosity coating weight of 0.01 lb/sq ft					
	Dacron	Lb/sq ft	0.03	0.032	0.015	0.12
	Operating temperature	F	220	200	370	150
	Nomex	Lb/sq ft	N/A	N/A	N/A	N/A
	Operating temperature	F	N/A	N/A	N/A	N/A
10	Total decelerator surface area	Sq ft	5540	6020	3955	1875

11	Total decelerator weight (based on Item 9)					
	Dacron	Lb	421	340	173.3	302
	Nomex	Lb	N/A	N/A	N/A	N/A
12	Auxiliary gas inflation aid weight based on gas source					
	BALLUTEs	Lb	45.5	54	29	. . .
	AIRMAT cone	Lb	. . .	. . .	. . .	25
13	Packaging volume required based on					
	Packing density = 20 lb/cu ft	Cu ft	21	17	8.67	15.1
	Packing density = 30 lb/cu ft	Cu ft	14	11.33	5.8	10.1
14	Inflated decelerator volume	Cu ft	25,600	30,350	16,000	1971
15	Specified inflation time (from start of deployment)	Sec	1.5	1.5	1.5	1.5
16	Mach number at deployment initiation		3.13	3.13	3.13	3.69
17	Dynamic pressure at deployment	Lb/sq ft	16.9	16.9	16.9	20.9
18	Adiabatic wall temperature at deployment	F	150	150	150	300
19	Centroid of inflated volume	X_v/D_v	5.489	1.147	0.555	0.265
20	Transverse radius of gyration of decelerator squared	Sq ft	173.8	194.3	186.7	96.6
21	Transverse radius of gyration of composite system squared	Sq ft	234.4	48.3	29.4	27.92
22	Rotational radius of gyration of decelerator squared	Sq ft	271.9	321.5	306.3	166.1
23	Rotational radius of gyration of composite system squared	Sq ft	60	58.2	37.45	36.35
24	Centroid of decelerator weight (from capsule base)	X_o/D_v	5.532	1.291	0.723	0.265
25	Composite system cg position	X_{cg}/D_v	1.114	0.416	0.299	0.284
26	Composite system cp position	X_{cp}/D_v	. . .	1.65	1.43	1.48
27	Estimated C_{N_α} (average) = C_{Y_β} (per degree)		0.01	0.01	0.02	0.005
28	Estimated $(C_{m_q} + C_{m_{\dot{\alpha}}})$	(qD_v/V) (ref)	0	-0.065	-0.11	-0.127
29	Added mass of inflation gas (approximate)	Slugs	1.9	2.25	1.2	N/A
30	Apparent mass effect of boundary layer	Slugs	0.437	0.507	0.392	0.18

*For explanation of each item, see comments at beginning of Appendix A.

TABLE A-V - COMPARISON OF DECELERATOR CHARACTERISTICS

Trajectory no. 37

Atmosphere VM8

Vehicle characteristics

Diameter, D_v (ft) 16

Mass (slugs) 84.5

Ballistic parameter, $\left(M/C_D A\right)_v$ 0.3

Drag area, $\left(C_D A\right)_v$

(sq ft) 281.5

Weight, W_E (Earth lb) 2720

Initial entry angle (deg) 28

Initial entry velocity (fps) 23,000

Target altitude (ft) 10,000

Target Mach no. 1.0

Decelerator configuration code

TB - trailing BALLUTE (80 deg with plain back)

AB - attached BALLUTE

TBB - tucked-back BALLUTE

AC - AIRMAT cone (120 deg)

Item no. *	Characteristic	Dimension	Decelerator configuration			
			TB	AB	TBB	AC
1	Optimum initial operating Mach number at full-drag effectiveness	M = V/C	5	4.23	4.7	5
2	Dynamic pressure at initial Mach number	Lb/sq ft	92	71	83	92
3	Altitude at initial Mach number	Ft × 10^3	20	17.5	19	20
4	Adiabatic wall temperature at initial Mach number	F	1000	700	900	1000
5	Drag area at initial Mach number ($C_D A$)	Sq ft	408	796	735	688
6	Diameter	Ft	25.4	28	30.4	24.8
7	Drag coefficient, C_D (total)		0.805	1.29	1.01	1.422
8	Decelerator weight based on					
	Dacron at 350F	Lb	802	672	190.2	776
	Nomex at 600F	Lb	1200	1008	290	1160
9	Minimum practical decelerator envelope unit weight for combined thermal and aerodynamic loading environment including porosity coating weight of 0.01 lb/sq ft					
	Dacron	Lb/sq ft	0.09	0.09	0.07	N/A
	Operating temperature	F	440	290	450	N/A
	Nomex	Lb/sq ft	0.084	0.091	0.05	N/A
	Operating temperature	F	500	300	670	N/A
10	Total decelerator surface area	Sq ft	2830	3170	1870	678

11	Total decelerator weight (based on Item 9)					
	Dacron	Lb	1061	631	351	776
	Nomex	Lb	1038	600	386	1160
12	Auxiliary gas inflation aid weight based on gas source					
	BALLUTEs	Lb	28	36	19.2	. . .
	AIRMAT cone	Lb	. . .	. . .	. . .	30
13	Packaging volume required based on					
	Packing density = 20 lb/cu ft	Cu ft	53.1	31.6	19.3	58
	Packing density = 30 lb/cu ft	Cu ft	35.4	21	12.9	38.6
14	Inflated decelerator volume	Cu ft	9360	12080	6410	637
15	Specified inflation time (from start of deployment)	Sec	1.5	1.5	1.5	1.5
16	Mach number at deployment initiation		5.72	4.83	5.4	5.72
17	Dynamic pressure at deployment	Lb/sq ft	112.5	88	103	112.5
18	Adiabatic wall temperature at deployment	F	1350	950	1190	1350
19	Centroid of inflated volume	X_v/D_v	5.06	0.758	0.381	0.145
20	Transverse radius of gyration of decelerator squared	Sq ft	90.3	106.0	88.7	57.0
21	Transverse radius of gyration of composite system squared	Sq ft	1062	52.4	29.67	33.65
22	Rotational radius of gyration of decelerator squared	Sq ft	140.5	182.3	145.6	99.4
23	Rotational radius of gyration of composite system squared	Sq ft	72.9	60.8	36.7	46.2
24	Centroid of decelerator weight (from capsule base)	X_o/D_v	5.09	0.871	0.501	0.145
25	Composite system cg position	X_{cg}/D_v	2.23	0.456	0.323	0.296
26	Composite system cp position	X_{cp}/D_v	. . .	1.22	1.33	1.085
27	Estimated C_{N_α} (average) = C_{Y_β} (per degree)		0.01	0.01	0.02	0.005
28	Estimated $(C_{m_q} + C_{m_{\dot{\alpha}}})$	(qD_v/V) (ref)	0	-0.08	-0.051	-0.083
29	Added mass of inflation gas (approximate)	Slugs	1.17	1.5	0.8	N/A
30	Apparent mass effect of boundary layer	Slugs	0.27	0.33	0.213	0.116

*For explanation of each item, see comments at beginning of Appendix A.

TABLE A-VI - COMPARISON OF DECELERATOR CHARACTERISTICS

Trajectory no. A4

Atmosphere VM7

Vehicle characteristics

Diameter, D_v (ft) 18.5

Mass (slugs) 94

Ballistic parameter, $\left(M/C_D A\right)_v$ 0.25

Drag area, $\left(C_D A\right)_v$

(sq ft) 376

Weight, W_E (Earth lb) 3025

Initial entry angle (deg) 25

Initial entry velocity (fps) 23,000

Target altitude (ft) 20,000

Target Mach no. 1.0

Decelerator configuration code

TB - trailing BALLUTE (80 deg with plain back)

AB - attached BALLUTE

TBB - tucked-back BALLUTE

AC - AIRMAT cone (120 deg)

Item no. *	Characteristic	Dimension	Decelerator configuration			
			TB+	AB	TBB	AC
1	Optimum initial operating Mach number at full-drag effectiveness	M = V/C		2	2	2.11
2	Dynamic pressure at initial Mach number	Lb/sq ft		14.8	14.8	16.5
3	Altitude at initial Mach number	Ft × 10^3		38.8	36.8	40.3
4	Adiabatic wall temperature at initial Mach number	F		250	250	295
5	Drag area at initial Mach number ($C_D A$)	Sq ft		431	431	440
6	Diameter	Ft		20.8	20.5	19.7
7	Drag coefficient, C_D (total)			1.27	1.305	1.44
8	Decelerator weight based on					
	Dacron at 350F	Lb		51.5	11.35	13.32
	Nomex at 600F	Lb		77.2	16.95	22.1
9	Minimum practical decelerator envelope unit weight for combined thermal and aerodynamic loading environment including porosity coating weight of 0.01 lb/sq ft					
	Dacron	Lb/sq ft		0.023	0.012	0.050
	Operating temperature	F		350	350	350
	Nomex	Lb/sq ft		0.028	0.012	0.167
	Operating temperature	F		400	600	400
10	Total decelerator surface area	Sq ft		1480	850	222
11	Total decelerator weight (based on Item 9)					

16

	Dacron	Lb		66	20.4	15.5
	Nomex	Lb		73.5	25.5	42
12	Auxiliary gas inflation aid weight based on gas source					
	BALLUTEs	Lb		4.6	2.2	. . .
	AIRMAT cone	Lb		. . .	. . .	5
13	Packaging volume required based on					
	Packing density = 20 lb/cu ft	Cu ft		3.7	1.3	2.1
	Packing density = 30 lb/cu ft	Cu ft		2.5	0.9	1.4
14	Inflated decelerator volume	Cu ft		4040	1975	75
15	Specified inflation time (from start of deployment)	Sec		1.5	1.5	1.5
16	Mach number at deployment initiation			2.11	2.11	2.22
17	Dynamic pressure at deployment	Lb/sq ft		16	16	17.4
18	Adiabatic wall temperature at deployment	F		350	350	370
19	Centroid of inflated volume	X_v/D_v		0.324	0.223	0.052
20	Transverse radius of gyration of decelerator squared	Sq ft		57.3	40.3	45.9
21	Transverse radius of gyration of composite system squared	Sq ft		27.4	26.4	26.35
22	Rotational radius of gyration of decelerator squared	Sq ft		106.1	66.2	80.8
23	Rotational radius of gyration of composite system squared	Sq ft		27.85	26	25.9
24	Centroid of decelerator weight (from capsule base)	X_o/D_v		0.563	0.29	0.052
25	Composite system cg position	X_{cg}/D_v		0.264	0.253	0.251
26	Composite system cp position	X_{cp}/D_v		0.788	0.776	0.745
27	Estimated C_{N_α} (average) = C_{Y_β} (per degree)			0.01	0.02	0.005
28	Estimated $(C_{m_q} + C_{m_{\dot{\alpha}}})$	(qD_v/V) (ref)		-0.05	-0.05	-0.056
29	Added mass of inflation gas (approximate)	Slugs		0.19	0.09	N/A
30	Apparent mass effect of boundary layer	Slugs		0.044	0.024	0.021

*For explanation of each item, see comments at beginning of Appendix A.

+Characteristics were not evaluated for this trajectory.

TABLE A-VII - COMPARISON OF DECELERATOR CHARACTERISTICS

Trajectory no. A4

Atmosphere VM7

Vehicle characteristics

Diameter, D_v (ft) 18.5

Mass (slugs) 94

Ballistic parameter, $\left(M/C_D A\right)_v$ 0.25

Drag area, $\left(C_D A\right)_v$

(sq ft) 376

Weight, W_E (Earth lb) 3025

Initial entry angle (deg) 25

Initial entry velocity (fps) 23,000

Target altitude (ft) 30,000

Target Mach no. 1.0

Decelerator configuration code

TB - trailing BALLUTE (80 deg with plain back)

AB - attached BALLUTE

TBB - tucked-back BALLUTE

AC - AIRMAT cone (120 deg)

Item no. *	Characteristic	Dimension	Decelerator configuration			
			TB	AB	TBB	AC
1	Optimum initial operating Mach number at full-drag effectiveness	M = V/C	2.75	2	2.13	2.55
2	Dynamic pressure at initial Mach number	Lb/sq ft	23	14.6	16	21
3	Altitude at initial Mach number	Ft × 10^3	46.8	39	40	45
4	Adiabatic wall temperature at initial Mach number	F	440	250	300	340
5	Drag area at initial Mach number ($C_D A$)	Sq ft	316	842	800	694
6	Diameter	Ft	21.1	28.6	31.5	24.8
7	Drag coefficient, C_D (total)		0.903	1.31	1.03	1.433
8	Decelerator weight based on					
	Dacron at 350F	Lb	171	149.8	41.75	148.2
	Nomex at 600F	Lb	227	227	63	222.5
9	Minimum practical decelerator envelope unit weight for combined thermal and aerodynamic loading environment including porosity coating weight of 0.01 lb/sq ft					
	Dacron	Lb/sq ft	0.025	0.028	0.014	0.15
	Operating temperature	F	350	350	350	350
	Nomex	Lb/sq ft	0.026	0.028	0.014	0.167
	Operating temperature	F	400	< 200	< 200	< 100
10	Total decelerator surface area	Sq ft	1958	3220	2000	678

11	Total decelerator weight (based on Item 9)					
	Dacron	Lb	185.9	183.5	65.6	151
	Nomex	Lb	172	137.5	46.9	235.5
12	Auxiliary gas inflation aid weight based on gas source					
	BALLUTEs	Lb	6.0	13.9	7.9	. . .
	AIRMAT cone	Lb	. . .	. . .	. . .	10
13	Packaging volume required based on					
	Packing density = 20 lb/cu ft	Cu ft	9.3	9.2	3.3	11.8
	Packing density = 30 lb/cu ft	Cu ft	6.2	6.1	2.2	7.85
14	Inflated decelerator volume	Cu ft	5380	12,520	7160	509
15	Specified inflation time (from start of deployment)	Sec	1.5	1.5	1.5	1.5
16	Mach number at deployment initiation		2.92	2.11	2.24	2.7
17	Dynamic pressure at deployment	Lb/sq ft	26.2	16	17.5	23.2
18	Adiabatic wall temperature at deployment	F	550	350	375	450
19	Centroid of inflated volume	X_v/D_v	4.77	0.624	0.342	0.103
20	Transverse radius of gyration of decelerator squared	Sq ft	61.2	110.4	95.3	61.4
21	Transverse radius of gyration of composite system squared	Sq ft	57.8	33.4	28.2	29.2
22	Rotational radius of gyration of decelerator squared	Sq ft	96.3	193.2	156.3	107.7
23	Rotational radius of gyration of composite system squared	Sq ft	31.4	37.2	28.88	30.9
24	Centroid of decelerator weight (from capsule base)	X_o/D_v	4.79	0.728	0.446	0.103
25	Composite system cg position	X_{cg}/D_v	0.536	0.291	0.259	0.257
26	Composite system cp position	X_{cp}/D_v	. . .	1.08	1.19	0.94
27	Estimated C_{N_α} (average) = C_{Y_β} (per degree)		0.01	0.01	0.02	0.005
28	Estimated $(C_{m_q} + C_{m_{\dot{\alpha}}})$	(qD_v/V) (ref)	0	-0.04	-0.077	-0.065
29	Added mass of inflation gas (approximate)	Slugs	0.25	0.58	0.33	N/A
30	Apparent mass effect of boundary layer	Slugs	0.058	0.128	0.087	0.0425

*For explanation of each item, see comments at beginning of Appendix A.

TABLE A-VIII - COMPARISON OF DECELERATOR CHARACTERISTICS

Trajectory no. B1
Atmosphere VM7

Vehicle characteristics

Diameter, D_v (ft) 12
Mass (slugs) 79
Ballistic parameter, $\left(M/C_D A\right)_v$ 0.5
Drag area, $\left(C_D A\right)_v$
(sq ft) 158
Weight, W_E (Earth lb) 2540

Initial entry angle (deg) 15
Initial entry velocity (fps) 15,000

Target altitude (ft) 20,000
Target Mach no. 1.0

Decelerator configuration code

TB - trailing BALLUTE (80 deg with plain back)
AB - attached BALLUTE
TBB - tucked-back BALLUTE
AC - AIRMAT cone (120 deg)

Item no. *	Characteristic	Dimension	Decelerator configuration			
			TB	AB	TBB	AC
1	Optimum initial operating Mach number at full-drag effectiveness	M = V/C	2.25	2	2	2.33
2	Dynamic pressure at initial Mach number	Lb/sq ft	17	15	15	18
3	Altitude at initial Mach number	Ft × 10^3	42.5	37	37	44
4	Adiabatic wall temperature at initial Mach number	F	295	250	250	300
5	Drag area at initial Mach number ($C_D A$)	Sq ft	183.1	363.5	363.5	324
6	Diameter	Ft	14.9	18.9	21.5	17
7	Drag coefficient, C_D (total)		1.05	1.23	1.0	1.43
8	Decelerator weight based on					
	Dacron at 350F	Lb	45.2	40.1	11.42	43.7
	Nomex at 600F	Lb	66.5	60.5	17.02	64.9
9	Minimum practical decelerator envelope unit weight for combined thermal and aerodynamic loading environment including porosity coating weight of 0.01 lb/sq ft					
	Dacron	Lb/sq ft	0.02	0.02	0.015	0.058
	Operating temperature	F	300	100	150	150
	Nomex	Lb/sq ft	N/A	N/A	N/A	N/A
	Operating temperature	F	N/A	N/A	N/A	N/A
10	Total decelerator surface area	Sq ft	974	1415	936	346

11	Total decelerator weight (based on Item 9)					
	Dacron	Lb	50.5	35.5	18.4	26.2
	Nomex	Lb	N/A	N/A	N/A	N/A
12	Auxiliary gas inflation aid weight based on gas source					
	BALLUTEs	Lb	3.4	6.2	3.8	. . .
	AIRMAT cone	Lb	. . .	. . .	. . .	5
13	Packaging volume required based on					
	Packing density = 20 lb/cu ft	Cu ft	2.53	1.78	0.92	1.31
	Packing density = 30 lb/cu ft	Cu ft	1.68	1.18	0.61	0.875
14	Inflated decelerator volume	Cu ft	1890	3630	2280	182
15	Specified inflation time (from start of deployment)	Sec	1.5	1.5	1.5	1.5
16	Mach number at deployment initiation		2.32	2.06	2.06	2.395
17	Dynamic pressure at deployment	Lb/sq ft	18.1	15.75	15.75	18.8
18	Adiabatic wall temperature at deployment	F	390	300	300	410
19	Centroid of inflated volume	X_v/D_v	4.832	0.643	0.360	0.118
20	Transverse radius of gyration of decelerator squared	Sq ft	30.5	48.2	44.4	28.0
21	Transverse radius of gyration of composite system squared	Sq ft	8.28	7.01	6.65	6.61
22	Rotational radius of gyration of decelerator squared	Sq ft	48.0	84.2	72.8	49.0
23	Rotational radius of gyration of composite system squared	Sq ft	8.43	8.645	8.0	7.97
24	Centroid of decelerator weight (from capsule base)	X_o/D_v	4.856	0.748	0.469	0.118
25	Composite system cg position	X_{cg}/D_v	0.347	0.261	0.254	0.252
26	Composite system cp position	X_{cp}/D_v	. . .	1.10	1.255	0.994
27	Estimated C_{N_α} (average) = C_{Y_β} (per degree)		0.01	0.01	0.02	0.005
28	Estimated $(C_{m_q} + C_{m_{\dot{\alpha}}})$	(qD_v/V) (ref)	0	-0.137	-0.155	-0.13
29	Added mass of inflation gas (approximate)	Slugs	0.14	0.26	0.16	N/A
30	Apparent mass effect of boundary layer	Slugs	0.032	0.058	0.042	0.021

*For explanation of each item, see comments at beginning of Appendix A.

TABLE A-IX - COMPARISON OF DECELERATOR CHARACTERISTICS

Trajectory no. B1
Atmosphere VM7

Vehicle characteristics
- Diameter, D_v (ft) 12
- Mass (slugs) 79
- Ballistic parameter, $\left(M/C_D A\right)_v$ 0.5
- Drag area, $\left(C_D A\right)_v$
- (sq ft) 158
- Weight, W_E (Earth lb) 2540

Initial entry angle (deg) 15
Initial entry velocity (fps) 15,000

Target altitude (ft) 30,000
Target Mach no. 1.0

Decelerator configuration code
- TB - trailing BALLUTE (80 deg with plain back)
- AB - attached BALLUTE
- TBB - tucked-back BALLUTE
- AC - AIRMAT cone (120 deg)

Item no. *	Characteristic	Dimension	Decelerator configuration			
			TB	AB	TBB	AC
1	Optimum initial operating Mach number at full-drag effectiveness	M = V/C	3	3	3	2.75
2	Dynamic pressure at initial Mach number	Lb/sq ft	25	25	25	22
3	Altitude at initial Mach number	Ft × 10^3	54.2	54.2	54.2	50.5
4	Adiabatic wall temperature at initial Mach number	F	520	520	520	420
5	Drag area at initial Mach number ($C_D A$)	Sq ft	200.5	358.5	358.5	370
6	Diameter	Ft	17.5	18.9	21.3	18.2
7	Drag coefficient, C_D (total)		0.832	1.28	1.005	1.42
8	Decelerator weight based on					
	Dacron at 350F	Lb	78.9	70.4	19.55	71.2
	Nomex at 600F	Lb	117.5	104.8	29.7	105.5
9	Minimum practical decelerator envelope unit weight for combined thermal and aerodynamic loading environment including porosity coating weight of 0.01 lb/sq ft					
	Dacron	Lb/sq ft	0.04	0.047	0.04	0.105
	Operating temperature	F	440	400	440	200
	Nomex	Lb/sq ft	N/A	N/A	N/A	N/A
	Operating temperature	F	N/A	N/A	N/A	N/A
10	Total decelerator surface area	Sq ft	1344	1415	918	431

10	Total decelerator surface area	Sq ft	[illegible]	[illegible]	918	191
11	Total decelerator weight (based on Item 9)					
	Dacron	Lb	132.9	116.3	58.8	58.7
	Nomex	Lb	N/A	N/A	N/A	N/A
12	Auxiliary gas inflation aid weight based on gas source					
	BALLUTEs	Lb	4	4.8	2.9	. . .
	AIRMAT cone	Lb	. . .	. . .	. . .	5
13	Packaging volume required based on					
	Packing density = 20 lb/cu ft	Cu ft	6.65	5.8	2.94	2.94
	Packing density = 30 lb/cu ft	Cu ft	4.43	3.9	1.96	1.96
14	Inflated decelerator volume	Cu ft	3030	3630	2220	246
15	Specified inflation time (from start of deployment)	Sec	1.5	1.5	1.5	1.5
16	Mach number at deployment initiation		3.1	3.1	3.1	2.83
17	Dynamic pressure at deployment	Lb/sq ft	25.4	25.4	25.4	22.93
18	Adiabatic wall temperature at deployment	F	570	570	570	500
19	Centroid of inflated volume	X_v/D_v	4.977	0.643	0.357	0.138
20	Transverse radius of gyration of decelerator squared	Sq ft	42.1	48.2	43.6	31.0
21	Transverse radius of gyration of composite system squared	Sq ft	18.4	8.72	7.36	7.04
22	Rotational radius of gyration of decelerator squared	Sq ft	66.2	84.2	71.4	54.1
23	Rotational radius of gyration of composite system squared	Sq ft	10.9	11.31	9.11	8.7
24	Centroid of decelerator weight (from capsule base)	X_o/D_v	5.005	0.748	0.465	0.138
25	Composite system cg position	X_{cg}/D_v	0.512	0.286	0.262	0.254
26	Composite system cp position	X_{cp}/D_v	. . .	1.10	1.24	1.06
27	Estimated C_{N_α} (average) = C_{Y_β} (per degree)		0.01	0.01	0.02	0.005
28	Estimated $(C_{m_q} + C_{m_{\dot{\alpha}}})$	(qD_v/V) (ref)	0	-0.084	-0.13	-0.13
29	Added mass of inflation gas (approximate)	Slugs	0.165	0.2	0.12	N/A
30	Apparent mass effect of boundary layer	Slugs	0.0384	0.044	0.032	0.02

*For explanation of each item, see comments at beginning of Appendix A.

TABLE A-X - COMPARISON OF DECELERATOR CHARACTERISTICS

Trajectory no. 22

Atmosphere VM7

Vehicle characteristics

Diameter, D_v (ft) 16

Mass (slugs) 84.5

Ballistic parameter, $\left(M/C_DA\right)_v$ 0.3

Drag area, $\left(C_DA\right)_v$

(sq ft) 281.5

Weight, W_E (Earth lb) 2720

Initial entry angle (deg) 16

Initial entry velocity (fps) 16,000

Target altitude (ft) 20,000

Target Mach no. 1.0

Decelerator configuration code

TB - trailing BALLUTE (80 deg with plain back)

AB - attached BALLUTE

TBB - tucked-back BALLUTE

AC - AIRMAT cone (120 deg)

Item no. *	Characteristic	Dimension	Decelerator configuration			
			TB	AB	TBB	AC
1	Optimum initial operating Mach number at full-drag effectiveness	M = V/C	2	2	2	2
2	Dynamic pressure at initial Mach number	Lb/sq ft	10.05	10.05	10.05	10.05
3	Altitude at initial Mach number	Ft × 10^3	58.1	58.1	58.1	58.1
4	Adiabatic wall temperature at initial Mach number	F	200	200	200	200
5	Drag area at initial Mach number (C_DA)	Sq ft	256	538	538	538
6	Diameter	Ft	17.2	22.95	25.37	21.8
7	Drag coefficient, C_D (total)		1.1	1.3	1.065	1.44
8	Decelerator weight based on					
	Dacron at 350F	Lb	46.3	50.6	13.3	48.2
	Nomex at 600F	Lb	65.8	76.8	20.2	72.6
9	Minimum practical decelerator envelope unit weight for combined thermal and aerodynamic loading environment including porosity coating weight of 0.01 lb/sq ft					
	Dacron	Lb/sq ft	0.02	0.019	0.013	0.046
	Operating temperature	F	250	260	350	100
	Nomex	Lb/sq ft	N/A	N/A	N/A	N/A
	Operating temperature	F	N/A	N/A	N/A	N/A
10	Total decelerator surface area	Sq ft	1297	2030	1282	538

11	Total decelerator weight (based on Item 9)					
	Dacron	Lb	52.5	62	28.7	29.3
	Nomex	Lb	N/A	N/A	N/A	N/A
12	Auxiliary gas inflation aid weight based on gas source					
	BALLUTEs	Lb	2.5	5.5	3.2	. . .
	AIRMAT cone	Lb	. . .	. . .	. . .	5
13	Packaging volume required based on					
	Packing density = 20 lb/cu ft	Cu ft	2.63	3.1	1.44	1.47
	Packing density = 30 lb/cu ft	Cu ft	1.75	2.07	0.957	0.977
14	Inflated decelerator volume	Cu ft	2900	6430	3680	358
15	Specified inflation time (from start of deployment)	Sec	1.5	1.5	1.5	1.5
16	Mach number at deployment initiation		2.05	2.05	2.05	2.05
17	Dynamic pressure at deployment	Lb/sq ft	10.4	10.4	10.4	10.4
18	Adiabatic wall temperature at deployment	F	250	250	250	250
19	Centroid of inflated volume	X_v/D_v	4.721	0.607	0.274	0.106
20	Transverse radius of gyration of decelerator squared	Sq ft	40.7	62.0	61.9	35.9
21	Transverse radius of gyration of composite system squared	Sq ft	19.8	18.36	17.51	17.22
22	Rotational radius of gyration of decelerator squared	Sq ft	64.0	124.8	101.5	82.4
23	Rotational radius of gyration of composite system squared	Sq ft	19.12	20.75	18.99	18.8
24	Centroid of decelerator weight (from capsule base)	X_o/D_v	4.741	0.713	0.357	0.106
25	Composite system cg position	X_{cg}/D_v	0.342	0.267	0.255	0.252
26	Composite system cp position	X_{cp}/D_v	. . .	1.003	1.11	0.955
27	Estimated C_{N_α} (average) = C_{Y_β} (per degree)		0.01	0.01	0.02	0.005
28	Estimated $(C_{m_q} + C_{m_{\dot{\alpha}}})$	(qD_v/V) (ref)	0	-0.125	-0.137	-0.10
29	Added mass of inflation gas (approximate)	Slugs	0.105	0.23	0.133	N/A
30	Apparent mass effect of boundary layer	Slugs	0.024	0.05	0.035	0.022

*For explanation of each item, see comments at beginning of Appendix A.

TABLE A-XI - COMPARISON OF DECELERATOR CHARACTERISTICS

Trajectory no. 22
Atmosphere VM7

Vehicle characteristics
Diameter, D_v (ft) 16
Mass (slugs) 84.5
Ballistic parameter, $\left(M/C_D A\right)_v$ 0.3
Drag area, $\left(C_D A\right)_v$
(sq ft) 281.5
Weight, W_E (Earth lb) 2720

Initial entry angle (deg) 16
Initial entry velocity (fps) 16,000

Target altitude (ft) 30,000
Target Mach no. 1.0

Decelerator configuration code
TB - trailing BALLUTE (80 deg with plain back)
AB - attached BALLUTE
TBB - tucked-back BALLUTE
AC - AIRMAT cone (120 deg)

Item no. *	Characteristic	Dimension	Decelerator configuration			
			TB	AB	TBB	AC
1	Optimum initial operating Mach number at full-drag effectiveness	M = V/C	2	2	2	2
2	Dynamic pressure at initial Mach number	Lb/sq ft	10.05	10.05	10.05	10.05
3	Altitude at initial Mach number	Ft × 10^3	58.1	58.1	58.1	58.1
4	Adiabatic wall temperature at initial Mach number	F	200	200	200	200
5	Drag area at initial Mach number ($C_D A$)	Sq ft	350.5	633	633	633
6	Diameter	Ft	19.95	24.9	28.07	23.7
7	Drag coefficient, C_D (total)		1.12	1.3	1.02	1.435
8	Decelerator weight based on					
	Dacron at 350F	Lb	68.7	65.2	17.9	70.4
	Nomex at 600F	Lb	102.8	98.4	48.5	102.1
9	Minimum practical decelerator envelope unit weight for combined thermal and aerodynamic loading environment including porosity coating weight of 0.01 lb/sq ft					
	Dacron	Lb/sq ft	0.02	0.019	0.013	0.046
	Operating temperature	F	250	260	350	100
	Nomex	Lb/sq ft	N/A	N/A	N/A	N/A
	Operating temperature	F	N/A	N/A	N/A	N/A
10	Total decelerator surface area	Sq ft	1750	2465	1600	710

11	Total decelerator weight (based on Item 9)					
	Dacron	Lb	74.3	77	36.9	39.4
	Nomex	Lb	N/A	N/A	N/A	N/A
12	Auxiliary gas inflation aid weight based on gas source					
	BALLUTEs	Lb	3.9	7.2	4.4	. . .
	AIRMAT cone	Lb	. . .	. . .	. . .	8
13	Packaging volume required based on					
	Packing density = 20 lb/cu ft	Cu ft	3.71	3.85	1.85	1.97
	Packing density = 30 lb/cu ft	Cu ft	2.48	2.56	1.23	1.31
14	Inflated decelerator volume	Cu ft	4530	8330	5090	526
15	Specified inflation time (from start of deployment)	Sec	1.5	1.5	1.5	1.5
16	Mach number at deployment initiation		2.05	2.05	2.05	2.05
17	Dynamic pressure at deployment	Lb/sq ft	10.4	10.4	10.4	10.4
18	Adiabatic wall temperature at deployment	F	250	250	250	250
19	Centroid of inflated volume	X_v/D_v	4.836	0.63	0.353	0.131
20	Transverse radius of gyration of decelerator squared	Sq ft	54.7	83.7	75.7	40.7
21	Transverse radius of gyration of composite system squared	Sq ft	22.9	19.33	17.9	17.45
22	Rotational radius of gyration of decelerator squared	Sq ft	86.1	146.2	124.2	92.9
23	Rotational radius of gyration of composite system squared	Sq ft	20.3	22.05	19.6	19.22
24	Centroid of decelerator weight (from capsule base)	X_o/D_v	4.861	0.737	0.459	0.131
25	Composite system cg position	X_{cg}/D_v	0.384	0.272	0.257	0.253
26	Composite system cp position	X_{cp}/D_v	. . .	1.09	1.23	1.038
27	Estimated C_{N_α} (average) = C_{Y_β} (per degree)		0.01	0.01	0.02	0.005
28	Estimated $(C_{m_q} + C_{m_{\dot{\alpha}}})$	(qD_v/V) (ref)	0	-0.104	-0.129	-0.109
29	Added mass of inflation gas (approximate)	Slugs	0.164	0.3	0.184	N/A
30	Apparent mass effect of boundary layer	Slugs	0.038	0.067	0.049	0.03

*For explanation of each item, see comments at beginning of Appendix A.

APPENDIX B - REFINED POINT-MASS TRAJECTORY COMPUTATIONS AND TRANSIENT HEATING CALCULATIONS

The figures in this appendix present the space/time and envelope transient temperature histories of the decelerator envelope fabric for the entry cases in Table III of this report. The envelope fabric in all cases was dacron.

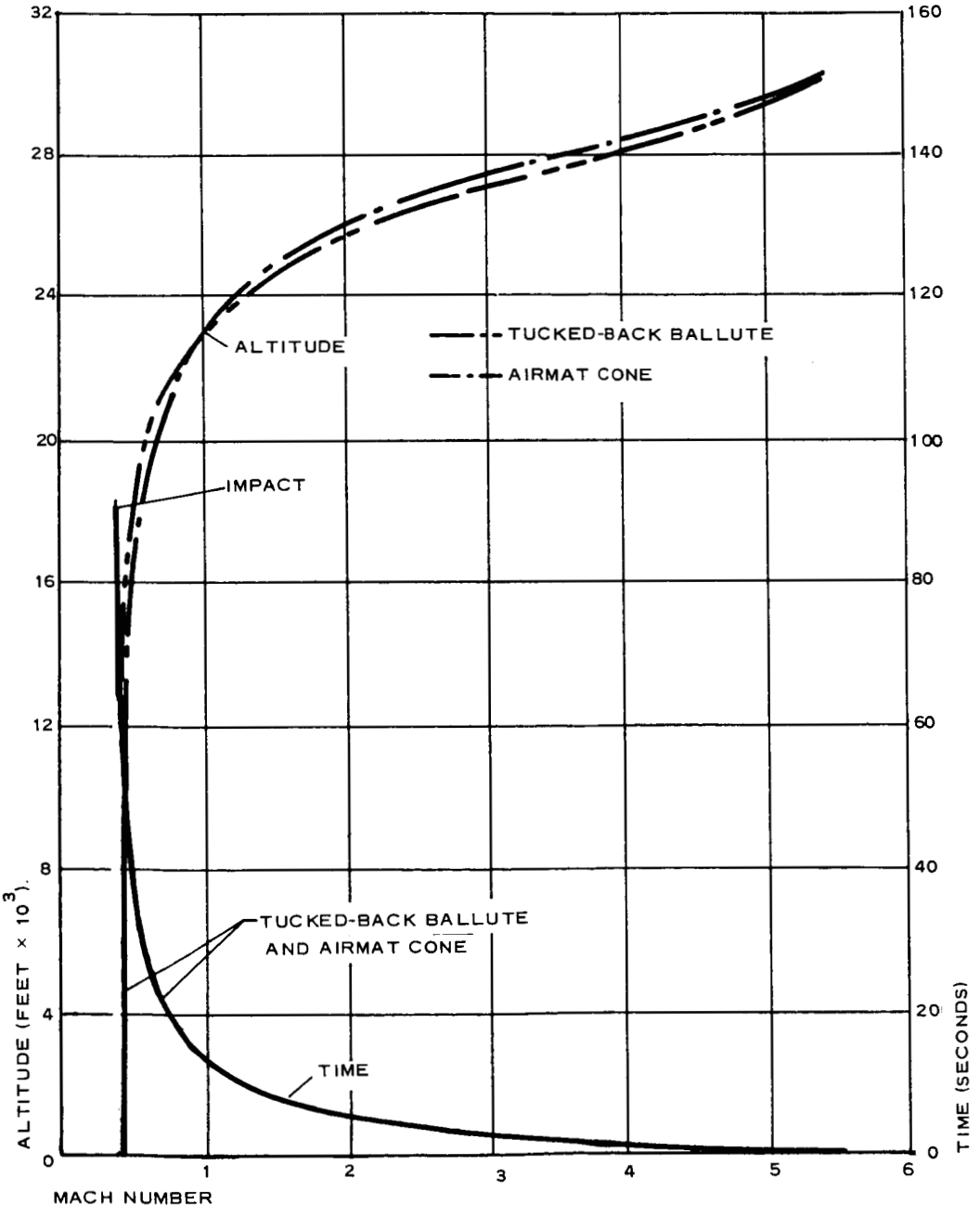
ALTITUDE
TUCKED-BACK BALLUTE
AIRMAT CONE
IMPACT
TUCKED-BACK BALLUTE
AND AIRMAT CONE
TIME
ALTITUDE (FEET × 10³)
TIME (SECONDS)
MACH NUMBER
0
4
8
12
16
20
24
28
32
0
20
40
60
80
100
120
140
160
1
2
3
4
5
6

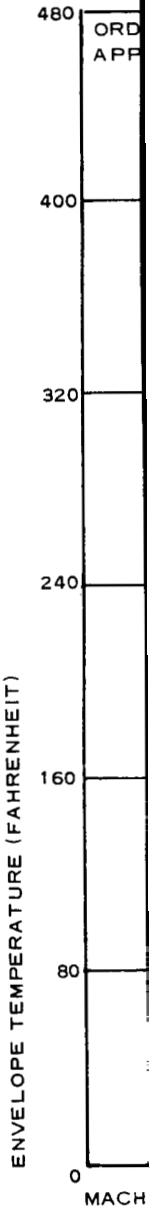
ENVELOPE TEMPERATURE (FAHRENHEIT)
480
400
320
240
160
80
0
MACH

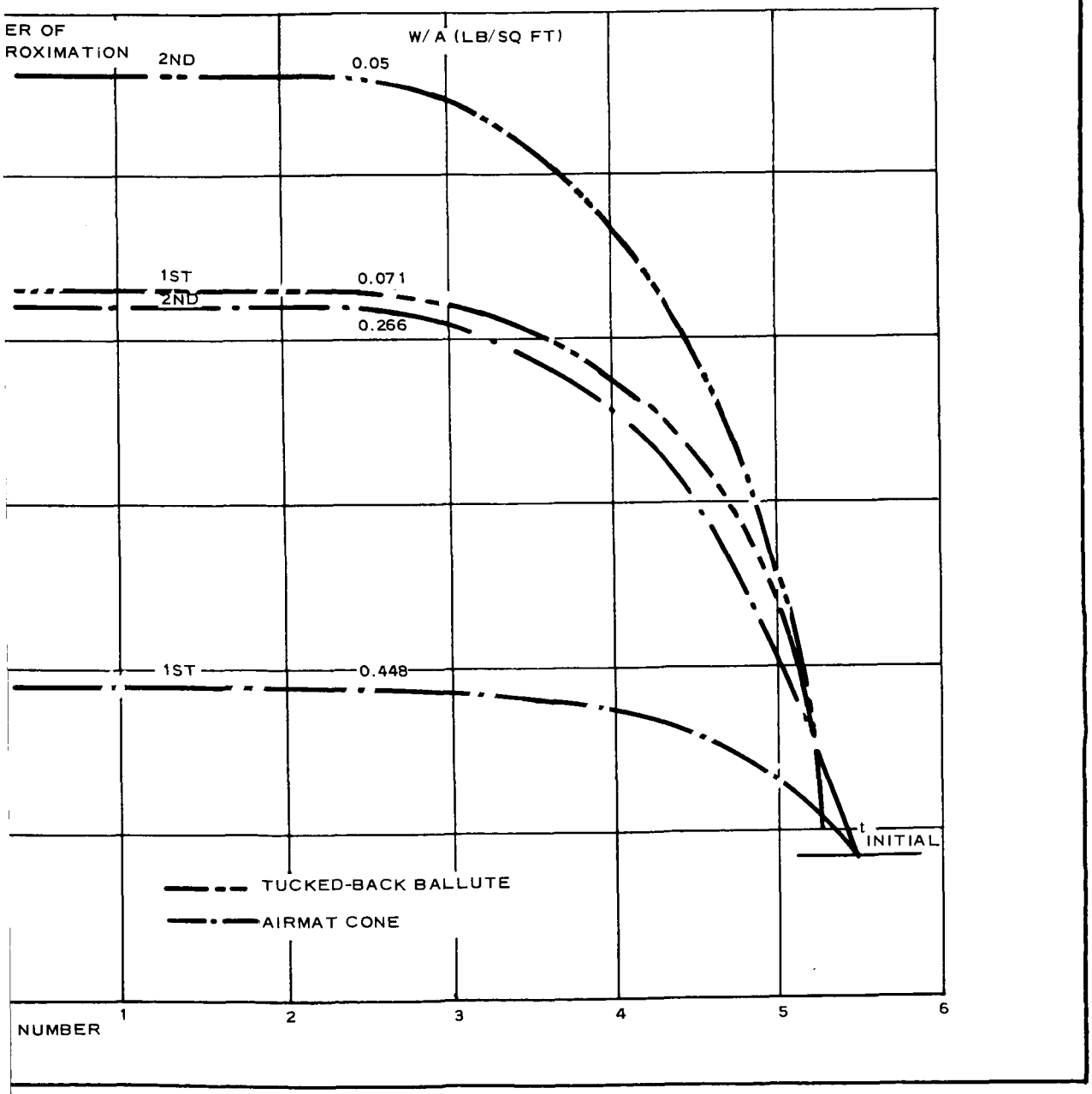

Figure B-1 - Space/Time and Envelope Transient Temperature versus Mach Number (Trajectory A1)

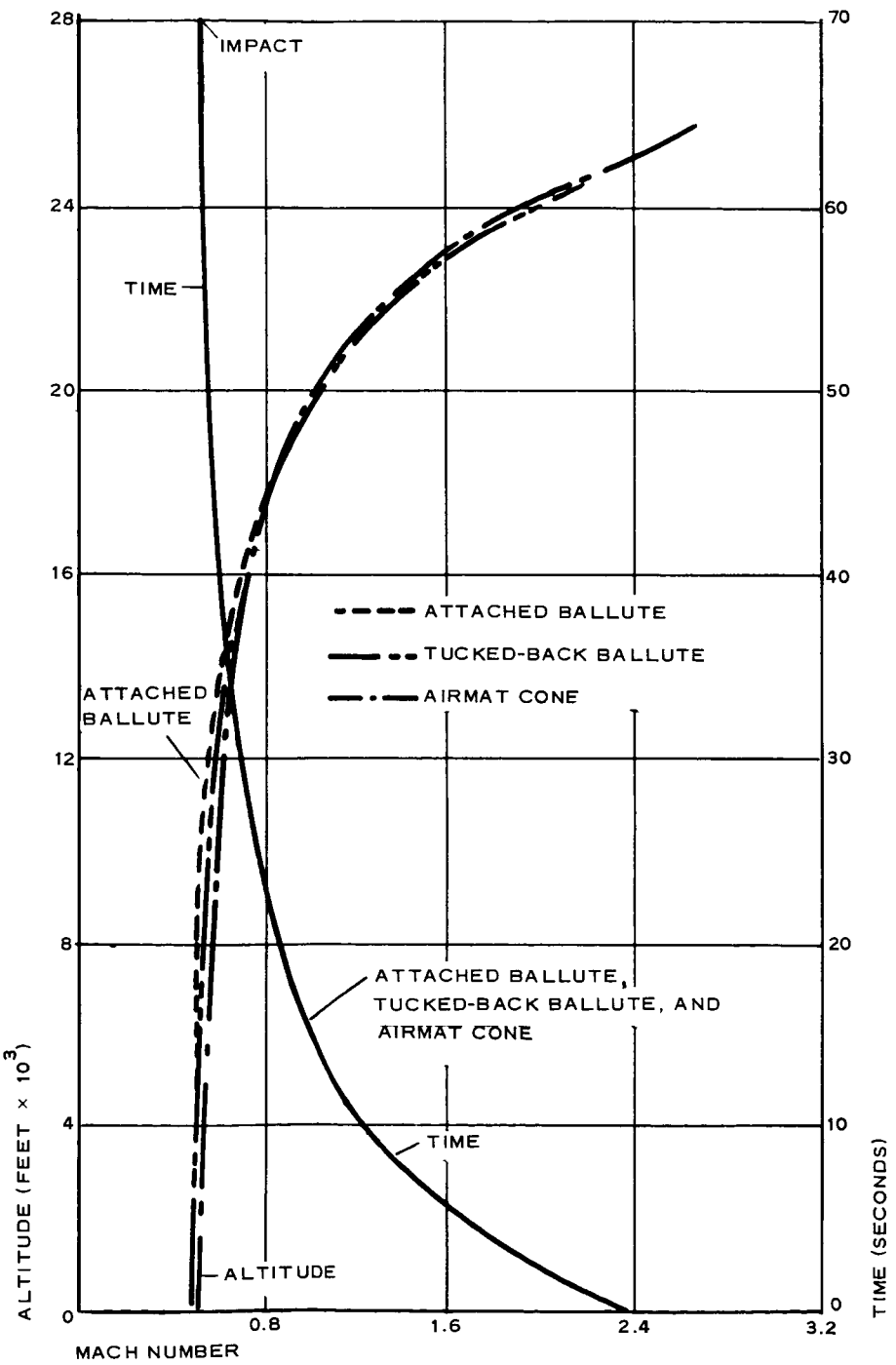
IMPACT
TIME
ATTACHED BALLUTE
TUCKED-BACK BALLUTE
AIRMAT CONE
ATTACHED BALLUTE
ATTACHED BALLUTE, TUCKED-BACK BALLUTE, AND AIRMAT CONE
TIME
ALTITUDE
ALTITUDE (FEET × 10^3)
TIME (SECONDS)
MACH NUMBER
0
4
8
12
16
20
24
28
0
10
20
30
40
50
60
70
0.8
1.6
2.4
3.2

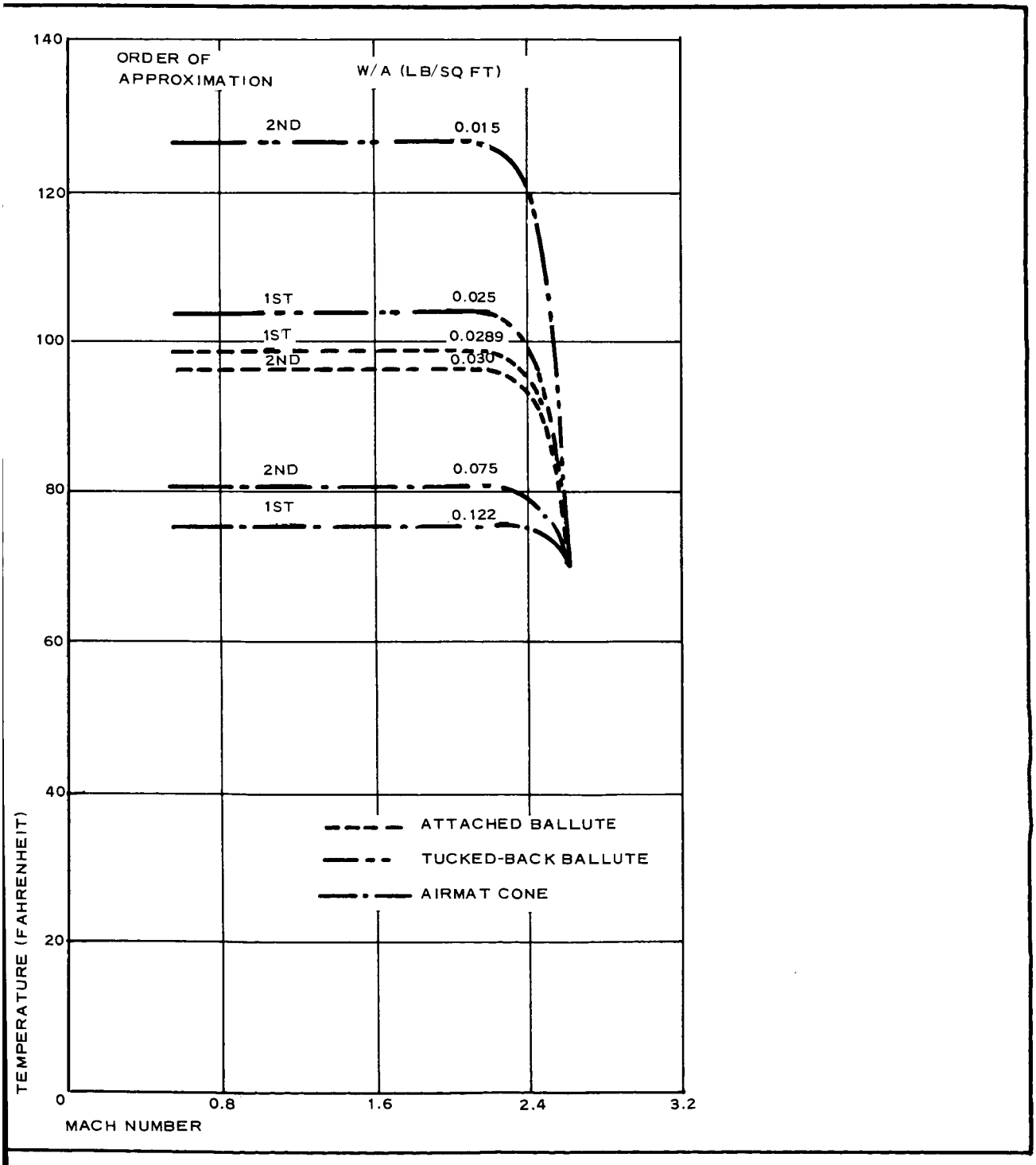

Figure B-2 - Space/Time and Envelope Transient Temperature versus Mach Number (Trajectory B3)

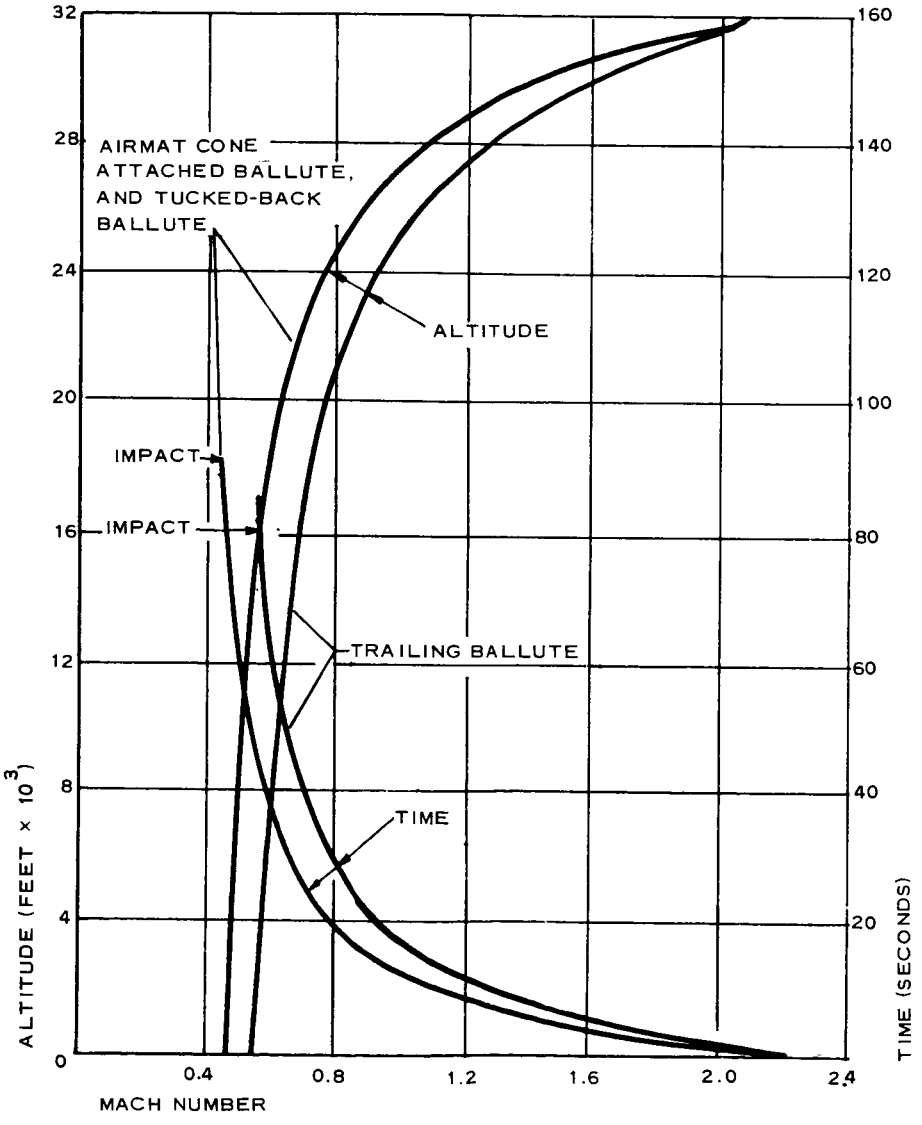
AIRMAT CONE ATTACHED BALLUTE, AND TUCKED-BACK BALLUTE
ALTITUDE
IMPACT
IMPACT
TRAILING BALLUTE
TIME
ALTITUDE (FEET x 10^3)
TIME (SECONDS)
MACH NUMBER
0
4
8
12
16
20
24
28
32
20
40
60
80
100
120
140
160
0.4
0.8
1.2
1.6
2.0
2.4

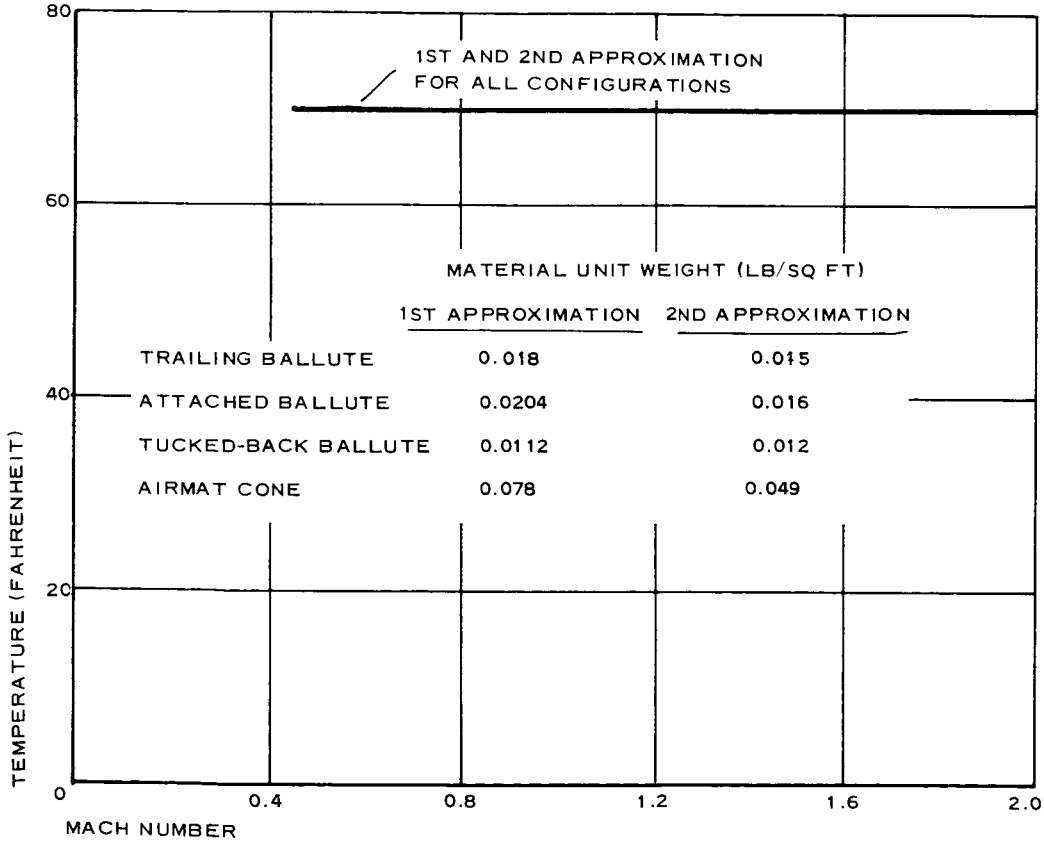

Figure B-3 - Space/Time and Envelope Transient Temperature versus Mach Number (Trajectory 19)

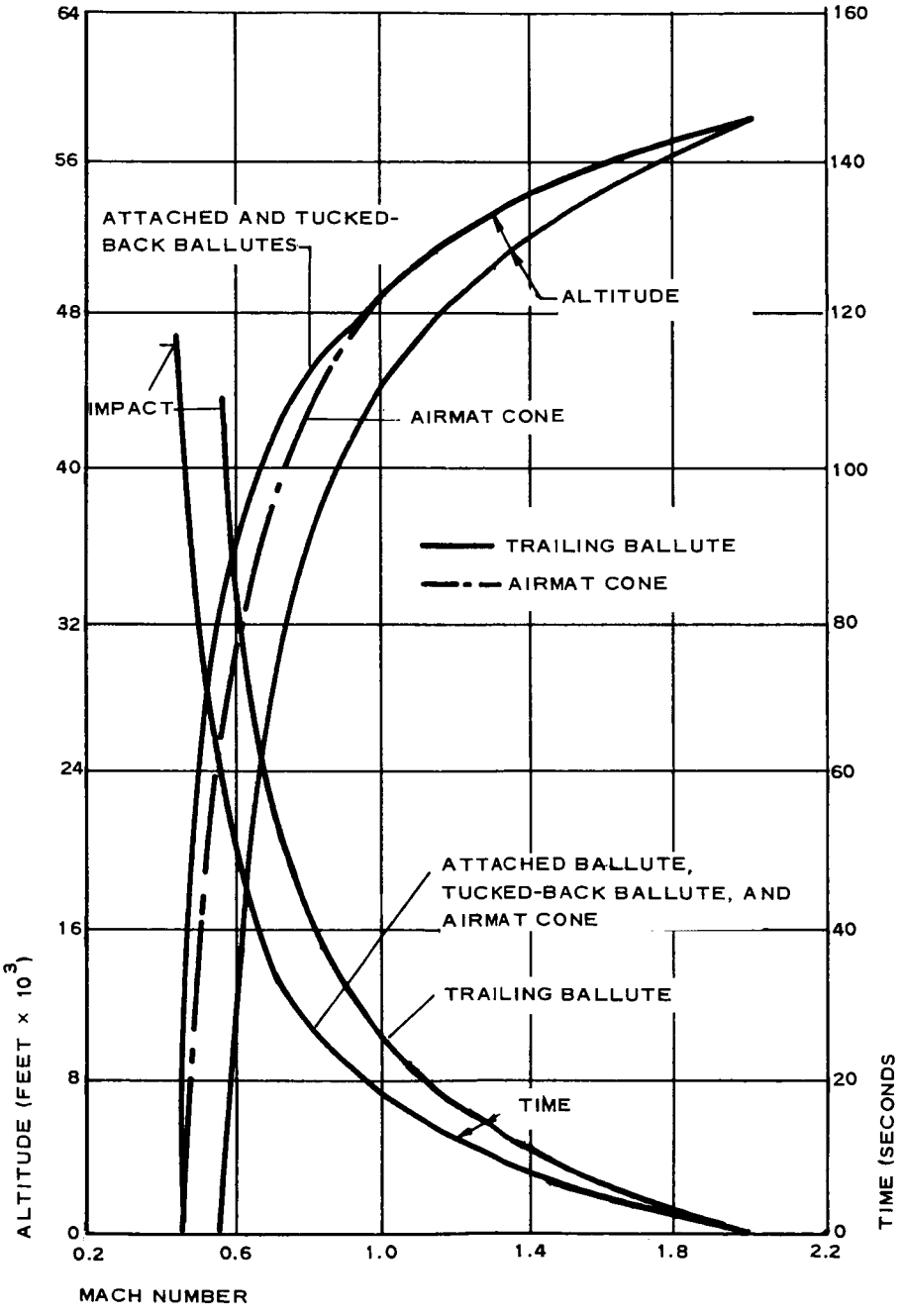
64
56
48
40
32
24
16
8
0
160
140
120
100
80
60
40
20
0
0.2
0.6
1.0
1.4
1.8
2.2
MACH NUMBER
ALTITUDE (FEET × 10³)
TIME (SECONDS
ATTACHED AND TUCKED-BACK BALLUTES
ALTITUDE
IMPACT
AIRMAT CONE
TRAILING BALLUTE
AIRMAT CONE
ATTACHED BALLUTE, TUCKED-BACK BALLUTE, AND AIRMAT CONE
TRAILING BALLUTE
TIME

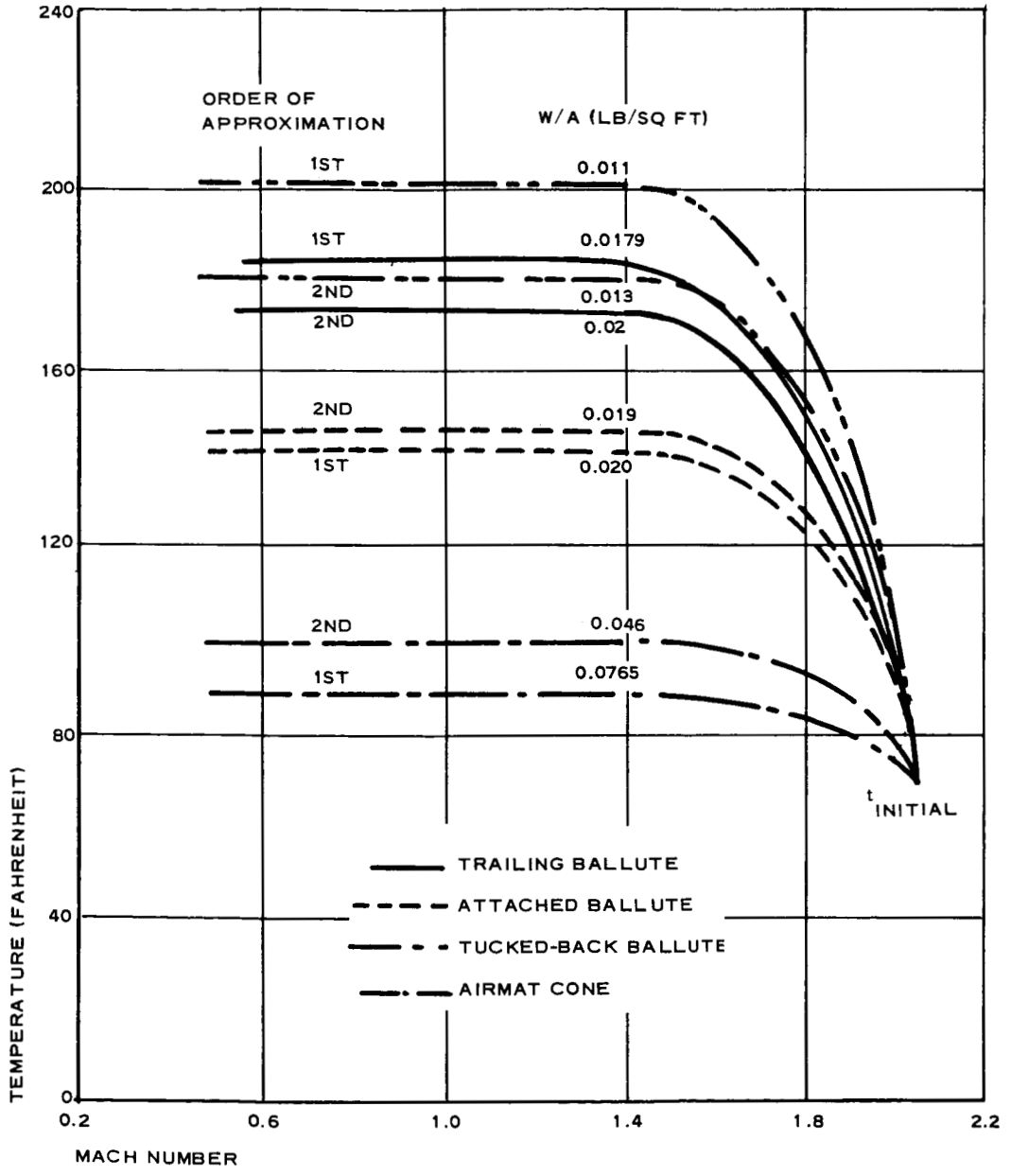

Figure B-4 - Space/Time and Envelope Transient Temperature versus Mach Number (Trajectory 22)

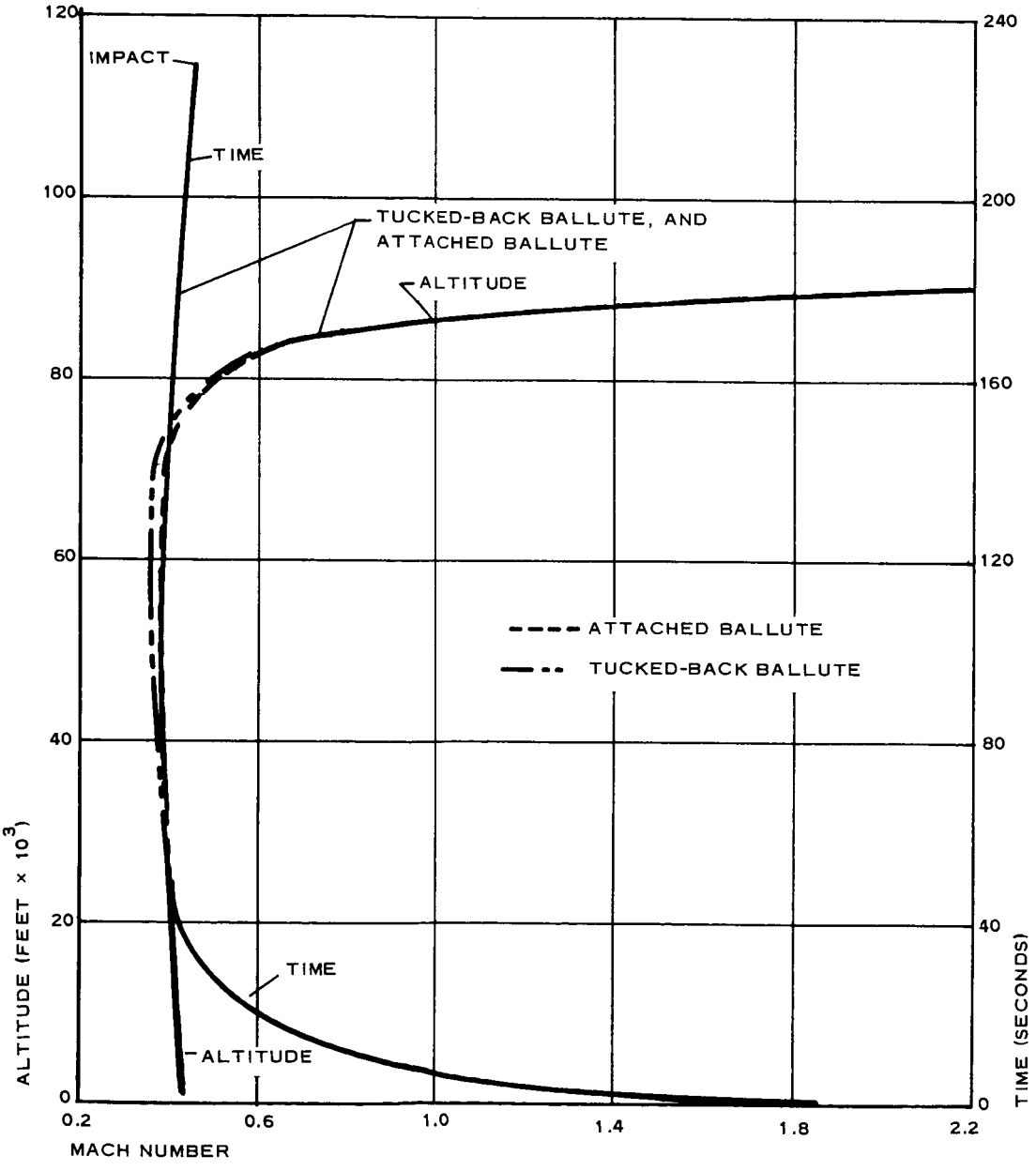
120
100
80
60
40
20
0
240
200
160
120
80
40
0
IMPACT
TIME
TUCKED-BACK BALLUTE, AND
ATTACHED BALLUTE
ALTITUDE
ATTACHED BALLUTE
TUCKED-BACK BALLUTE
TIME
ALTITUDE
0.2
0.6
1.0
1.4
1.8
2.2
MACH NUMBER
ALTITUDE (FEET x 10^3)
TIME (SECONDS)

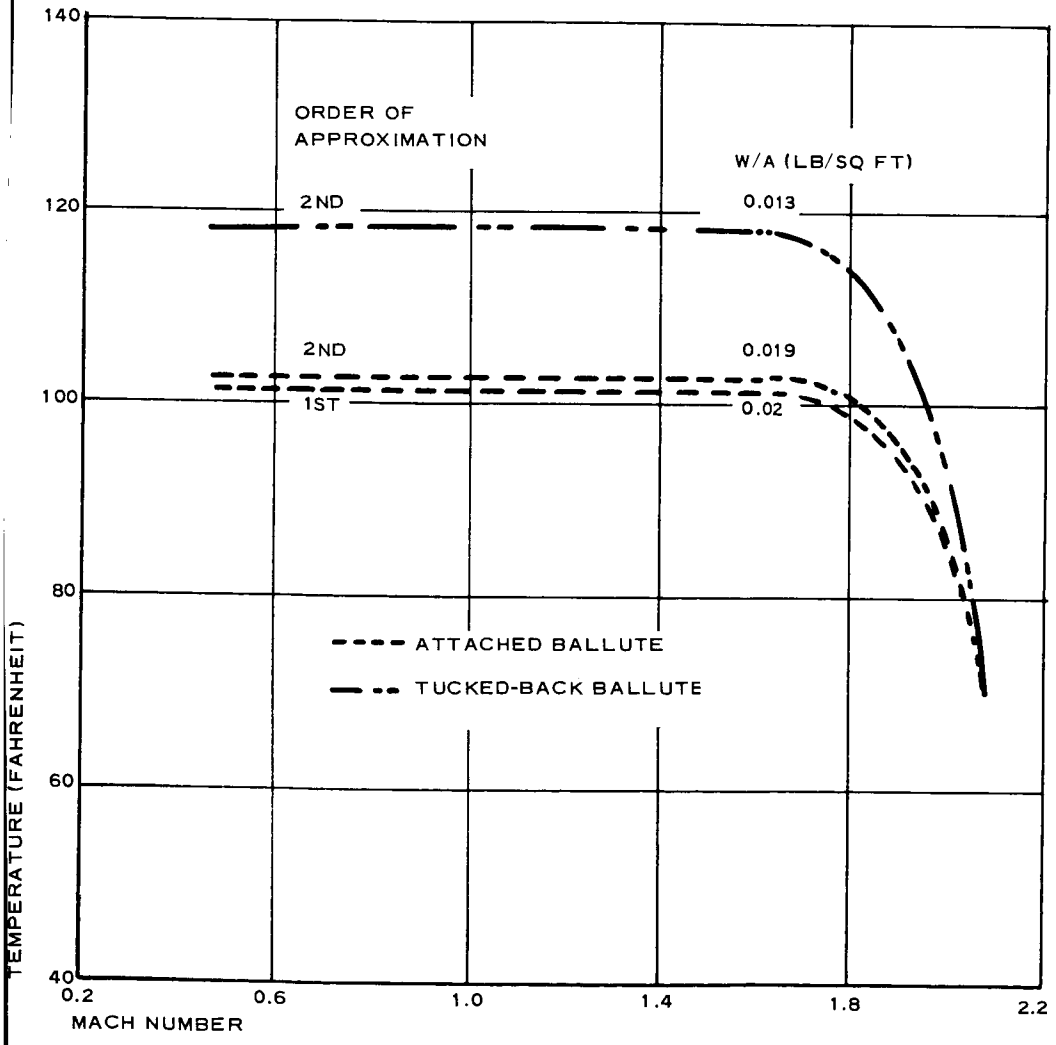

Figure B-5 - Space/Time and Envelope Transient Temperature versus Mach Number (Trajectory 23)

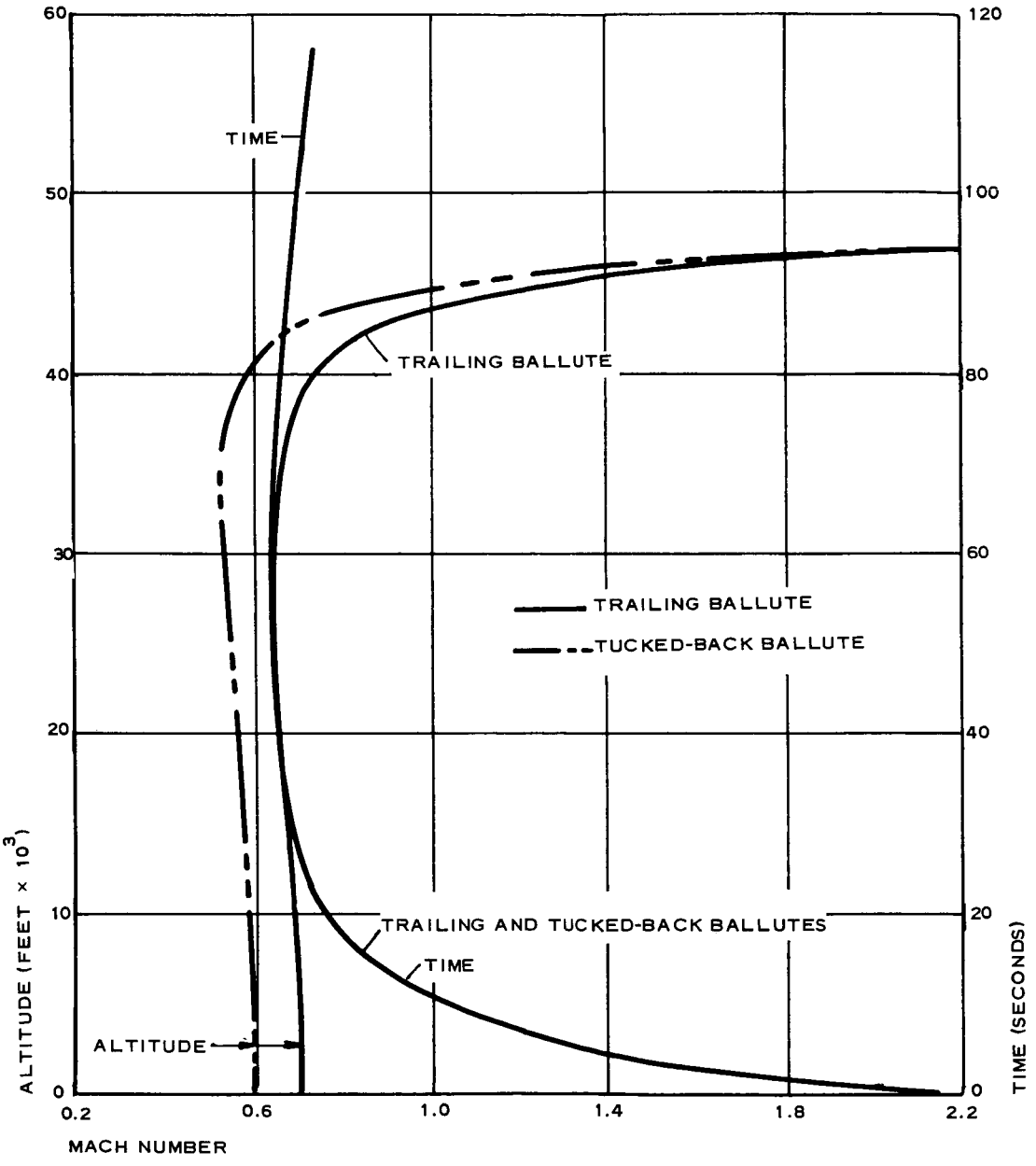
60
50
40
30
20
10
0
120
100
80
60
40
20
0
TIME
TRAILING BALLUTE
TRAILING BALLUTE
TUCKED-BACK BALLUTE
TRAILING AND TUCKED-BACK BALLUTES
TIME
ALTITUDE
ALTITUDE (FEET × 10^3)
TIME (SECONDS)
0.2
0.6
1.0
1.4
1.8
2.2
MACH NUMBER

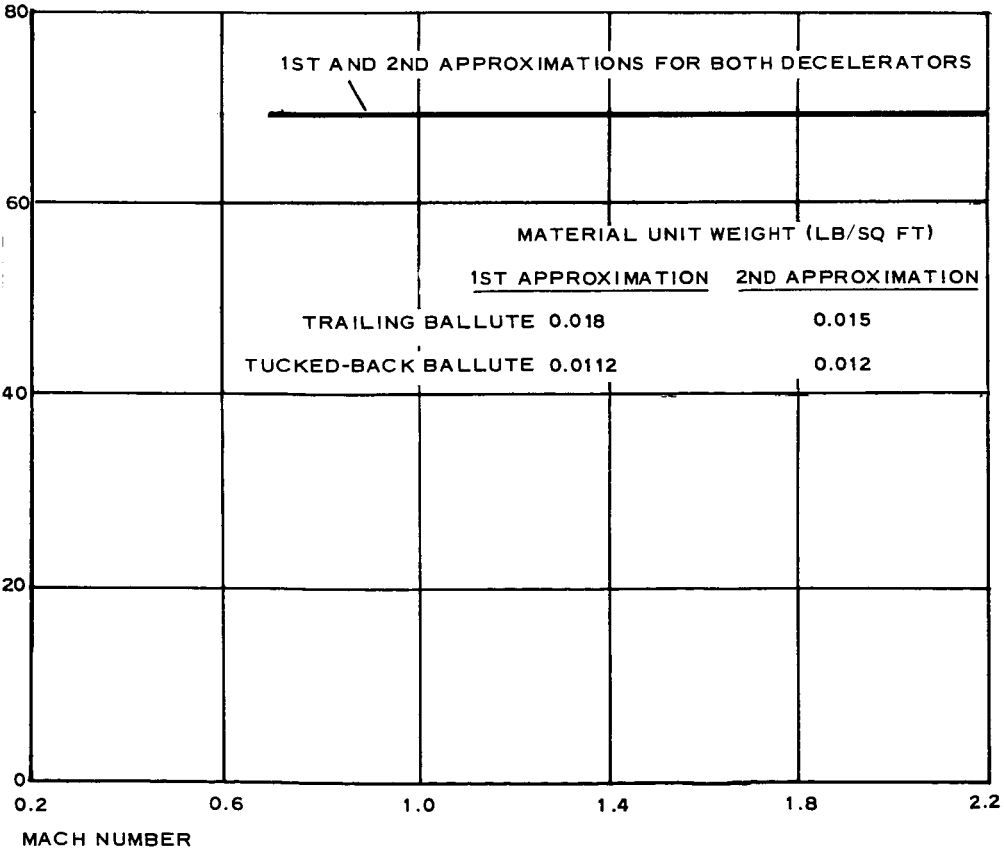

Figure B-6 - Space/Time and Envelope Transient Temperature versus Mach Number (Trajectory 30)

APPENDIX C - DISCUSSION OF DYNAMIC STABILITY ANALYSES

1. INTRODUCTION

The determination of the dynamic motion characteristics for a recoverable space vehicle landing on the surface of Mars with attached or trailing aerodynamic decelerators is a primary requirement. The motion characteristics will predominantly affect the design of terminal impact control systems, whether they are of the hard- or soft-landing type.

Additionally, as shown by the results of this study, there is relatively little weight advantage indicated for a particular decelerator configuration on a drag performance basis. Consequently, the choice of a particular configuration largely could be dictated by dynamic performance characteristics.

The weight analysis developed in this study was based on static aerodynamic loading relationships with empirically determined, quasi-static load, temperature and design factors employed to account for operating environmental effects and material characteristics. This weight analysis of necessity preceeded the dynamic analysis, assuming adequate aerodynamic stability of the various configurations and little dynamics interaction with the decelerator strength-weight requirements. This interaction is discussed subsequently in this appendix as related to the attached decelerator configurations.

The development of an adequate mathematical model formulated for use with high-speed digital computer equipment is a prerequisite to analyze dynamic motion and to secure results within reasonable time scales.

The dynamic motion about the flight path of an aerodynamic expandable

decelerator is quite complex; particularly, if spin about the longitudinal axis of the entry capsule is present prior to deployment of the decelerator device. Spin may be induced intentionally or be present inherently for rotationally symmetric bodies traversing entry-flight paths. Intentionally induced spin (usually small, about 1.0 rad/sec or less and not intended for spin stabilization) primarily minimizes deviations from the flight path as a result of lateral cg tolerance and ensures symmetry of heating over the forward portion of the entry capsule.

During the early IRBM and ICBM nose cone development programs, it was found that nose cones not intentionally spun would develop inherent spin during entry through the earth's atmosphere as a result of lateral cg tolerance and asymmetric ablation when incorporating this method of heat insulation. Typical spin rates encountered in this manner were of the order of 0.2 rad/sec. The alternative to spinning is an active, three-axis control system with aerodynamic or jet-reaction controls.

For the case of an aerodynamic body with a trailing aerodynamic decelerator, there are 18 deg of freedom when the motions of the riser and suspension system between the forebody and trailing decelerator are considered. This assumes that each of the separate components, i.e., forebody, riser and suspension lines, and trailing decelerator can be treated as rigid bodies. If flexibility and torsional deflection modes were considered for each component, then the system has 36 deg of freedom. The solution of this motion description during the real-time trajectory of an entry body and trailing decelerator from deployment to impact, using the required integration intervals, would be prohibitive or at least unrealistic even with the highest speed and capacity digital computers available.

Experience has indicated (at least for purposes of parametric analyses) that the physical description for the dynamic motion of a body can be approximated reasonably by neglecting flexibility effects or by introducing this consideration as a modification to rigid-body parameters

and coefficients. Additional simplifications in the mathematical formulations can be made with appropriate assumptions and approximations such as linearization of non-linear terms, small angle approximations, invariant parameters, constant coefficients, etc. For bodies defined as having rotational symmetry and weight distribution, the proper choice of body reference axes about and along which the motions can be described eliminates cross products of inertia and decouples pitch and yaw angular rates from the roll mode since the transverse moments of inertia of the body are implicitly equal. Additionally, if the capsule is not accelerating in longitudinal flight or is near terminal velocity conditions, the longitudinal force equation usually may be surpressed and the space-time history adequately described by separate, more simple point-mass trajectory computations.

2. ANALYSIS

Goodyear Aerospace has developed in Appendix B of Volume II, equations of motion with six and eight degrees of freedom to describe the characteristics of composite systems with attached or trailing aerodynamic decelerators entering planetary atmospheres. The formulations were developed for use with the IBM 360 computer system available at the Goodyear Aerospace computer facilities. No additional explanation of this formulation is made in this appendix. However, to illustrate what factors and parameters are important in the force and moments affecting the motion characteristics of composite entry capsule/-decelerator systems, the following simplified equations are set forth using conventional airframe-dynamic-stability notation. This notation is not the same as employed in Appendix B of Volume II.

For the cases of an entry capsule with attached decelerator configurations, the force and moment equations may be written in terms of principal axes of a body. Thus, the system moments of inertia are independent of the angular motions about the axes and are constant with the result that all products of inertia are eliminated.

Force equations[a]

$$\ddot{x} = \sum\left(C_X\right)\left(\frac{\bar{q}A}{m}\right)$$

$$\ddot{y} = \sum\left(C_Y\right)\left(\frac{\bar{q}A}{m}\right)$$

$$\ddot{z} = \sum\left(C_Z\right)\left(\frac{\bar{q}A}{m}\right)$$

Moment equations

$$\dot{p} = \sum\left(C\right)\left(\frac{\bar{q}Ad}{I_x}\right) - qr\left(\frac{I_z - I_y}{I_x}\right)$$

$$\dot{q} = \sum\left(C_m\right)\left(\frac{\bar{q}Ad}{I_y}\right) - pr\left(\frac{I_x - I_z}{I_y}\right)$$

$$\dot{r} = \sum\left(C_n\right)\left(\frac{\bar{q}Ad}{I_z}\right) - pq\left(\frac{I_y - I_x}{I_z}\right)$$

The summation sign implies consideration of all approriate aerodynamic factors for both the vehicle and decelerator. As previously noted above and as used in the study, the transverse moments of inertia were defined as equal, eliminating effects of inertia coupling in the roll-angular acceleration equation. Using Items 21 and 23 of Tables A-III and A-XI of Appendix A, the inertia coupling effect is about 10 percent of the cross-plane angular velocity for either the pitch or yaw angular acceleration equations. The effect will be oscillatory in accordance with the sign of the cross-plane angular velocity since the roll damping was negligible and the roll rate remained constant in the computations of this analysis. Thus, the roll-angular acceleration equation is eliminated from further discussion in this appendix.

The parameters $\left(\frac{\bar{q}A}{m}\right)$ and $\left(\frac{\bar{q}Ad}{I_{y,z}}\right)$ given below for trajectories 19 and 22 are

[a]See List of Symbols at the end of this appendix for definition of terms.

evaluated at initial operation and near terminal conditions for each attached decelerator configuration from Tables A-III and A-XI.

Parameters for trajectory 19 (VM8)

	AB	TBB	AC
$\left(\frac{\bar{q}A}{m}\right)_i$	65	85	59
$\left(\frac{\bar{q}A}{m}\right)_t$	12.3	14.4	12.4
$\left(\frac{\bar{q}Ad}{I_{y,z}}\right)_i$	91	147	85
$\left(\frac{\bar{q}Ad}{I_{y,z}}\right)_t$	17.3	25	17.8

Parameters for trajectory 22 (VM7)

	AB	TBB	AC
$\left(\frac{\bar{q}A}{m}\right)_i$	58	74	52
$\left(\frac{\bar{q}A}{m}\right)_t$	12.3	13.5	12.9
$\left(\frac{\bar{q}Ad}{I_{y,z}}\right)_i$	66	106	65
$\left(\frac{\bar{q}Ad}{I_{y,z}}\right)_t$	13.9	19.4	15.1

The variation in values tabulated above are indicative only of the differences in geometry of the decelerators since, for practical purposes, the dynamic pressure, $\bar{q}$, is the same and the mass (m) is identical for all cases. Note that the values for these parameters in both the force and moment equations are of comparable magnitude.

The factors comprising the aerodynamic terms contained in the force and moment equations with all coefficients referred to body axes are given below.

Force equations:

$$\frac{\sum F_x}{\bar{q}A} = -C_x$$

$$\frac{\sum F_y}{\bar{q}A} = -C_{N_\mu}\beta + \left[C_{N_q} r + C_{N_\alpha}(\alpha p) - C_{N_{\dot\alpha}}\dot\beta\right]\frac{d}{2V}$$

$$\frac{\sum F_z}{\bar{q}A} = -C_{N_\mu}\alpha - \left[C_{N_q} q + C_{N_\alpha}(\alpha p) + C_{N_{\dot\alpha}}\dot\alpha\right]\frac{d}{2V}$$

Moment equations:

$$\frac{M_x}{\bar{q}Ad} = \sum(C_\ell) = -C_{\ell_p}\frac{pd}{2V} \sim 0 \text{ in this study}$$

$$\frac{M_y}{\bar{q}Ad} = \sum(C_m) = C_{m_\mu}\alpha + \left[C_{m_q} q + C_{m_\alpha}(\alpha p) + C_{m_{\dot\alpha}}\dot\alpha\right]\frac{d}{2V}$$

$$\frac{M_z}{\bar{q}Ad} = \sum(C_n) = C_{m_\mu}\beta + \left[C_{m_q} r + C_{m_\alpha}(\beta p) - C_{m_{\dot\alpha}}\dot\beta\right]\frac{d}{2V}$$

where typically (assuming small angular displacements)

$$\mu \doteq \sqrt{\alpha^2 + \beta^2} = \sqrt{\frac{\dot x^2 + \dot y^2}{V}}$$

$$u \doteq \dot x\ddot x + \dot y\ddot y + \dot z\ddot z$$

$$\dot\alpha \doteq \frac{V\ddot z - \alpha u}{V^2}$$

$$\dot\beta \doteq \frac{V\ddot y - \beta u}{V^2}$$

Note again that the above notation is not the same as that employed in Appendix B of Volume II but is introduced in this appendix to gain an appreciation of what aerodynamic terms may be important. Note that the parenthetical products, (αp) and (βp), which essentially provide damping forces and moments, are generally referred to as the kinematic coupling terms in conventional airframe-dynamic-stability analyses. These terms can have an appreciable effect on the dynamic motion characteristic of a spinning body if large angular excursions in angle of attack and yaw are encountered. Note further that the effect of these terms for a constant roll rate can alternately aid or aggravate the oscillation tendency of the system in the cross-plane modes of motion.

3. RESULTS FOR ATTACHED CONFIGURATIONS

In this study, all aerodynamic damping terms were neglected in the force equations. Pitch and yaw damping was considered in the moment equations. Although no separate coefficient term was introduced to account for the kinematic coupling as defined in the above notation, the coupling effect may be interpreted as being present through the formulation of the angular rate matrix in Appendix B of Volume II.

Now, considering the aerodynamic force and moment equations above, the evaluation of the parameter $(\frac{d}{2V})$ is made for each attached decelerator configuration at initial operation and near terminal conditions as follows:

Parameter for Trajectory 19

	AB	TBB	AC
$(\frac{d}{2V})_i$	0.021	0.024	0.02
$(\frac{d}{2V})_t$	0.041	0.047	0.04

Parameter for trajectory 22

	AB	TBB	AC
$(\frac{d}{2V})_i$	0.014	0.015	0.013
$(\frac{d}{2V})_t$	0.025	0.028	0.024

The values for the parameters given below are taken from Tables A-III and A-XI of Appendix A (Items 25, 26, 27, and 28):

Parameters for trajectory 19

	AB	TBB	AC
$\frac{\Delta X_{cp}}{D_v}$	-0.92	-1.104	-0.876
$C_{N_\alpha} = C_{Y_\beta}$ (per degree)	0.01	0.02	0.005
$C_{m_\alpha} = C_{n_\beta} = C_{N_\alpha} \frac{\Delta X_{cp}}{D_v}$ (per degree)	-0.0092	-0.0221	-0.00438
$C_{m_q} + C_{m_{\dot\alpha}}$ (per radian)	-0.27	-0.336	-0.28

Parameters for trajectory 22

	AB	TBB	AC
$\frac{\Delta X_{cp}}{D_v}$	-0.818	-0.973	-0.785
$C_{N_\alpha} = C_{Y_\beta}$ (per degree)	0.01	0.02	0.005
$C_{m_\alpha} = C_{n_\beta}$ (per degree)	-0.0082	-0.0195	-0.00393
$(C_{m_q} + C_{m_\alpha})$ (per radian)	-0.208	-0.258	-0.218

The aerodynamic force and moment equations at initial operation of the decelerators reduce approximately to the following values:

Force and moment equations for trajectory 19

	AB	TBB	AC
$\frac{\sum F_x}{\bar{q}A} = -C_X = C_D$	1.3	0.99	1.43
$\frac{\sum F_y}{\bar{q}A} = -C_Y$	-0.01β	-0.02β	-0.005β
$\frac{\sum F_z}{\bar{q}A} = -C_N$	-0.01α	-0.02α	-0.005α
$\sum(C_m)$	$-(0.0092\alpha + 0.0057q)$	$-(0.022\alpha + 0.0081q)$	$-(0.0044\alpha + 0.0056q)$
$\sum(C_n)$	$-(0.0092\beta + 0.0057r)$	$-(0.0022\beta + 0.0081r)$	$-(0.0044\beta + 0.0056r)$

Force and moment equations for trajectory 22

	AB	TBB	AC
$\frac{\sum F_x}{\bar{q}A} = -C_X = C_D$	1.3	10.2	1.435
$\frac{\sum F_y}{\bar{q}A} = -C_Y$	-0.01β	-0.02β	-0.005β
$\frac{\sum F_z}{\bar{q}A} = -C_N$	-0.01α	-0.02α	-0.005α
$\sum(C_m)$	$-(0.0082\alpha + 0.0039q)$	$-(0.0192\alpha + 0.0039q)$	$-(0.0039\alpha + 0.00284q)$
$\sum(C_n)$	$-(0.0082\beta + 0.0039r)$	$-(0.0195\beta + 0.0039r)$	$-(0.0039\beta + 0.0028r)$

The linear and angular accelerations due to the aerodynamic forces and moments plus inertia coupling (approximated as 10 percent of the cross-plane angular velocity) at initial operation are as follows.

Linear and angular accelerations for trajectory 19

AB

$$\ddot{x} = -84.5$$
$$\ddot{y} = -0.65\beta$$
$$\ddot{z} = -0.65\alpha$$
$$\dot{p} = 0$$
$$\dot{q} = -0.837\alpha - 0.519q - 0.1r$$
$$\dot{r} = -0.837\beta - 0.519r - 0.1q$$

TBB

$$\ddot{x} = -84.1$$
$$\ddot{y} = -1.7\beta$$
$$\ddot{z} = -1.7\alpha$$
$$\dot{p} = 0$$
$$\dot{q} = -3.23\alpha - 1.19q - 0.1r$$
$$\dot{r} = -3.23\beta - 1.19r - 0.1q$$

AC

$$\ddot{x} = -84.4$$
$$\ddot{y} = -0.295\beta$$
$$\ddot{z} = -0.295\alpha$$
$$\dot{p} = 0$$
$$\dot{q} = -0.374\alpha - 0.476q - 0.1r$$
$$\dot{r} = -0.374\beta - 0.476r - 0.1q$$

Linear and angular accelerations for trajectory 22

AB

$$\ddot{x} = -75.4$$
$$\ddot{y} = -0.58\beta$$
$$\ddot{z} = -0.58\alpha$$
$$\dot{p} = 0$$
$$\dot{q} = -0.541\alpha - 0.257q - 0.1r$$
$$\dot{r} = -0.541\beta - 0.257r - 0.1q$$

TBB

$$\ddot{x} = -75.4$$
$$\ddot{y} = -1.48\beta$$
$$\ddot{z} = -1.48\alpha$$
$$\dot{p} = 0$$
$$\dot{q} = -2.065\alpha - 0.414q - 0.1r$$
$$\dot{r} = -2.065\beta - 0.414r - 0.1q$$

AC

$$\ddot{x} = -74.6$$
$$\ddot{y} = -0.26\beta$$
$$\ddot{z} = -0.26\alpha$$
$$\dot{p} = 0$$
$$\dot{q} = -0.253\alpha - 0.185q - 0.1r$$
$$\dot{r} = -0.253\beta - 0.185r - 0.1q$$

Refer now to Figures 27 and 28 of this volume. In terms of the analysis, it is shown by inspection of the figures and the reduced equations above that the difference in the angular oscillation characteristics among the three attached decelerator configurations is primarily affected by the magnitude of the static aerodynamic force coefficient and the static stability margin. That is, the size and geometry of the expandable attached decelerator configuration is of primary importance to ensure desirable dynamic stability characteristics for a specific terminal descent performance. This is further emphasized by consideration of the oscillation rate characteristics for each configuration. The value for the damping factor ($C_{m_q} + C_{m_{\dot{\alpha}}}$) is for practical purposes nearly the same for each configuration (see Item 28, Tables A-III and A-XI of Appendix A). However, upon reduction of the equations of motion at initial operation where the configuration geometry parameters are introduced, the effect of the decelerator geometry is substantial.

Again, considering the above reduced dynamic motion equations for each

of the attached decelerator configurations at initial operation, the degree of accuracy may be approximated in basing the previous weight analyses on the assumptions that adequate stability would exist and that there would be little dynamic interaction with stress-weight requirements. The total translational deceleration load along the longitudinal axis on the composite entry-body decelerator is approximated as follows:

$$N_{\ddot{x},\, q,\, r} = \frac{1}{g_e}\left[\ddot{x} + k\sqrt{(q)^2 + (r)^2}\right]$$

where

g_e = earth g's (32.2 ft/sec/sec),

k = transverse radius of gyration of composite system (from Item 21, Tables A-III and A-XI of Appendix A),

q and r = maximum values from Figures 27 and 28.

The composite system lateral acceleration is approximated as:

$$N_{\ddot{y},\, \ddot{z},\, \dot{q},\, \dot{r}} = \frac{1}{g_e}\left\{\left[(\ddot{y})^2 + (\ddot{z})^2\right]^{1/2} + k\left[(\dot{q})^2 + (\dot{r})^2\right]^{1/2}\right\}$$

Conservatively, the composite maximum g's can be approximated as:

$$N_{tot} = \left[(N_{\ddot{x},\, q,\, r})^2 + (N_{\ddot{y},\, \ddot{z},\, \dot{q},\, \dot{r}})^2\right]^{1/2}$$

The following values are the equivalent earth-g loads acting on the system for each of the attached decelerator configurations at initial operation for trajectories 19 and 22:

Earth-g loads for trajectory 19

	AB	TBB	AC
$N_{\ddot{x}, q, r}$	-2.69	-2.72	-2.68
$N_{\ddot{y}, \ddot{z}, \dot{q}, \dot{r}}$	-1.13	-3.41	-0.52
N_{tot}	-2.92	-4.35	-2.72

Earth-g loads for trajectory 22

	AB	TBB	AC
$N_{\ddot{x}, q, r}$	-2.41	-2.44	-2.37
$N_{\ddot{y}, \ddot{z}, \dot{q}, \dot{r}}$	-0.61	-2.24	-0.36
N_{tot}	-2.48	-3.31	-2.4

Compare, now, the above tabulated values of g-loads with Item 15 in Table IV of this summary report. It is seen (with exception of the tucked-back BALLUTE for trajectory 19) that basing the strength-weight requirements of the decelerators on quasi-static design strength, load, and safety factors will, in general, tend to be conservative as compared to the maximum loads predicted by the dynamic analysis.

This trend is only as far as the attached decelerators are concerned. This observation must, of course, also be tempered in light of the accuracy of the assumptions and approximations made throughout the parametric study. On the basis of previous engineering design experience and application, it is considered that the indicated trends are valid.

4. RESULTS FOR TRAILING CONFIGURATION

As described in Appendix B of Volume II, the trailing decelerator is attached to the forebody through a suspension system assumed to be rigid. The confluence point is defined as the intersection of the suspension

system and riser. In the analysis, this point retains a constant geometrical relationship with respect to the forebody regardless of the motion of either the forebody or trailing decelerator. The riser line is treated as essentially a rigid rod free to pivot at any angle and in any plane at the confluence point.

The decelerator attached to the end of the riser also is defined as retaining a fixed geometrical relationship with the riser (essentially a rigid sphere at the end of a rigid rod free to pivot at the confluence point). The motion of the trailing decelerator and riser is described as having two degrees of freedom about the confluence point. This motion is influenced by the aerodynamic lift and side-force as a function of angle of attack and yaw (i.e., angular displacement of the riser) as well as the drag force and mass characteristics of the decelerator. The spin of the forebody is not considered to affect the decelerator motion as far as rotational, inertial, and aerodynamic effects are concerned.

Thus, the analysis has neglected any consideration of inertial or aerodynamic coupling in describing the motion of the trailing decelerator. The effect of the trailing decelerator motion and loads on the forebody motion is assumed to be transmitted as a tension force through the riser to the fixed confluence point.

Thus, for this program the motion of the composite forebody and trailing decelerator has been described by the eight-degree-of-freedom formulation presented in Appendix B of Volume II.

Referring now to Figures 27 and 28 and Figures C-1 through C-6 of this appendix for the trailing decelerator, it is shown that the present mathematical model describes an apparent coupling effect and resonance between rolling velocity and angular attitude. This coupling causes the composite capsule motion to diverge to large attack, yaw, and coning angles for trajectories 19 and 22. Figures C-1 through C-6 have been developed from additional computer runs for the same capsule/trailing decelerator characteristics for different values of rolling velocity. The

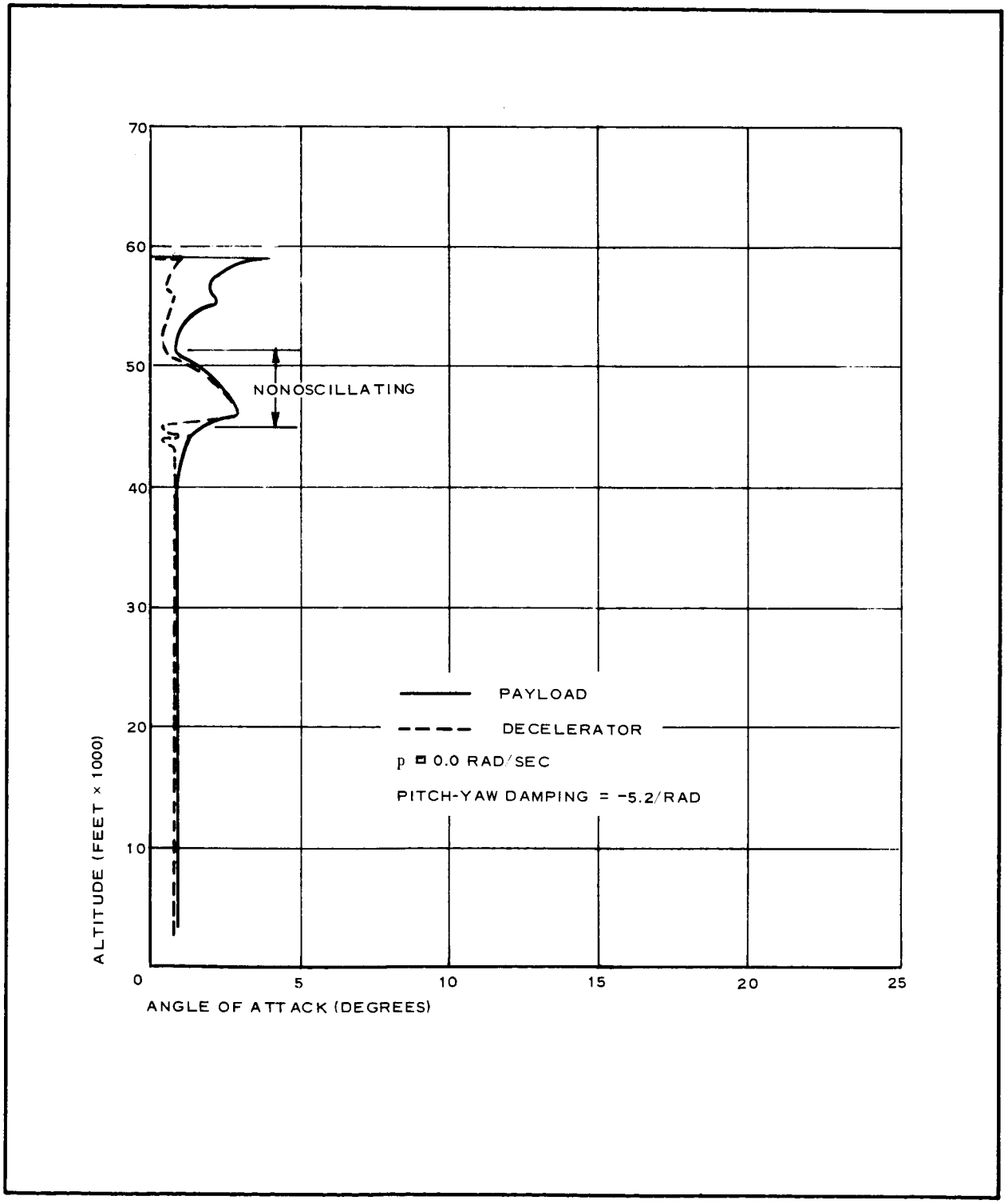

C-1 - Decelerator Oscillation Characteristics for Trailing BALLUTE (Atmosphere VM7; Trajectory 22; p = 0.0 rad/sec)

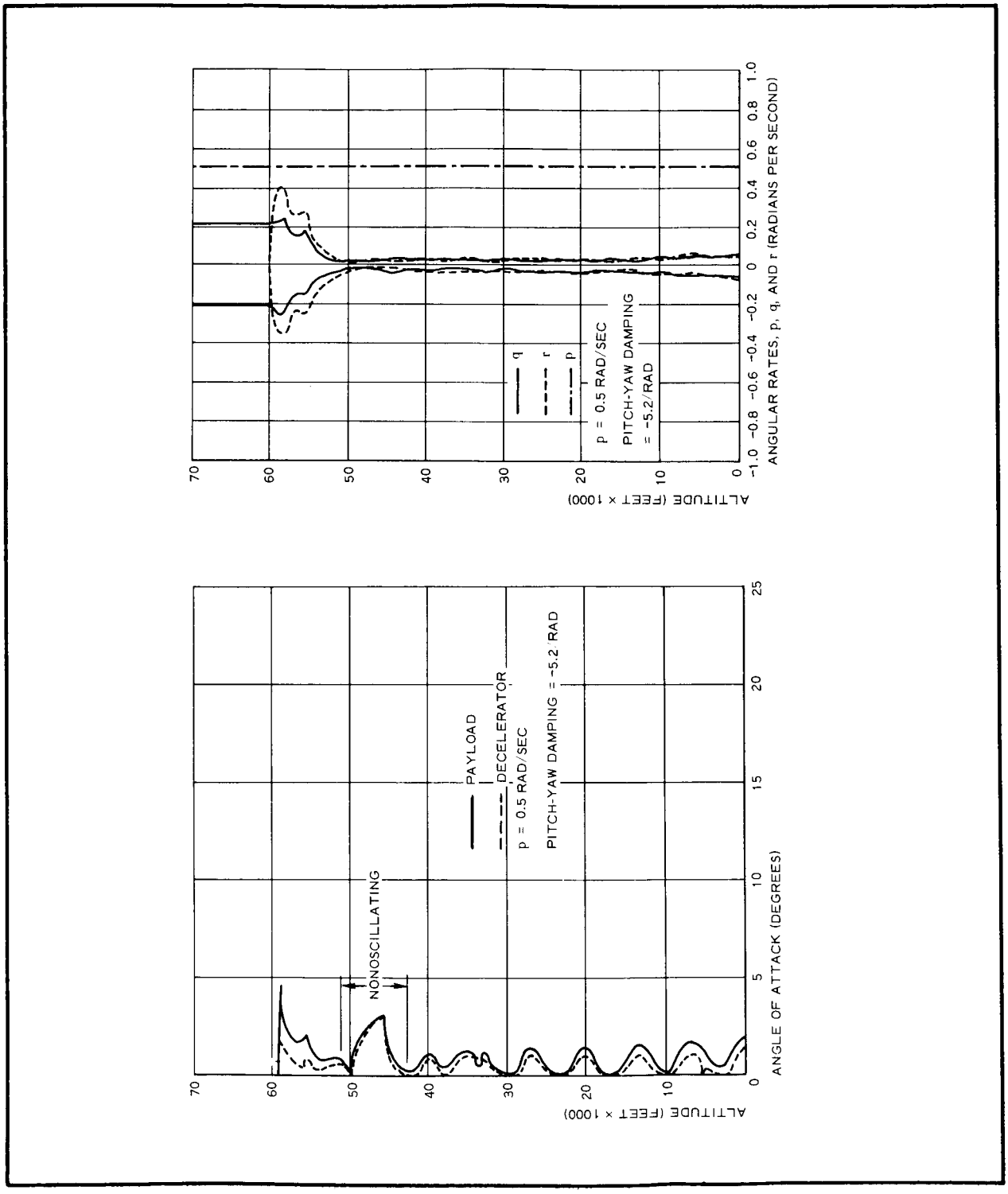

C-2 - Decelerator Oscillation Characteristics for Trailing BALLUTE (Atmosphere VM7; Trajectory 22; p = 0.5 rad/sec)

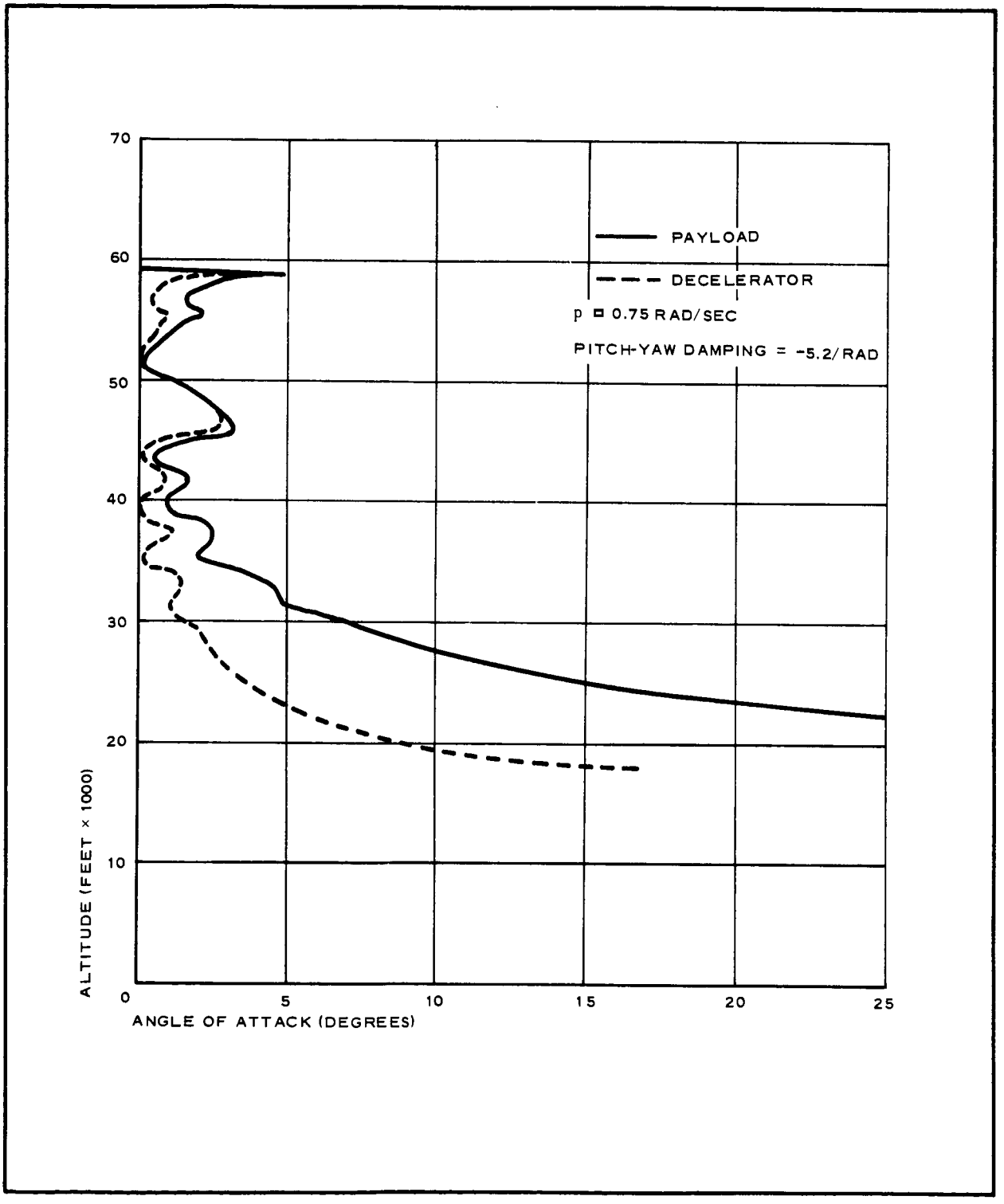

C-3 - Decelerator Oscillation Characteristics for Trailing BALLUTE (Atmosphere VM7; Trajectory 22; p = 0.75 rad/sec)

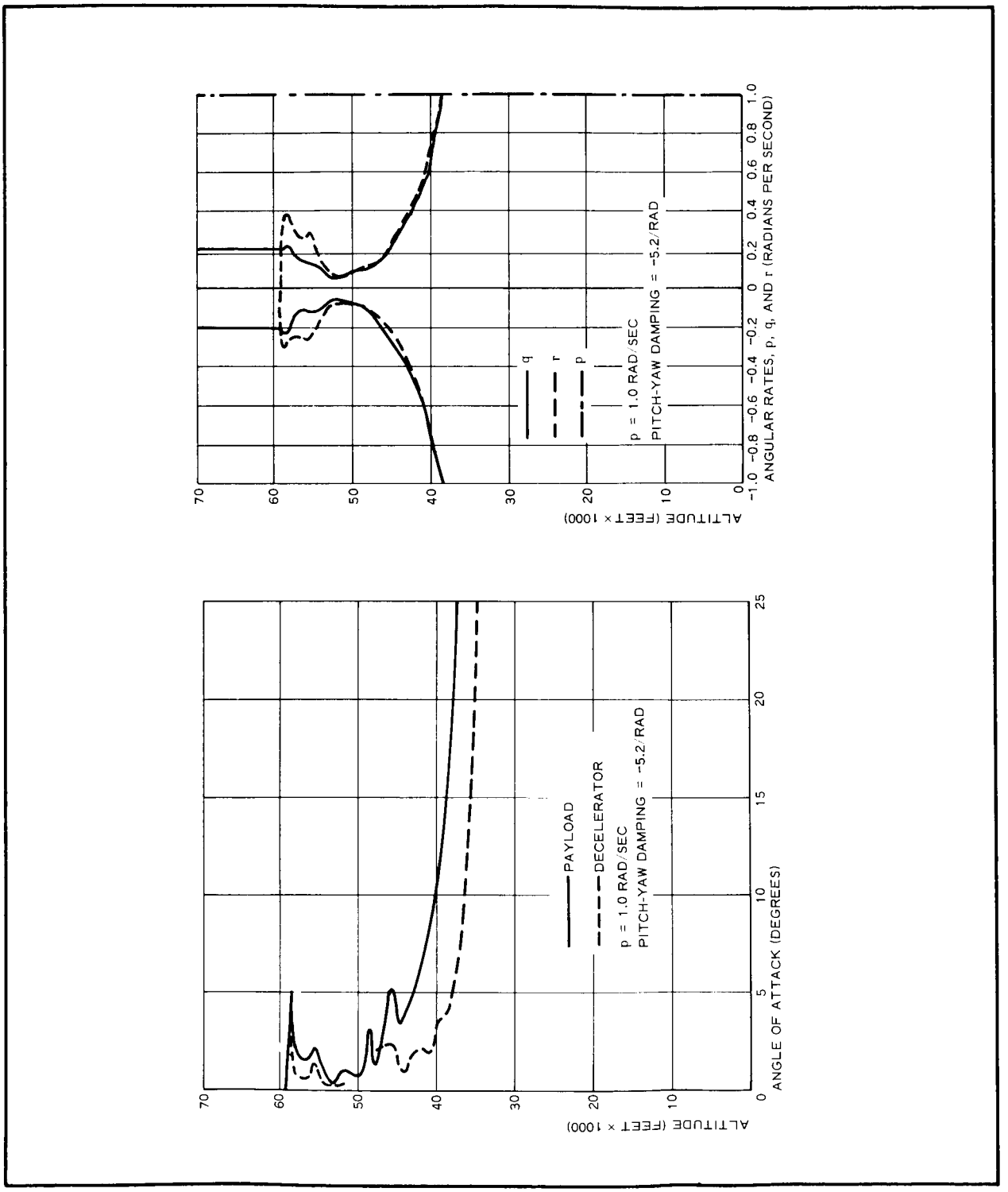

C-4 - Decelerator Oscillation Characteristics for Trailing BALLUTE (Atmosphere VM7; Trajectory 22; p = 1.0 rad/sec)

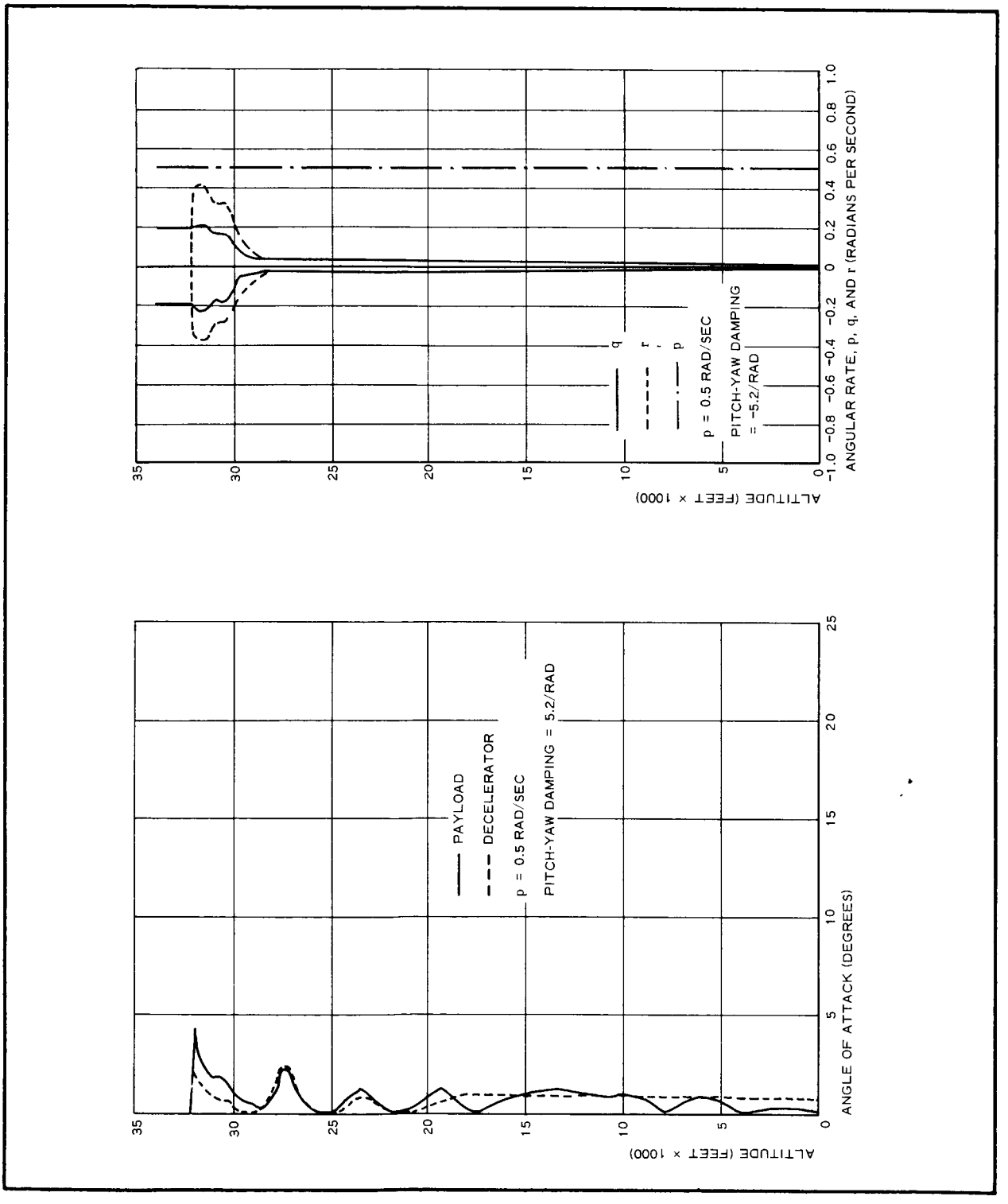

C-5 - Decelerator Oscillation Characteristics for Trailing BALLUTE (Atmosphere VM8; Trajectory 19; p = 0.5 rad/sec)

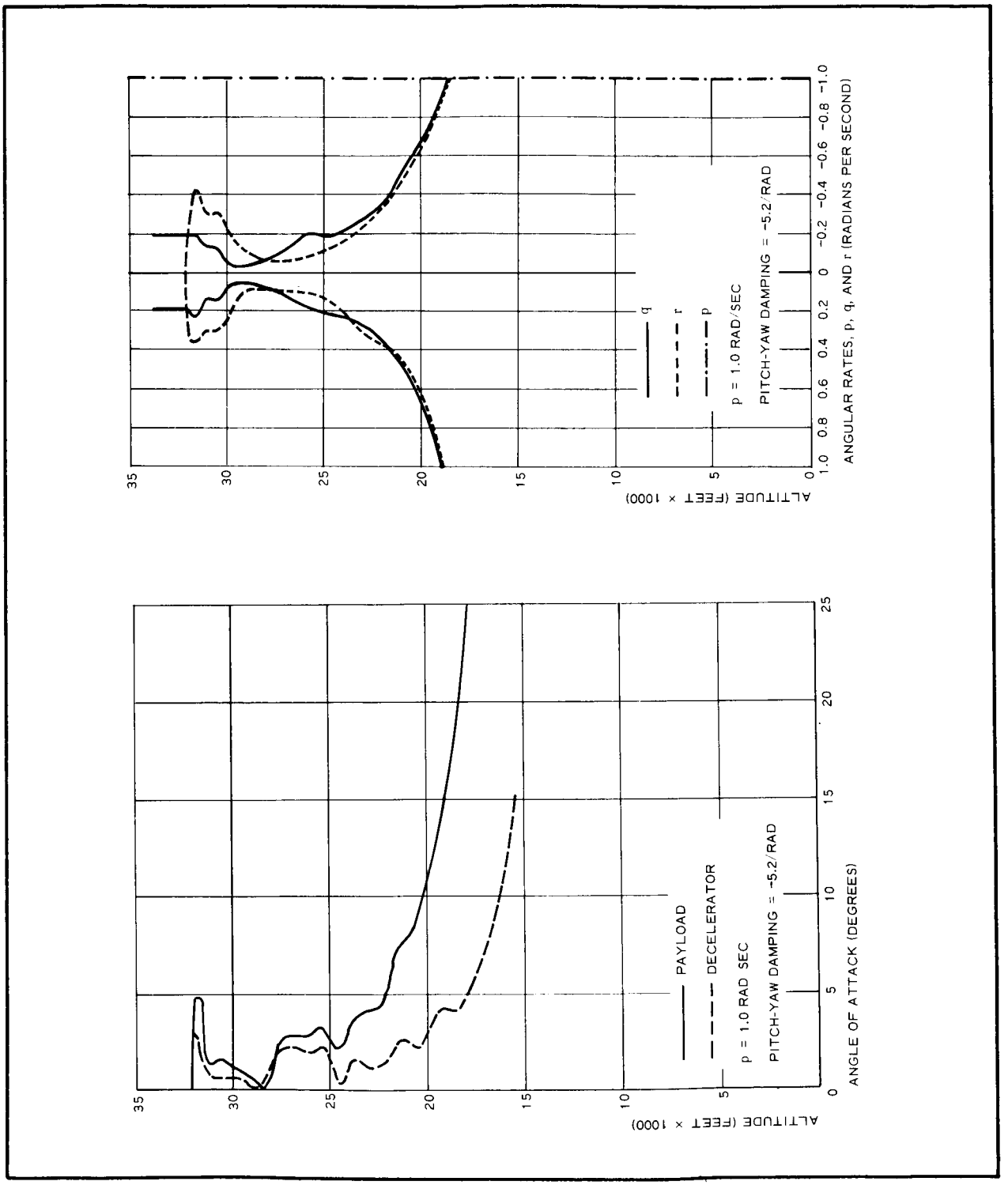

C-6 - Decelerator Oscillation Characteristics for Trailing BALLUTE (Atmosphere VM8; Trajectory 19; p = 1.0 rad/sec)

apparent effect of roll coupling on the system motion as described by the present mathematical model is strongly in evidence.

The drag force and moment of the trailing decelerator has the natural effect of providing stabilization for the composite capsule/decelerator system as demonstrated by the case for the rolling velocity equal to zero. Additionally, as shown by the figures of this appendix, the magnitude of roll rate is important in determining whether the system will converge to or diverge from a stable attitude in terminal descent. While the possibility of coupling and resonance is recognized to exist for the motion of a spining entry capsule with a trailing decelerator, Goodyear Aerospace's experience with such applications (including cases of a spinning forebody) has not exhibited generally a divergence tendency, at least to the magnitude encountered in this study.

Therefore, the motion of a forebody with a trailing decelerator as presently decribed by the eight-degree-of-freedom formulation presented in Appendix B of Volume II is not considered to be a completely adequate description. The analytical description of the system dynamics for use of trailing decelerators should be studied and evaluated in greater detail than encompassed in this program in view of the importance for the recovery and safe landing of planetary entry vehicles.

5. CONCLUSIONS AND RECOMMENDATIONS

1. The present six-degree-of-freedom mathematical model describing the dynamic motion of composite entry body and attached expandable decelerator configurations is adequate. As shown by the results of this study, it is not necessary to include additional sophisticated parameters such as kinematic aerodynamic coupling terms or non-linear variation of coefficients with angular attitude for preliminary parametric analyses of the dynamic motion characteristics.

2. For the initial conditions established by the specified JPL entry trajectories for this study corresponding to the time of decelerator deployment and operation, the transient distrubance as a result of decelerator deployment does not result in excessive angular excursions and rates. For all of the attached expandable decelerator configurations, the trend is toward convergence to reasonable magnitudes of angular attitude and damping of angular rates of motion.

3. For the attached expandable decelerator configurations, the magnitude of the static normal force coefficient and static margin of stability (center of pressure), which are indicative of the shape of the device combined with the device size and configuration geometry, profoundly affect the dynamic motion characteristics and damping of the composite system.

4. The computer results using the present eight-degree-of-freedom formulation describing the system dynamics for an entry capsule and trailing decelerator point out that kinematic (roll-yaw) coupling effects can result in angular attitude and rate divergence when an initial roll rate exceeding about 0.5 rad/sec is present at deployment. The computer results also indicate that there is resonance, i.e., coupling between the trailing decelerator and entry capsule motion, that causes a pronounced divergence trend. The formulation presented in Appendix B of Volume II and the computer program have been determined to be mathematically correct and provide an accurate description of the system motion as described by the formulation.

5. In this event, the present eight-degree-of-freedom mathematical model for the entry capsule and trailing decelerator does not appear to be a completely accurate description of the system dynamics. This observation stems from actual free-flight experience of Goodyear Aerospace personnel with similar loading environments. Apparently, more sophisticated forms are required to describe the dynamics such as riser-line elasticity and additional degrees of freedom to describe confluence point motion, at least in the lateral planes. A description of the trailing decelerator motion at the end of the riser line by two additional degrees of freedom also might be desirable. Thus, it appears that at least twelve degrees of freedom may be necessary to adequately describe the system dynamics.

   A survey should be made of past free-flight trailing decelerator data. More complete information should be gathered to estimate static stability and damping coefficient derivatives for use with the dynamic stability analyses of trailing decelerator configurations.

LIST OF SYMBOLS FOR APPENDIX C

A = reference area

C_ℓ = rolling moment coefficient

C_{ℓ_p} = rolling moment coefficient derivative with rolling velocity (damping in roll)

C_m = pitching moment coefficient

C_{m_q} = pitching moment coefficient derivative with pitching velocity

C_{m_α} = pitching moment coefficient derivative with angle of attack (X-body axis)

$C_{m_{\dot{\alpha}}}$ = pitching moment coefficient derivative with angle of attack rate

C_{m_μ} = pitching moment coefficient derivative with total angle of attack

C_{N_q} = normal force coefficient derivative with pitch rate

C_{N_α} = normal force coefficient derivative with angle of attack (X-body axis)

$C_{N_{\dot{\alpha}}}$ = normal force coefficient derivative with angle of attack rate

C_{N_μ} = normal force coefficient derivative with total angle of attack

C_n = yawing moment coefficient

C_{n_β} = yawing moment coefficient derivative with angle of yaw

C_X = axial force coefficient

C_Y = side force coefficient

C_{Y_β} = side-force coefficient derivative with angle of yaw

C_Z = vertical force coefficient

d = reference diameter

D_v = system reference diameter

F_x = axial aerodynamic force along X-body axis

F_y = side aerodynamic force along Y-body axis

F_z = vertical aerodynamic force along Z-body axis

g_e = earth gravity

I_x = moment of inertia about X-body axis

I_y = moment of inertia about Y-body axis

I_z = moment of inertia about Z-body axis

k = transverse radius of gyration

m = system mass

M_x = aerodynamic moment about X-body axis

M_y = aerodynamic moment about Y-body axis

M_z = aerodynamic moment about Z-body axis

N_{tot} = total (rms) gravity load factor

$N_{\ddot{x}, q, r}$ = axial gravity load factor due to linear acceleration along X-body axis and centrifugal acceleration due to pitching and yawing angular velocities

$N_{\ddot{y}, \ddot{z}, \dot{q}, \dot{r}}$ = transverse gravity load factor due to linear accelerations along Y and Z body axis and pitching and yawing angular accelerations

p = rolling angular velocity

$\dot{p}$ = rolling angular acceleration

q = pitching angular velocity

$\bar{q}$ = dynamic pressure

$\dot{q}$ = pitching angular acceleration

r = yawing angular velocity

$\dot{r}$ = yawing angular acceleration

V = velocity (total)

$\dot{x}$ = linear velocity component along X-body axis

$\ddot{x}$ = linear acceleration along X-body axis

$\dot{y}$ = linear velocity component along Y-body axis

$\ddot{y}$ = linear acceleration along Y-body axis

$\dot{z}$ = linear velocity component along Z-body axis

$\ddot{z}$ = linear acceleration along Z-body axis

α = angle of attack

$\dot{\alpha}$ = angle of attack rate

β = angle of yaw

$\dot{\beta}$ = angle of yaw rate

ΔX_{cp} = center of pressure position with respect to system center of gravity

Σ = summation of related factors or terms